ROOM USE CHEY

MH2800 MA2800

082404

ARSTRACT

STRUCTURE AND BONDING IN METAL-AMINE SOLUTIONS AS DETERMINED BY ELECTRON PARAMAGNETIC RESONANCE AND OPTICAL SPECTRA

by Larry Raymond Dalton

An extensive study has been made of the magnetic and eptical properties of solutions of the alkali metals dissolved in a number of amine, dismine, and amine-ether solvents.

The results of these studies emphasize the differences as well as the similarities between metal-amine and metal ammonia solutions. At least two additional species not present in metal-ammonia solutions appear to be required to explain the physical properties of metal-amine solutions.

The various models for metal-amine solutions have been examined in the light of the experimental evidence. Correlation of the optical and EPR results precludes the assignment of the visible absorption to the monomeric species responsible for hyperfine splitting.

A detailed analysis of hyperfine splittings, g values, spin concentrations, and relaxation processes has permitted the development of semi-quantitative models for the monomeric species. Although both stationary single-state and dynamic multi-state models are considered, the dependence of the magnetic parameters upon temperature and upon

metal and solvent composition indicates that a multi-state equilibrium among memomeric species of different electronic configurations is operative in the solutions.

The nature of the singlet observed at $g = 2.0019 \pm 0.0002$ in the EPR spectra is considered. Evidence is presented supporting the assignment of this singlet to the selvated electron, $e^{-}(selv_{*})$.

Measurements of the viscosities of methylamine and ethylamine permit further analysis of melear spin-dependent relaxation processes in metal-amine solutions. In particular, the dependence of the linewidth upon the muclear spin quantum number $\mathbf{n}_{\underline{\mathbf{r}}}$ is evaluated in the light of a two-state equilibrium and a multi-state distribution. These two expressions are shown to result in the same functional dependence upon $\mathbf{n}_{\underline{\mathbf{r}}}$.

STRUCTURE AND BONDING IN METAL-AMINE SOLUTIONS AS DETERMINED BY ELECTRON PARAMAGNETIC RESONANCE AND OPTICAL SPECTRA

by

Larry Raymond Dalton

A THESIS

Submitted to

Michigan State University

in partial fulfillment of the requirements

for the degree of

MASTER OF SCIENCE

Department of Chemistry

9/1/2/16 5/1/2/1

To my wife Leuraine

ACKNOWLEDOMENTS

The author wishes to express his sincere appreciation to Professor

J. L. Dye for his continued interest, counsel, and encouragement during

the course of this investigation.

I would also like to thank Professor H. M. McConnell of Stanford University, Professors C. Kikuchi and R. H. Sands of the University of Michigan, and Professor J. Cowen of Michigan State University for making their magnetic resonance facilities available to me and for many helpful and stimulating discussions.

I am pleased to acknowledge valuable discussions with Professor D. Kivelson of the University of California at Les Angeles and I wish to thank him for making available preprints of related papers.

It is also a pleasure to acknowledge the advice of Dr. L. S. Singer of Union Carbide Corporation concerning the measurement of spin concentrations and spin-lattice relaxation times. Moreover, I wish to thank him for providing pertinent data concerning reference samples.

Particular thanks are due V. A. Ricely, J. D. Rymbrandt, E. M. Hansen, and A. Ulland-Hoss for experimental assistance.

Last, but certainly not least, I wish to thank my wife Lauraine for typing this thesis, assistance with calculations, and continued encouragement.

This research was supported by the United States Atomic Energy Commission.

TABLE OF CONTENTS

I.	INTRODUCTION		1
n.	HISTO	RICAL	5
	A.	Models for Metal-Amine Solutions	. 5
	B.	Nodels for the Konsser	11
	c.	Paramagnetie Relexation in Motal-Amine Solutions	23
	D.	Perenagnetic Relexation in Alkali Notals	32
m.	EXPER	imental.	35
	A.	Glassware Cleaning and Resgont Purification	35
	B.	EPR Measurements	46
	C.	Optical Measurements	68
	D_{\bullet}	Conductance Measurements	69
	E.	Viscosity Measurements	69
IV.	RESUL	.73	70
	Å.	EPR Mossurements en Metal-Amine Solutions (Magnetic Parameters)	70
	₿.	EPR Monagrements en Hotel-Amino Solutions (Paramagnetic Relexation)	94
٧.	CONCI	CUSIONS	103
	A.	The Assignment of the Optical Absorptions	103
	B.	The Assignment of the EPR Absorptions	109
	C.	Mudleer Spin-Dependent Relexation	127
	D.	Wuclear Spin-Independent Relaxation	137

TABLE OF CONTENTS - Continued

VI.	APPENDIX	138
VII.	refundaces	142

LIST OF TABLES

TABLE		page
I.	Least-Squares Values from Analysis of Atom-Monomer Equilibria	15
II.	Equilibrium Constants for the Solvation and Complexation Equilibria as Calculated from Spin Concentration and Hfs Measurements	21
III.	Coefficients of m_ in the Linewidth Expression using the Two-State Model	27
IV.	Alkali Metals and Solvents Employed and their Commercial Sources	36
V.	Reference Standards used for Determination of Spin Concentrations	37
VI.	Qualitative Nature of the Electron Paramagnetic Resonance Spectra of Metal-Amine Solutions	71
VII.	The Hyperfine Splitting, A., of the Monomeric Species as a Function of the Metalland Solvent Employed	72
VIII.	The Hyperfine Splitting, A., of the Monomeric Species as a Function of Temperature	73
IX.	The g-value, gn, of the Monomeric Species as a Function of Alkali Metal and Solvent for a Number of Metal-Amine Solutions	78
х.	The g-value, g, of the Monomeric Species as a Function of Temperature	80
XI.	The Spin Concentration (at 23°C) of the Monomeric Species as a Function of Metal and Solvent for a Number of Saturated Metal-Amine Solutions	81
XII.	The Spin Concentration (at 23°C) and g-value of the Solvated Electron for a Number of Metal-Amine Systems	83
XIII.	EPR Parameters of the HTs Pattern and Extra Absorption as Obtained by Computer Analysis	85

LIST OF TABLES - Continued

TABLE		page
XIV.	Summary of EPR Results for Lithium in EthylaminsAmmonia Mixtures	87
• VX	g-values of Solutions Dimibiting only a Single Line .	91
XVI.	Linewidth of Sodium-Mothylamine Solutions	93
XVII.	Analysis of Muclear-Spin Dependent Relaxation for Soveral Metal-Amine and Metal-Amine Ammonia Solutions	988
XVIII.	Linewidths of the Solvated Electron	981
XIX.	Summary of the Optical Spectra of Metal-Amine and Metal-Ammonia Solutions	100
XX.	Conductance of Sodium in Ethylenediamine	101
XXI.	Viscosities of Methylamine and Ethylamine	102
XXII.	Concentration of the Solvated Dimer Predicted from Monomer Spin Concentration Measurement by Use of Gas Phase Equilibrium Constant	lc4
XXIII.	Calculated Secular Linewidths of Na_2^+	107
XXIV.	The Ratio $p_p/(p_a + p_p)$ Obtained from g-shift Analysis and Independently from Analysis of Hyperfine Splitting for a Solution of Cesium in Ethylamine	118

LIST OF FIGURES

PIGURE		Page
1.	Separation of Hyperfine Splitting into Atomic and Honomorie Contributions	16
2.	Calculation of Complexation Constants from Spin Con- centration Data and Independently from Hfs Data	20
3.	EPR Spectra of Alkali Metals in Some Amines	24
4.	Variation of the Coefficients of the Expression $T_2^{-1} = C_0 + C_1 m_1 + C_2 m_1^2 + C_3 m_1^3 \text{ with } 1/T \dots \dots \dots$	30
5.	Vessel Used to Prepare Solutions of Sodium, Potassium, Rubidium, and Cesium in Amine Solvents for EFR Measure- ment	41
6.	Vessel Used to Prepare Lithium-Amine Solutions for EPR Studies	42
7•	Vessel Used to Propare Sample for Measurement of H ₁ inside of Metal-Amine Sample	45
8.	Line Shape Analysis of Some Typical Ketal-Amine Spectra	58
9.	Inhomogeneously Breadened Resonance Line	64
10.	Saturation Curve for a Typical Metal-Amine Sample and Rydrasyl	67
11.	Block Diagrem of Apparetus Used to Obtain the Viscosities of Methylamine and Ethylamine as a Function of Temperature	69 1
12.	Hyperfine Splitting of Monomeric Species as a Func- tion of Temperature and Solvent	74
13.	The Hyperfine Splitting, A. of the Monomeric Species as a Function of Armonia Concentration for Some Ketal-Amine-Armonia Mixtures	76

LIST OF FIGURES - Continued

FIGURE		page
14.	Temperature Variation of A. for Some Metal-AmineAmmonia Solutions	77
15.	Variation of g-value with Temperature for Some Netal-Amine Solutions	79
16.	A Potassium-Ethylamine-Armonia Solution Shouling the Presence of the Extra Absorption	86
17.	EPR Spectra of Lithium im Some Ethylamine-Aumonia Mixtures	83
18.	Decay of the EPR Absorption of a Cosium-Ethylandre Solution	95
19.	Cosium in 1,2- and 1,3-propanediamine	96
20.	Comparison of $p_{\rm p}$ obtained from Analysis of Hyperfine Data and Independently from g-shift Analysis	119
21.	High Temperature g-shift Behavior in Light of Models for the Solvated Atom	121
22.	Effect of Decomposition on the Temperature Dependence of the Hyperfine Splitting	124
23.	Variation of the Coefficients of the Expression $T_2^{-1} = C_0 + C_1 m_1 + C_2 m_1^2 + C_3 m_2^2 \text{with } n/T \bullet \bullet \bullet \bullet \bullet$	129

INTRODUCTION

There are two reasons for studying solutions of the alkali metals dissolved in amount and the amines. From a theoretical standpoint these solutions are of interest in that they represent systems of solvated fundamental particles. That is, the solutions are considered to be characterised by equilibria involving solvated electrons, metal memores and dimers, metal molecule ions, and metal amions and cations. In the gas phase these fundamental particles and their interestions and reactions have been the subject of detailed quantum mechanical, thermodynamical, and statistical thermodynamical analyses. The study of these particles in solution provides considerable insight into the nature of the dissolution precess and the nature of the liquid state. Insight is also provided into the methods of applied mathematics and the limitations of these methods.

From a practical standpoint these solutions are of interest because they represent a convenient source of electrons to be used in chamical rescutions. The solutions are of particular value in the study of the kinetics of electron-attachment reactions.

The physical properties of alkali and alkaline earth metals in ammenia have been the subject of experimental and theoretical interest for ever one hundred years. Since the early work of Weyl (1) many chemists and physicists have studied these systems because of their unusual physical and chemical properties. When metals dissolve in ammenia, netastable blue solutions are formed which become copper-bronze in color as the solutions because more concentrated.

Much of the early work on metal-ammonia solutions was carried out by C. A. Krane. France (2) hypothesized that the disselved metal issued according to the mass action expression

$$H + x(RH_3) \Longrightarrow H^+ + \bullet^-(RH_3)_x$$

where H is the notal stan, H⁺ is the positive notal ion, and e⁻ is the solvated electron. It was also hypothesised that the equilibrium shifted to the right as the concentration decreased giving only notal ions and solvated electrons at infinite dilution.

The solutions should be paramagnetic if they contain unpaired electrons. This was verified by Freed and Sugarman (3) and by Haster (4,5). These workers measured the static susceptibility of sedium, potassium, cosium, calcium, and berium in assemble as a function of temperature and concentration. At high dilution the static susceptibility appreaches the value expected for free spins. Dilute barium solutions have susceptibilities greater than expected for one electron per barium stam indicating that both valuese electrons are ionized. Quantitative electron paramagnetic resonance experiments have shown the paramagnetic susceptibility of sedium and potassium in sementa (6) and potassium in deutero-assemble (7) increases but the melar susceptibility decreases with increasing concentrations. These results are in agreement with the static measurements and show that a concentration-dependent equilibrium exists between the perumagnetic and dismagnetic species.

Transference number measurements (8,9,10) have shown the primary convent carrier to be existing. The negative species carries about seven times more current at low exposurations than does the positive earrier. The percentage of the current carried by the negative species increases with increasing concentration until it is greater than 99% at high concentrations.

Nuclear magnetic resonance experiments on metal-ammonia solutions (11,12,13,14) have shown a chemical shift for the mitrogen and metal muclei (Knight shift) but no detectable chemical shift for the protons. These results indicate considerable electron density at the mitrogen and metal muclei but very little electron density at the proton mucleus.

In contrast to solutions of inorganic salts in amount, which increase in density and viscosity with increasing concentration, solutions of metals in amounts show a decrease in both density and viscosity with increasing concentration (15,16).

The optical spectra of metal-ammenia solutions have been investigated extensively (17,18,19,20). All solutions are characterised by a
single broad peak in the near infrared which is asymmetrically broadened
en the high energy side. The spectra are independent of the nature of the
satism, and there is no marked change in the form of the spectra when
temperature and concentration are varied.

The preceding paragraphs indicate the intensity of experimental investigation directed toward metal-sumenia solutions. Theoretical efforts have been no less exhaustive. Several theories have been proposed, two of which gained early prominence (21,22). Both models involve the inmination of the metal in dilute solution to give a metal extien and a solvated electron, as first postulated by Kraus. The main difference between the theories relates to the position of the electron in the intermediate concentration range (0.005 to 0.1 molar). The "cavity" model (21) considers the electron to be completely removed from the metal and located in a "cavity" within the solvent. The Becker, Lindquist, Alder (BIA) model (22) considers the electron to be in an orbit about the metal ism but sutside of its solvation sheath. Both models also consider the dimerisation of the species just described.

Arnold and Patterson (23) have shown that correlation of the magnetic and conductance data necessitates the existence of a dismagnetic, negatively-charged species. This observation has generated extended interest in models for metal-smine solutions (24,25). Unfortunately me model capable of explaining the full range of physical properties has yet been forthcoming.

Alkali metals have also been observed to dissolve in a number of smines, dismines, and others forming strongly reducing blue solutions. The visual and chemical similarity of these solutions to metal-ammenia solutions has prompted the idea that these solutions are stoichiometrically equivalent to metal-ammonia solutions. Unfortunately the metal-erganic solvent systems have until recently received only cursory attention.

The purpose of this project was to investigate extensively notal—
-axine solutions by optical and magnetic resonance techniques. It was
hoped that the relationship of these solutions to metal—axine solutions
could be deduced and that a detailed model for metal—axine solutions
could be developed.

HISTORICAL.

A. Models for Motel-Amine Selutions

In spite of the complexity of the optical spectra of metal-animo solutions including the appearance of several bands not found for metal-amounts solutions, there existed an initial tendency to describe metal-amounts solutions by extension or medification of the existing theories of metal-amounts solutions (21,22).

Blades and Hodgins (26), after studying solutions of certain of the alkali metals in methylamine, ethylamine, and amine-amenia mixtures, attributed the three characteristic optical absorptions of motal-cuine solutions to solveted electrons existing in different types of solvent treps. In metal-amenia solutions the positive end of the amenia meloouls is made up of three hydrogen stems and is symmetrical so that the array of molecules at the edge of any hole will be identical. This will make the configurational op-ordinates and consequently the transition levels for each hele identical, with the result that a single maximum is observed for all the colutions in liquid amounts. It was further arrued that since the nothylemine and othylemine melecules are not symmetrical shout the nitrogen it was possible that two different aspects of the nelecule might be presented at the boundary of a trop. These tre erientations may or may not be mixed depending on how readily they fit around the hole, the size of the hole, and on what other forces are at work in the rest of the liquid. On the basis of this model the methylamine

spectra were broken into two groups, called by Blades and Hedgins, amine bands and aliphatic bands. The former represented the condition where the methylamine melecules are eriented so that an amenia-like trap is produced. This trap was viewed as giving rise to the infrared band (1250 to 1400 mm). Aliphatic bands, accounting for the absorption at 650 to 725 mm (visible band), are so from traps in which the methyl group per-ticipated in the formation of the trap boundary. The red band (840 to 1000 mm) observed for dilute solutions of petassium in methylamine was considered to arise from a mixture of the two possible orientations.

Symons (27) viewed motal-amine solutions as being characterised by two absorptions, the visible band and the infrared band. On the brais of existing experimental evidence and by analogy with F centers in alkali halide exystals and P centers in exystalling silicen, Symons assigned the visible absorption to a dismagnetic species such as the dimer of the model of Booker, Lindquist and Alder (BLA). Continuing, he assigned the infrared absorption to the selvated or cavity electron. From analogy with the results of addition of large concentrations of sedium salt to dilute solutions of sedium in essents (28), Symons attributed the red band to a measurer of the BLA type.

Cafasse and Sundheim (29) presented results for solutions of the alkali metals in others which seemed to fit the general description given by Symons (27,30). On the basis of studies of the alkali metals in othylenediamine, Windsor and Sundheim (31) postulated that the visible (650 to 725 mm) absorption is due to a species which shows no electron paramagnetic resonance (EPR) absorption and that the intermediate absorptions (800 to 900 mm) for K and Rb solutions might be associated with a dimer. Dainton, Wiles, and Wright (32) have presented strong evidence that the visible absorption peak for petassium in disethemyotheme and tetrohydrofuren arises from the heterogeneous nature of the solutions. They were able repeatedly to decrease the absorbance significantly by contribustion of the solutions. This suggested that the solutions are actually colloided in nature. It has been pointed out that these results might be due to the presence of undissolved notal or precipitated decomposition products.

The first detailed medel for metal-anime solutions was developed by Dre and Devald (33). This medel was unique in that it viewed the visible and red bands as arising from species not characteristic of metal-emmonia solutions. Covalent dimers, similar to those existing in the gas phase for the alkali metals, were considered responsible for the red band. This assignment was based upon correlation of this band with the intense ${}^{1}\Gamma_{ji}^{+} \longleftarrow {}^{2}\Gamma_{g}^{+}$ transition for the gaseous dimers of K and Cs (34) and upon the fact that, consistent with the assignment to a dimerie species, the red bend is favored at high metal concentrations. The visible band was attributed to a combination of a solvated melecula-tion, $\mathtt{H}_{2^{n}}^{\bullet}$ with an electron trapped in the field of this ion. The dissociation of \mathbb{N}_2^* would involve the breaking of a covalent notal-notal bond, accounting for the slaw rate of interconversion of optical species. The slaw interconversion rate also explained the lack of reproducibility of results by different investigators (31,35,36). Since the resultant electron density would be largely outside of the primary solvation layer, the nature of the estion in the H2 species would be expected to here little effect upon the electronic energy levels, which explains the independence of peak position and shape upon the particular notal used. Comparison of optical

spectra and conductance measurements for alkali metals in ethylenediamine with the corresponding measurements for metal-amonia solutions led these investigators to attribute the infrared absorption in smine systems to the solvated electron in the species: (\bullet^-) , $(H^+ \bullet \bullet^-)$, $(H^+ \bullet \bullet^-)$, and $(H^+ \bullet \bullet^-)_2$. Those species were collectively referred to as "solvated electrons".

A new era of metal-amine research was introduced when Yos and Dye (37) at Michigan State University and Bar-Eli and Tuttle (38) independently at Brendeds University observed hyperfine splitting from a single metal nucleus in the EPR spectra of selutions of rebidium and contam in methylamine and of potassium in ethylamine. These observations established unequivecedly the existence of a species of statebonetry M in metal-amine solutions. It also suggested the possibility that by comparison of the EPR and optical spectra of a given solution one could establish or dispreve the assignment of the visible absorption to the moments.

Ottologhi, Ber-Eli, Linschite, and Tuttle (39) examined the decay kinetics of solutions of potentium and rubidium in othylamine. Comparison of the rate of change of shootbance with that of the EPR signal during decomposition of a potentium-ethylamine solution, and comparison of the rates of disappearance of the shootbances at 675 and at 915 mm for solutions of potentium and rubidium in othylamine led them to assign the visible shootption to a memomer of the ELA type. These authors were in agreement with Dye and Dewald (33) with regard to the assignment of the red and infrared bends.

More recently, Ottolenghi, Bar-Eli, and Linschitz (40) have studied solutions of the alkali metals in othylamine by flash photolysis. Relying

upon the assignments made in Ref. 39 these authors evaluate their data in terms of a model involving BLA species and excited BLA species.

Thus despite the dissimilarities in the EPR and optical spectra of metal-amine and metal-ammonia solutions, it appeared that the preparties of both systems could be explained by the same model. To investigate further the relationship between splittiens of the alkali metals in the suines and in amounts, workers in this laboratory (41.42) undertack the study of solutions of the alkali metals in amine-amonia mixtures. This investigation conclusively showed the assignment by Ottolonghi et al. (39) of the visible band to the monamer to be in error. The reasons may be summarised as follows: (a) Measurement of soin concentrations for solutions of notessium in animo-ammonia mixtures (42) in solutions of lew emments content show the concentration of the hyperfine species to be eppreximately 10-6 M. Even if the molar absorptivity of this species were as high as 5 x 10 cm -1-mole -1-liter, the abserbance in a 1-mm cell would have a value of only 0.005. However, the absorbance of the visible peck observed in these solutions was unity or higher, more than 200 times that possible if the same species were responsible for both phanesum. (b) The absorbance of the optical species and the spin concentration of the hyperfine species change in eppecite directions with changing temperature (41.42). (c) The dependence of spin concentration of the hyperfine species and the absorbance of the optical band (corrected to unit noth length) upon sumenia concentration also show that different species are responsible for these two effects (41,42). (d) Bar-Kli and Tuttle(43) contend that the contributions to the EPR and optical spectra are determined by the equilibria:

$$\begin{array}{c}
K & \stackrel{K_1}{\longleftrightarrow} & H^+ + \bullet^* \\
K + K & \stackrel{K_2}{\longleftrightarrow} & H_2
\end{array}$$

Since me electron peak is observed in the EPR spectra of potassium in ethylenine, they assume that $K_1 \ll 10^{-h}$. They then reason that the concentration of H_2 will increase when the concentration of H decreases. Dalton at al. (41,42) found the appearite to be true. (a) Although the kinetics of decomposition observed by Ottolonghi at al. (39) would indicate that the visible and red band species are in a 2:1 steichiometric relationship, decomposition studies in this laboratory (42) do not yield this result but rather are in a 1:1 relationship.

Since the presence of an EPR absorption attributable to the selvated electron accounted for only a fraction of the total infrared absorption, the work perferred in this laboratory (51,52) showed electron-pairing reactions to be important in metal-axime solutions. It also showed that the red band should be assigned to the $\frac{1}{11}$ $\frac{1}{11}$ $\frac{1}{11}$ transition of the alkali metal dimers rather than the $\frac{1}{11}$ $\frac{1}{11}$ transition as was originally proposed by Dye and Dewald (33).

The model of Dye and Devald (33) was further challenged by the pulsed radiolysis studies of Amber and Hart (44). These workers reported that pulsing solutions of anhydrous ethylenedismine resulted in an absorption maximum at 920 mm in direct disagreement with the assignment by Dye and Devald of the infrared absorption at 1280 mm observed for solutions of the alkali metals in ethylenedismine to the solvated electron. This disagreement was particularly surprising in light of the excellent agreement between the assignment of the solvated electron in metal-ammenia solutions and the electron absorption found in the pulse radiolysis studies of anhydrous ammenia by Compton and so-workers (45).

Subsequent pulse radiolysis studies of anhydrous aminos and disminos by Dalton, Dye, Fielden and Hart (46) showed the results of Anhar and Hart to be in error. Moreover, this study tended to confirm the assignment by Dye and Dewald (33) of the infrared band to the solvated electron.

Although the recent studies in this laboratory (40,41,45) have previded support for the assignments of Dye and Devald (33) of the red band to covalent metal dimers and the infrared band to solvated electrons and aggregates and have shown the assignment of Ottolenghi at al. (39) of the visible band to alkali metal monomers to be in error, these investigations have not elucidated the nature of the species responsible for the visible band.

Most recently J. D. Rymbrandt (47) has attempted to explain the properties of metal-amine solutions by assignment of the visible band to species of stoichiometry K.. This model, although capable of explaining many of the experimental data and in particular the flesh photolysis results of Cttolenghi, Bar-Eli, and Linschits (40), possesses several faults common to other models. The model will be discussed in greater detail later in this dissertation.

B. Models for the Moment

The observation of hyperfine splitting by a single metal smeleus (37.33) showed conclusively that monomeric metal species exist in metal-amine solutions. The magnitude and marked dependence of this hyperfine interaction upon temperature and solvent rules out the assignment solely to a species whose electronic configuration is identical with that of a gaseous alkali metal atom.

The first detailed description of the monomeric species was attempted by Bar-Eli and Tuttle (43). They assumed that the monomeric species in

metal-amine solutions was essentially a moment of the BIA type. They also assumed that the spherically symmetrical "shape" of the wavefunction does not change with temperature but that an expansion occurs as the temperature is decreased. This expansion presumably results from an increase in the size of the moment as additional selvation spheres are added. The unpaired electron density is assumed to be distributed ever the solvation layers according to the ratio of the solvent binding emergy to kT. Over the temperature range which they studied, Bar-Eli and Tuttle (43) found the scaling factor for the wavefunction to be linear in 1/T. Workers in this laboratory (42) found, however, that extending the temperature range yields a scaling factor that is not a linear function of 1/T. Furthermore, calculations using this model require the average radius of the electron distribution to increase by a factor of two over a 100 degree temperature range.

O'Reilly (48,49), also using a monomer model, proposed a different explanation of the temperature dependence of the hyperfine splitting in metal-anime solutions. The alkali-metal ion was assumed to be established ally surrounded by solvent molecules at a distance r = a, while the remainder of the solvent (r > b) was treated as a continuous dielectric medium. The potential function used was that of the free gaseous atem plus an inverted square well of radius a to account for dipelar, quadrupolar, and pelarisability effects of the solvent. An approximate calculation, ignoring the quadrupolar term, indicated that the temperature variation of the hyperfine splitting could be accounted for on the basis of an expansion of the cation-solvent distance of about 0.2% per degree. In attempting to apply 0'Reilly's model to their results, Dalton at al. (42) found that the high and low temperature regions require different coefficients of expansion.

Using an iterative precedure to calculate a as a function of temperature (50) gives (1/a) $(da/dt) = 5.84 \times 10^{-4}$ below 40° C and 4.73×10^{-3} above this temperature.

Both of these models require rather large changes in monomer dimensions with temperature. Moreover none of the models predicts the sharp change in the temperature dependence of the hyperfine interaction observed in this laboratory (41,42). Neither do these models explain the strong dependence of the hyperfine splitting upon ammonia concentration observed for amine-ammonia mixtures (41,42).

Dalton, Rynbrandt, Hansen, and Dye (42) have developed a model which meets these objections and which gives emcellent quantitative agreement with experimental results. In this model they consider an equilibrium among two or more measured species with distinct magnetic properties. The relaxation time for the interconversion of these species must be faster than the reciprocal of the hyperfine interaction frequency but slower than molecular rotation. Because of the extrapolation of the hyperfine splitting (hfs) to the free-atom value at high temperatures, one of the species (A) is considered to be the selvated atom, with a splitting the same as that for gaseous atoms. The amount dependence of the hfs requires, in addition to atoms, two selvated monomeric species $H(EthH_2)_X$, and $H(EthH_2)_{X=1}(HH_3)$ represented by B and C, respectively. Asserting to this scheme the following equilibria are involved:

$$A \rightleftharpoons B$$

$$E_{a} = [B]/[A] \qquad (1)$$

$$E_{a} = [C]/[B] \{(1-x)/x\}$$

in which I is the mole fraction of amounts. The measured hyperfine splitting A_p is related to the concentration of these species and their respective splittings by

 $A_{p} = (n_{A}A_{A}^{0} + n_{B}A_{B}^{0} + n_{C}A_{C}^{0})/n$ with, of source, $n = n_{A} + n_{B} + n_{C}$. (2) For the case of saturated solutions, it would be expected that the consentration of atoms would vary according to

$$ln [A] = (\Delta H^0/RT) + (\Delta S^0/R)$$
 (3)

in which ΔH^0 and ΔS^0 are the molar enthalpy and entropy of solution of the metal to give atoms. The strong dependence of A_p upon temperature above $A0^0$ C indicates that the temperature dependence of atom concentration is much greater than that of the other two species. This permitted an approximate separation of the splitting due to atoms from that due to the species B and C by extrapolation of the low-temperature behavior. This separation was accomplished using the approximation

$$\mathbf{n}_{\mathbf{A}} = \mathbf{n}(\mathbf{A}_{\mathbf{F}}^{\mathbf{O}} - \mathbf{A}_{\mathbf{H}}^{\mathbf{O}})/(\mathbf{A}_{\mathbf{A}}^{\mathbf{O}} - \mathbf{A}_{\mathbf{H}}^{\mathbf{O}}) \tag{4}$$

in which $A_{\rm H}^0$ was first obtained from a linear continuation of the low--temperature splitting. The stem concentration was used with Eq. 3 to evaluate ΔH^0 and ΔS^0 . Then calculated stem concentrations were combined with the experimental splittings to yield now $A_{\rm H}^0$ values. The correct value of $A_{\rm H}^0$ represented the splitting which would be observed in the observe of stems. It is given by

$$A_{\rm H}^0 = (n_{\rm B} A_{\rm B}^0 + n_{\rm C} A_{\rm C}^0)/(n_{\rm B} + n_{\rm C}) \tag{5}$$

These were fitted to a linear equation in temperature using a leastsquares technique. Iteration gave the results in Table I. Calculated
and experimental splittings are shown in Fig. 1 for a 2.7 mole \$ ammenta solution.

It is seen from Table I that the value of ΔG^{\bullet} is reasonably independent of associate concentration as are ΔH^{\bullet} and ΔS^{\bullet} at the lawer concentrations. This provided support for the treatment used, especially in the light of the large variation of A_{μ} and a with associate concentration.

TABLE I. Loast-Squares Valmes from Analysis of Atom-Monomor Equilibria

Hole percent	(keal)	△s [●] (exl/degree)	△G [©] (25 [©] C) (keal)
1.2	8.3	-9.8	11.2
2.7	9.8	-5-5	11.4
5.8	9.1	-7.2	11.9
9.6	12.9	5.6	11.3
22.8	14.6	12.5	10.8
14.2	15.1	15.4	10.5

[&]quot;Standard states are one note per liter for both gaseous and solvated atoms.

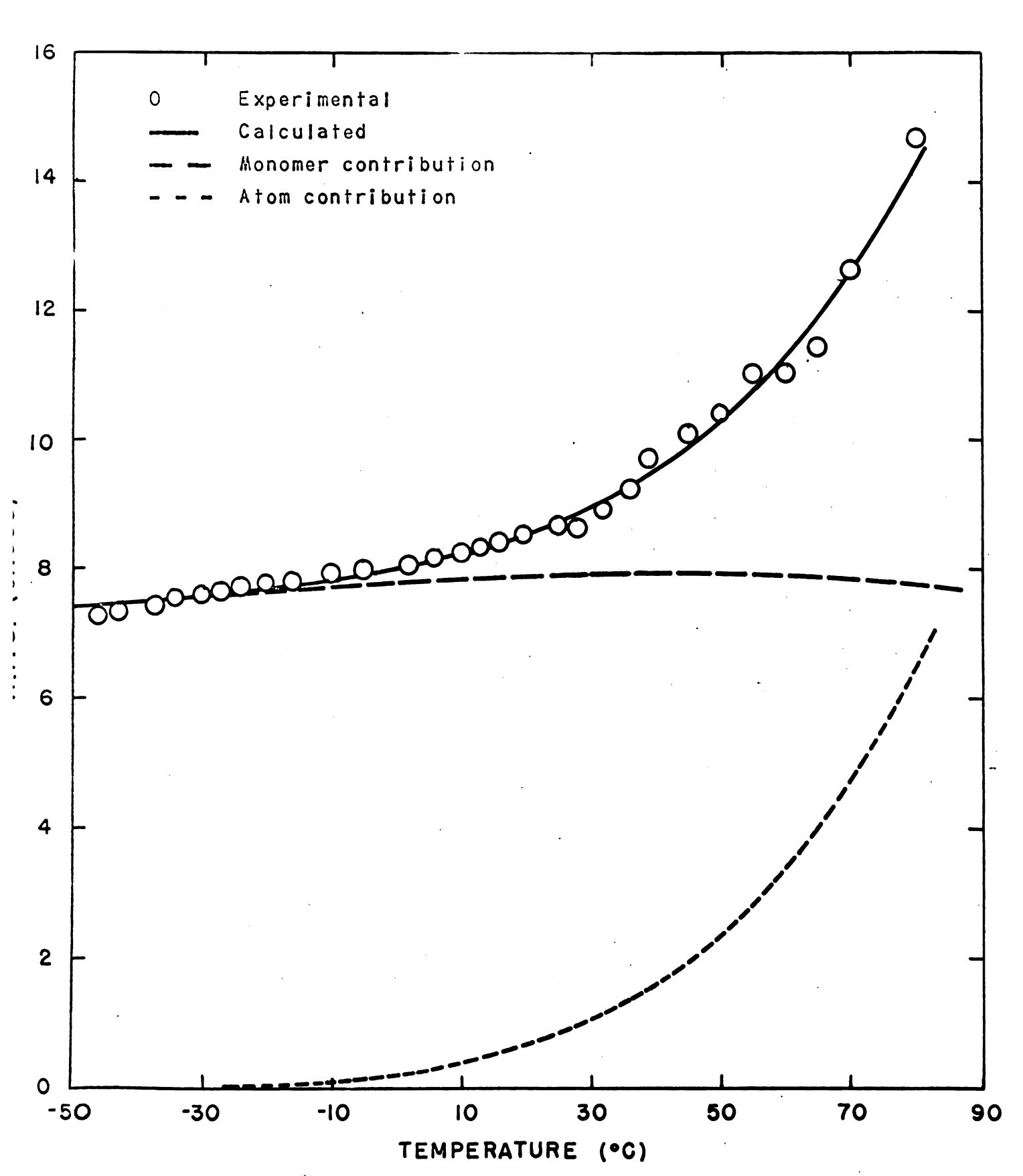


Figure 1. Separation of hyperfine splitting into atomic and monomeric contributions

The everage value of ΔG^0 , combined with the free energy of fernation of the gaseous atoms yields ΔG^0 m -5.2 keel nois⁻¹ for the solvation process

using standard states of 1 mole/liter for both the gas phase and the solution. Results for the three levest amonia concentrations yield $\Delta H^0 = -12.4$ kmal mole⁻¹ and $\Delta S^0 = -24.2$ cal mole⁻¹ deg⁻¹ for this process. Because of the limited studies at higher amonia concentration and possible unsaturation of the solutions, the values of ΔH^0 and ΔS^0 especially in the high amonia region, are subject to considerable uncertainty.

However, Dalton et al. (42) point out that even if the solutions were unsaturated above room temperature, the atom-moment model could be used to explain the variation of the hyperfine splitting with temperature. Using the equilibria given in Eq. 1, and the expressions for hyperfine splitting one obtains

$$K_{a}\left\{1+K_{1}^{(0)}\left[1/(1-K)\right]\right\}=(A_{A}^{0}-A_{Y})/(A_{Y}-A_{Y}^{0}),$$
 (7) which is valid whether or not the solutions are saturated. Because of its sensitivity to the small value of $(A_{Y}-A_{Y}^{0})$ at less temperatures, this equation was used only to evaluate K_{a} by extrapolation to $X=0$. Use was made in this extrapolation of the $X_{1}^{(0)}$ values obtained as described below.

Variation of K_a with temperature gave $\Delta H_a^0 = -6.6$ heal male⁻¹. $\Delta S_a^0 = -14.7$ cal \log^{-1} male⁻¹ and $\Delta G_a^0 = -2.2$ heal male⁻¹ at 25°C. These values agree with those obtained from the previous experiment.

While inclusion of atoms in the equilibrium model successfully accounts for the high-temperature behavior of the hfs including the

The average value of ΔG^0 , combined with the free energy of fernation of the gaseous atoms yields ΔG^0 m -5.2 hoal male⁻¹ for the solvation process

$$K(gas) \rightleftharpoons K(solution)$$
 (6)

using standard states of 1 mole/liter for both the gas phase and the solution. Results for the three levest summin concentrations yield $\Delta H^0 \approx -12.4$ kmal mole⁻¹ and $\Delta S^0 \approx -24.2$ cel mole⁻¹ deg⁻¹ for this process. Because of the limited studies at higher summin concentration and possible unsaturation of the solutions, the values of ΔH^0 and ΔS^0 especially in the high summin region, are subject to considerable unsaturation.

However, Dalton ot als (42) point out that even if the solutions were unsaturated above room temperature, the atom-moment model could be used to explain the variation of the hyperfine splitting with temperature. Using the equilibria given in Eq. 1, and the expressions for hyperfine splitting one obtains

$$K_{a}\left\{1+K_{1}^{(a)}\left[1/(1-K)\right]\right\} = (A_{A}^{0}-A_{y})/(A_{y}-A_{y}^{0}),$$
 (7) which is valid whether or not the solutions are saturated. Because of its sensitivity to the small value of $(A_{y}+A_{y}^{0})$ at low temperatures, this equation was used only to evaluate K_{a} by extrapolation to $I=0$. Use was made in this extrapolation of the $K_{1}^{(a)}$ values obtained as described below.

Variation of K_a with temperature gave $\Delta H_a^0 = -6.6$ has $mole^{-1}$. $\Delta S_a^0 = -14.7$ cal dog^{-1} mole⁻¹ and $\Delta G_a^0 = -2.2$ has mole⁻¹ at 25°C. These values agree with those obtained from the previous experiment.

While inclusion of atoms in the equilibrium model successfully accounts for the high-temperature behavior of the his including the

sharp break just above room temperature, the residual variation with summis concentration requires further consideration. Dalton et al., point out that this suggests an equilibrium involving substitution of summis for ethylamine in the vicinity of the metal sucleus. Such a substitution might involve simple replacement of ethylamine by ammonia in the first co-ordination sphere of a monomer unit, or else a significant alteration of the monomer structure by ammonia. The possible substitution reactions are represented by

$$K_{1}^{(o)}$$
 $K_{1}^{(o)}$
 $K_{1}^{(o)}$
 $K_{2}^{(o)}$
 K_{2

M(EtHH₂)_{x=1}(HH₃) + HH₃ M(EtHH₂)_{x=2}(HH₃)₂ + EtHH₂, etc.

Since saturated solutions are involved, the following solubility equilibries are also involved:

$$M(o) + xEthH_{2} \xrightarrow{K_{0}^{(s)}} M(EthH_{2})_{x},$$

$$M(o) + (x-1)EthH_{2} + NH_{3} \xrightarrow{K_{1}^{(s)}} M(EthH_{2})_{x-1}NH_{3}, \text{ etc.}$$
Where, of course,

$$E_{1}^{(a)} = E_{0}^{(a)}E_{1}^{(c)},$$
 $E_{2}^{(a)} = E_{1}^{(a)}E_{2}^{(c)} = E_{0}^{(a)}E_{1}^{(a)}E_{2}^{(c)}, \text{ etc.}$

To determine the extent of summis substitution at a given temperature one can independently expuise the variation of spin concentration and of his with summis concentration. Consideration of the equilibria (assuming mole fractions equal to activities for summis and ethylamine) yields

for small mole fractions of sumenia and

$$\mathbf{z} - \mathbf{z}_{A} = \mathbf{f}_{\Phi}^{(\bullet)} (1 - \mathbf{x})^{X} \left[1 + \frac{\mathbf{f}_{A}^{(\bullet)} \mathbf{x}}{(1 - \mathbf{x})} + \frac{\mathbf{f}_{A}^{(\bullet)} \mathbf{f}_{2}^{(\bullet)} \mathbf{x}^{2}}{(1 - \mathbf{x})^{2}} + \cdots \right] + \frac{\mathbf{f}_{A}^{(\bullet)} \mathbf{f}_{2}^{(\bullet)} \cdot \cdots \cdot \mathbf{f}_{X}^{(\bullet)} \mathbf{x}^{X}}{(1 - \mathbf{x})^{X}} \right]$$

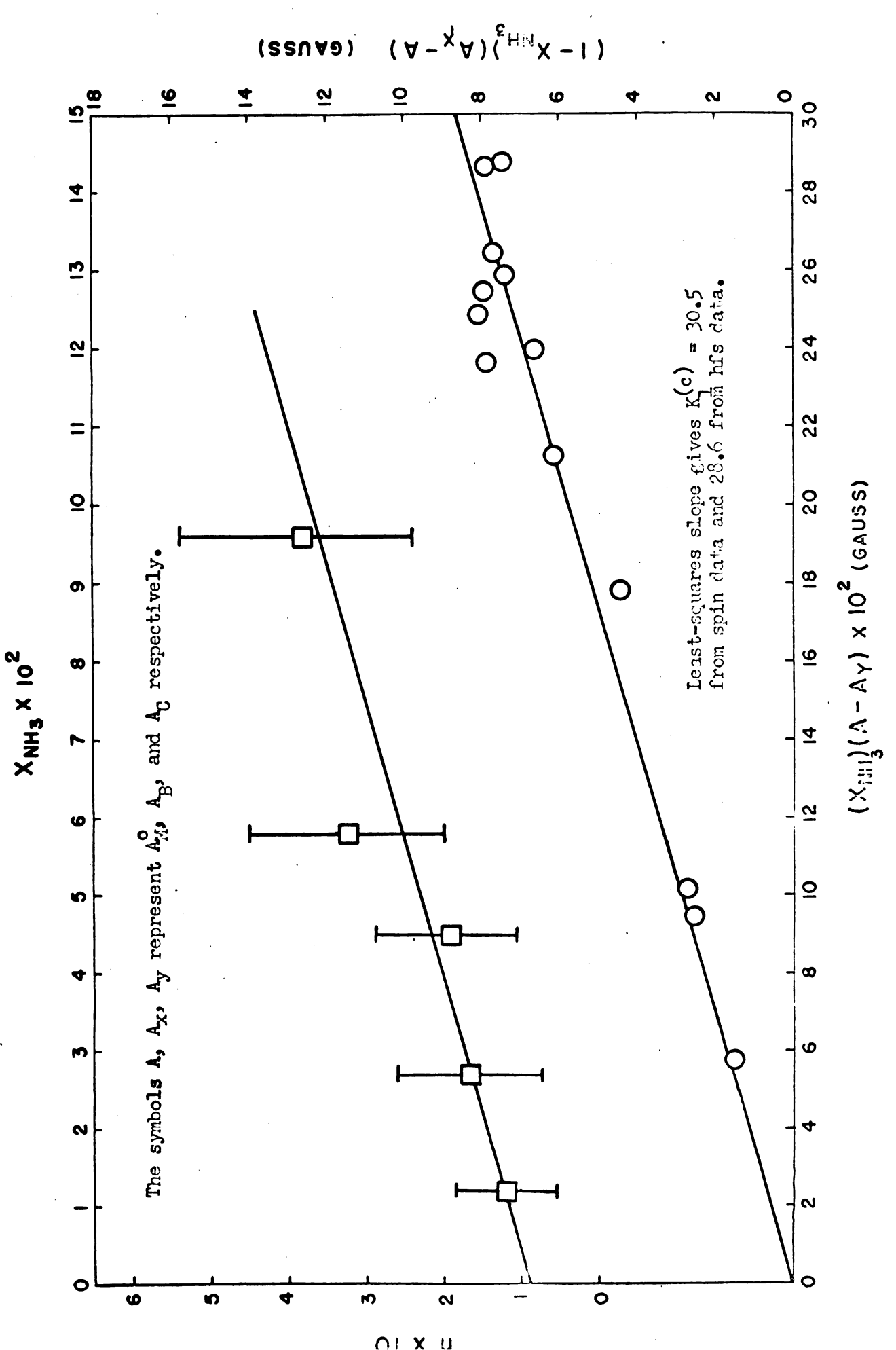
for larger nole fractions of summia. Within experimental error, graphs of $[n-n_A]$ versus $\mathbf{I}_{\mathrm{HH}_3}$ at various temperatures are linear up to about 10 nole \$ summia (top line, Fig. 2), showing that the addition of only one nolecule of summia is important ever this range. Values of $\mathbf{E}_{a}^{(s)}$ and $\mathbf{E}_{a}^{(s)}$ obtained from spin necomments are given in Table II.

An independent shock on $K_{\lambda}^{(a)}$ can be used using the hfs data and the assumption that species B and C have different splittings which are independent of temperature. The residual splitting $k_{\rm H}^{a}$ obtained by climinating the contribution from atoms is related to the concentrations and splittings of B and C by

$$A_{\rm H}^0 = (n_{\rm H} A_{\rm H} + n_{\rm C} A_{\rm C})/(n_{\rm H} + n_{\rm C}). \tag{11}$$

(It is to be noted that the contribution from atoms is negligible below about 10° C. Above this temperature, $A_{\rm H}^{\circ}$ must be calculated from the total splitting and procused atom concentration.)

From the equilibrium (1) with $\mathbf{x} = \mathbf{mole}$ fraction of summate, one obtains



Calculation of complexation constants from spin concentration data (squares) and independently from his data (circles). Figure 2.

TABLE II. Equilibrium Comstants for the Solvation and Complexation Equilibria as Calculated from Spin Concentration and Hfs Heasurements.

Tongo C	E(*) = 10 ⁷	K(+)	r(e)
	(from min on	nosstrations)	(from his values)
75 ⁴			18.9
40ª			22,4
25 ⁴	2.3	24.2	23.9
0	2.1	22.9	22.5
-25	1.7	27.7	27.7
مد_	1.5	30.5	28.6
-60	1.3	35.4	37.6

Above 25°C the effects of the stem-memorar equilibria were taken into account. Molar concentrations were used for potassium; mele fractions for amount and ethylamine.

$$E_1^{(o)} = (n_C/n_B)[(1-x)/x],$$

which yields

$$\mathbf{x}_{3}^{(o)} = [(\mathbf{A}_{3} - \mathbf{A}_{M}^{0})/(\mathbf{A}_{M}^{0} - \mathbf{A}_{C})][(\mathbf{1} - \mathbf{x})/\mathbf{x}].$$
 (12)

Extrapolation of $A_{\rm H}^0$ versus I to I = 0 gives an intercept of $A_{\rm B}^0$, while extrapolation of $A_{\rm H}^0$ versus (1-X)/X to I = 1 gives an intercept of $A_{\rm C}^0$. Using those values, $K_{\rm I}^{(0)}$ was calculated by a least-equares fit of Eq. 12 as shown in Fig. 2. The results are given in Table II. Since little deviation of $A_{\rm B}^0$ and $A_{\rm C}^0$ with temperature was noted, constant values were used. In addition, $K_{\rm I}^{(0)}$ is nearly independent of temperature. The agreement of $K_{\rm I}^{(0)}$ obtained from hyperfine splittings and from the completely independent spin concentration measurements is gratifying.

In summary, the equilibrium model not only describes such qualitative features as the unusual dependence upon temperature and summais concentration, but also is in quantitative agreement with the experimental results. Although three species were required to fit the data, the nature of the effects observed makes it very difficult to describe them with a simpler model.

It is possible to describe the variation of his with ements concentration at a single temperature using Eq. 19 of Bar-Eli and Tuttle (20):

$$= \frac{x_1 \exp(\Delta E/M) + x_2}{x_2}$$

and a suitable value of E. For example, at -40° C, using $a_1 = 12.0$ G, $a_2 = 0$, and E = -1.48 koal mole. An excellent fit of the Ms data

is obtained. Using the same value of $\triangle E$ at 25°C, however, gives a very poor fit even when the values of a_1 and a_2 are adjusted.

The large change of his upon substitution of a single amount nelecule for ethylamine is rather surprising. However, within the framework of the equilibrium model, one is ferred to the conclusion that only one amount nelecule is involved. In view of this, the substitution of amount for ethylamine must result in considerable distortion of the electron distribution in the memore. This could result from the introduction of considerable p character in the ground-state wavefunction, or, in the extreme case, by stabilisation of an ion pair between the estion and a solvated electron.

Catterell of al. (51.52) have employed an equilibrium fermalism very similar to that developed in this laboratory to describe hyperfine interactions in potassium-anime solutions. The major contributor to the observed hyperfine splitting is considered to be the solvated atom.

C. Paramagnetic Relaxation in Notal-Amine Solutions

One of the most pussling features of the EPR spectra of motel-duine solutions is the dependence of the linewidth upon hyperfine
component (see Fig. 3) observed for solutions of rebidium and commuin methylamine and for solutions of potassium, rubidium, and comium
in othylamine and propylamine (59). The usual explanation for such
behavior is in terms of a strong amisotropy of the electric field at
the splitting muclous, modulated by tunbling of the paramegnetic
species. This "McConnell mechanism" (54) requires the linewidths to
be dependent upon both viscosity and frequency and has successfully

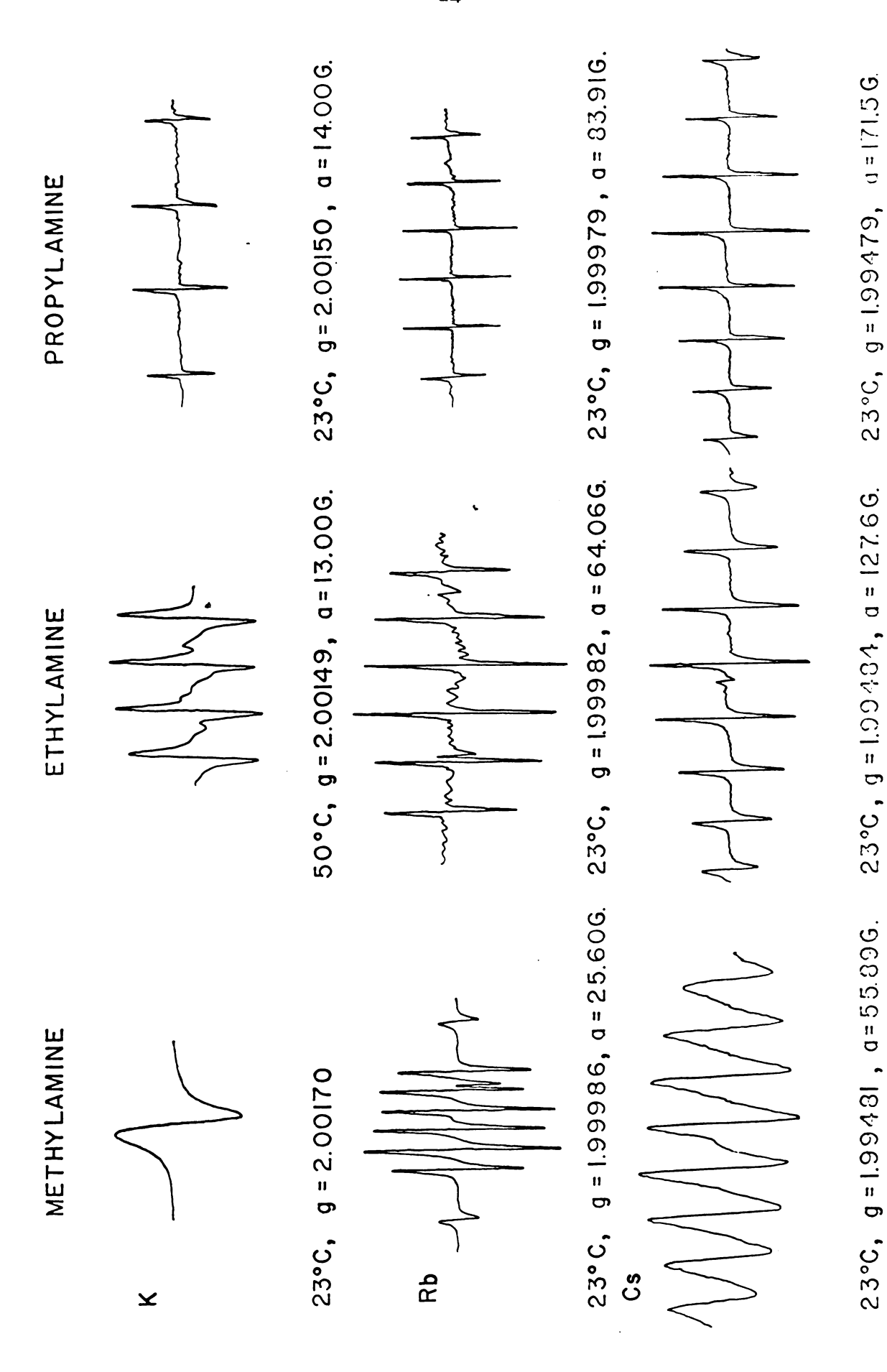


Figure 3. EPR spectra of alkali metals in some amines; data given for 39K, 85Rb, and 131cs.

explained the EPR spectra of several first and second row transition metal ions and complexes (54,55,56,57,58,59). In all these cases, a merted asymmetry of the field can legisally arise from the geometry of the ion in the presence of its ligands.

Severel refinements of the original treatment of McConnell have been made (56,60). Recently, Wilson and Rivelson (57) have medicated the treatment for the case of large hyperfine interactions by including second-order effects and have given expressions for the dependence of linewidth upon m, through third-order.

It is difficult to retievalise interactions between alkali metal ions and amine solvent molecules which are strong enough to result in a marked asymmetry of the electric field. However, the introduction of such a field anisotropy is required to explain the experimental linewidths by the McConnell mechanism.

Dalton et al. (42) have proposed an alternate mechanism which could also result in a dependence of linewidth upon m_{χ} . This mechanism involves the repid interconversion of the measures species, A and B, having different hyperfine contact densities. For exchange slaver than the embange-narrowed limit, this loads to an expression for linewidths (42)

 $T_2^{-1} = p_A/T_{2A} + p_B/T_{2B} + p_A^2 p_B^2 (a_A - a_B)^2 (\tau_A + \tau_B) n_A^2$ (13) in which a_A and a_B are the time-independent hyperfine splitting frequencies of the two species undergoing exchange, p_A and p_B are the respective fractions of these species, T_{2A} and T_{2B} are the relaxation times of A and B in the absence of exchange, and τ_A and τ_B are the note lifetimes of the two species. Although Eq. 13 shows dependence

only upon m_1^2 , the high-field approximation was used, and it was assumed that A and B have the same g-values.

Dye and Dalton (53) have recently modified the exchange mechanism to include the case of intermediate splittings (15 to 150 gauss) and the case for which $\mathbf{g}_{A} \neq \mathbf{g}_{B}$. Using third order corrections obtained from perturbation theory they wrote for the frequency of the transition involving hyperfine component \mathbf{m}_{I} in species A in the absence of exchange,

$$\omega_{\Lambda}^{\bullet}(\mathbf{n}_{\mathbf{I}}) = \omega_{\Lambda}^{\bullet} - \mathbf{a}_{\Lambda}\mathbf{n}_{\mathbf{I}} - \mathbf{a}_{\Lambda}^{2}[\mathbf{I}(\mathbf{I}+\mathbf{I}) - \mathbf{n}_{\mathbf{I}}^{2}]/2 \omega_{\Lambda}^{\bullet}(\mathbf{n}_{\mathbf{I}}) + \mathbf{a}_{\Lambda}^{3}/4 \omega_{\Lambda}^{\bullet}(\mathbf{n}_{\mathbf{I}})^{2}$$
 (14) in which $\omega_{\Lambda}^{\bullet}(\mathbf{n}_{\mathbf{I}})$ is the transition frequency of a particular line, ω_{Λ} is the transition frequency in the absence of hyperfine interestion, and \mathbf{a}_{Λ} is the hyperfine splitting frequency. A similar expression decembes the transition frequencies of species B.

If A and B are repidly interconverted, the inverse relaxation time of the exchange-marrowed line may be approximated by

$$[T_{2}(\mathbf{m}_{1})]^{-1} = p_{A}/T_{2A} + p_{B}/T_{2B} + p_{A}^{2}p_{B}^{2}(\gamma_{A} + \gamma_{B})[\omega_{A}^{\bullet}(\mathbf{m}_{1}) - \omega_{B}^{\bullet}(\mathbf{m}_{1})]^{2}$$
(15)

Eq. 15 assumes exchange narrowing to a single Lorentzian line for each hyperfine component. Substitution of the frequencies given by Eq. 14 into Eq. 15 leads to an expression of the form

$$[T_{2}(\mathbf{m}_{1})]^{-1} = p_{A}/T_{2A} + p_{B}/T_{2B} + p_{A}^{2}p_{B}^{2}v_{A}v_{B}[\alpha + \beta \mathbf{m}_{1} + \gamma \mathbf{m}_{1}^{2} + \delta \mathbf{m}_{1}^{3} + \xi \mathbf{m}_{1}^{4}]$$
(16)

Expressions for the coefficients of verious powers of $\mathbf{n}_{\underline{I}}$ are given in Table III.

Instead of describing the variation of magnetic parameters with temperature in terms of two or more interconverting species,

TABLE III. Coefficients of m, in the Linewidth Expression using the

$$T_{2}(n_{1})^{-\frac{1}{2}} = \frac{P_{A}}{T_{2A}} + \frac{P_{B}}{T_{2B}} + p_{A}^{2}p_{B}^{2}(\gamma_{A} + \gamma_{B})[\alpha + \beta n_{1} + \gamma m_{1}^{2} + \delta n_{1}^{3} + \epsilon n_{1}^{4}]$$

$$\alpha = \{F_{1} + F_{3}I(I+1)\}^{2}$$

$$\beta = 2\{F_{1} + F_{3}I(I+1)\} \{(F_{2} + \frac{1}{4}F_{A} - I(I+1)F_{A})\}$$

$$\forall = [\{F_{2} + \frac{1}{2}F_{A} - I(I+1)F_{A}\}^{2} - 2F_{3}\{F_{1} + F_{3}I(I+1)\}]$$

$$\delta = [2F_{A}\{F_{1} + F_{3}I(I+1)\} - 2F_{3}\{F_{2} + \frac{1}{2}F_{A} - I(I+1)F_{A}\}]$$

$$\epsilon = [2F_{A}\{F_{2} + \frac{1}{2}F_{A} - I(I+1)F_{A} + F_{3}^{2}\}]$$
where
$$F_{2} = (\omega^{0} - \omega^{0})$$

$$T_1 = (\omega_A^0 - \omega_B^0)$$

$$F_2 = (a_A - a_B)$$

$$F_3 = \frac{a_A^2}{2\omega_A} - \frac{a_B^2}{2\omega_B}$$

$$F_4 = \frac{a_A^3}{2\omega_A^2} - \frac{a_B^3}{2\omega_B^2}$$

The above coefficients of Eq. 16 are obtained when Eq. 14 is Peplaced by the expension of the Breit-Rabi equation given by Fessenden and Schuler.84

$$\omega_{A}(\mathbf{x}_{1}) = \omega_{A}^{0} + a_{A}\mathbf{x}_{1} + \frac{a_{A}^{2}}{2\omega_{A}}[I(I+1) - \mathbf{x}_{1}^{2}] + \frac{a_{A}^{3}}{2\omega_{A}^{2}} \left\{ \mathbf{x}_{1}[\mathbf{x}_{1}^{2} + \frac{1}{2} - I(I+1)] \right\}$$

R. W. Fessenden and R. H. Schuler, J. Chem. Phys., 23, 2704 (1965).

Dye and Dalton (53) point out that one can consider stationary-state models in which the wavefunction for the unpaired electron is strengly dependent upon solvent configuration about the H unit. Two models based upon this assumption have been used to explain hyperfine interactions in metal-anime solutions (43,49).

These models require a distribution of electron environments in the solution with a broad range of hyperfine centest densities. Such a distribution is necessary since a change in temperature brings about a change in the observed hyperfine splitting. Prosumbly this distribution arises from variations in solvent structure about the monemer. If the correlation time associated with fluctuations of the selvent environment is long enough to contribute significantly to line--breadening, then the linewidths of the individual hyperfine components will be different, with broader lines resulting for the higher m, walnes. If a significent portion of the distribution of solvent structures arises from molecules enteride of the primary solvetion layer, one would expect abrupt changes in hyperfine splitting and linewidth at the freezing point. A questitative treatment of this model would reonire busiledge of the distribution of hyperfine splittings and gwelmes, and has not yet been carried out. It should be possible. using the observed variation of these two parameters with temperature and the assumption of a Conscien distribution, to describe the linewidth behavior with a temperature-dependent correlation time.

Dye and Dalton (53) have attempted to determine which of those mechanisms is operative for metal-anime solutions by intensively investigating the spectra of cosium in ethylamine. The analysis of the my-dependent relaxation observed in metal-anime solutions was carried

out by evaluating the coefficients of $1/T_2$ to various powers of n_1 . To eliminate the effect of intermolecular relexation processes (e.g. spin exchange and chanical exchange) only solutions estimated to be less than 5×10^{-3} molar in notel were used in this analysis. The experimentally observed coefficients for several cosium-othylamine solutions are shown in Fig. 4 as functions of temperature. Analysis of the results showed that only terms throught the third power in n_2 are significant. Of particular interest is the opposite temperature dependence exhibited by the coefficients of the linear and quadratic terms.

The predominent term is quadratic in n_{χ} . Since the sign of the coefficient of the cubic term is opposite to that of the first-power term, both of these coefficients are very sensitive to experimental error and show considerable scatter. The dependence upon n_{χ} is significant. Of particular interest is the opposite temperature dependence exhibited by the coefficients of the linear and quadratic terms.

The predominent term is quadratic in n_{χ} . Since the sign of the coefficient of the subic term is opposite to that of the first-power term, both of these coefficients are very sensitive to experimental error and show considerable conttor. The dependence upon n_{χ} through third order is real but the deviations from a symmetric pattern are so small that it is difficult to measure the coefficients of the first and third-order terms.

When considered in detail, none of the treatments described above was able to explain all aspects of the observed $n_{\chi^{-}}$ -dependent relevation.

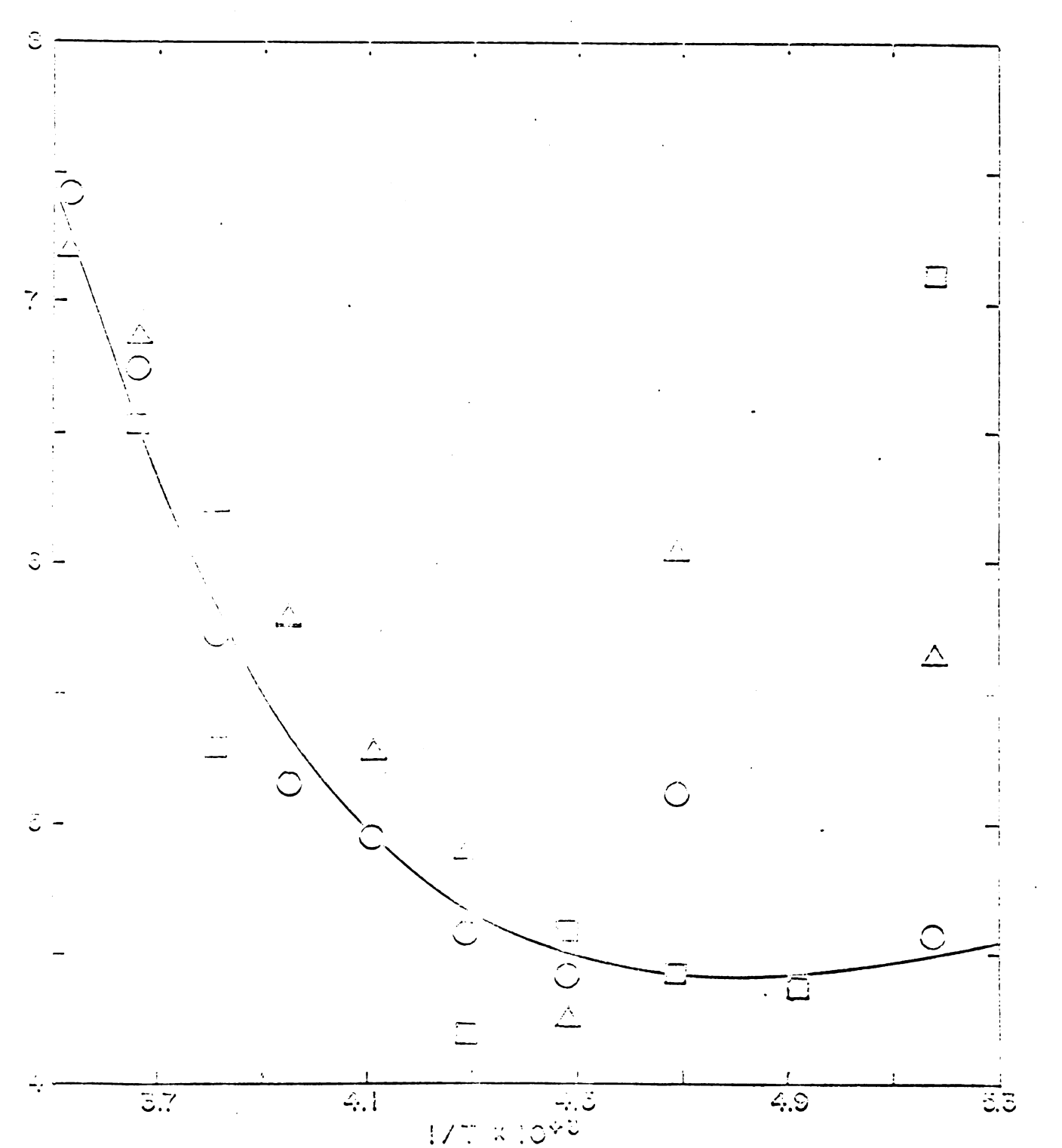


Figure 4a. Variation of the residual linewidth (Co) with 1/T: Cs in ethylamine. Results are shown for three different sample preparations.

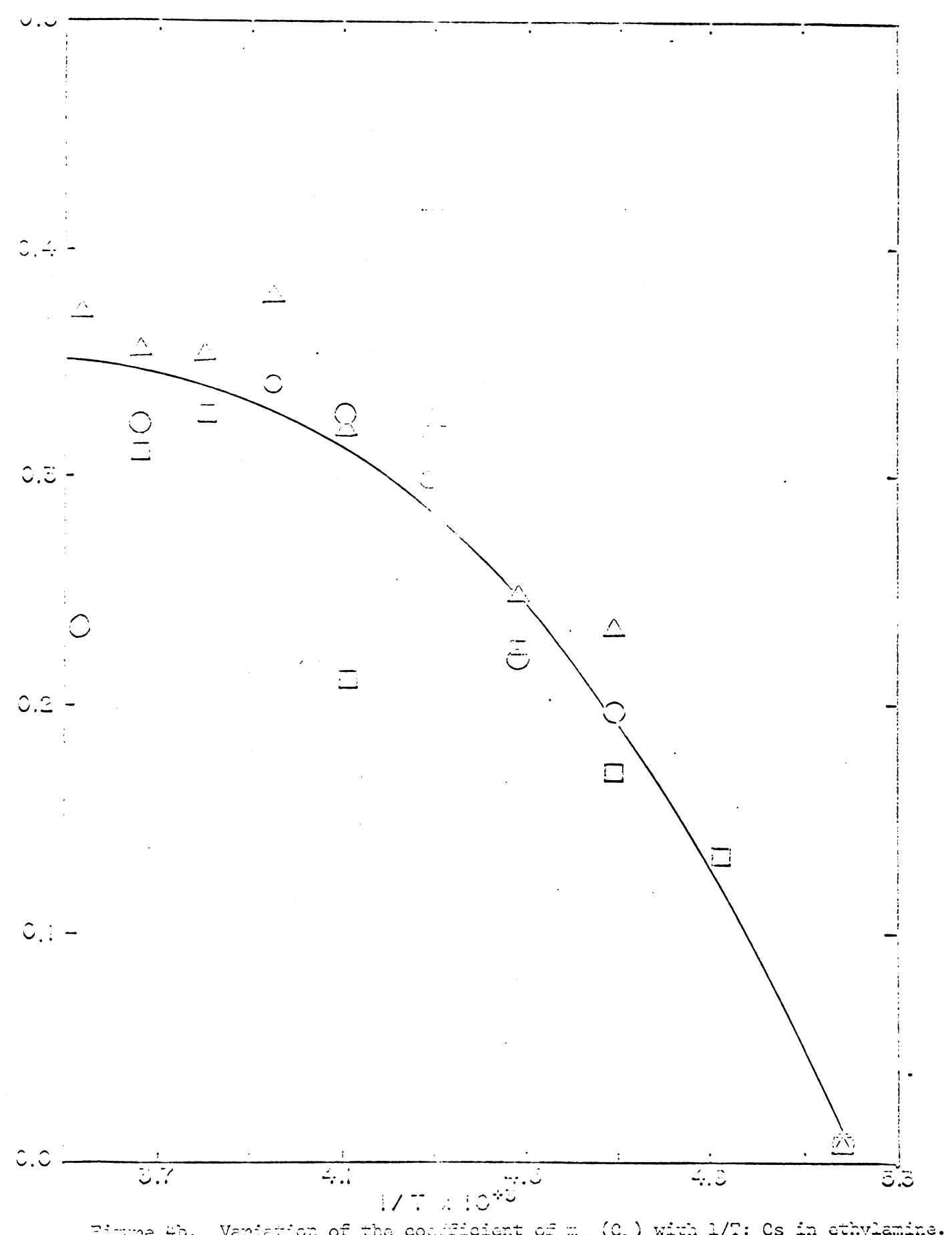


Figure 4b. Variation of the coefficient of $m_{\rm e}$ (C₁) with 1/T: Cs in ethylamine. Results are chosen for three different sample proparations.

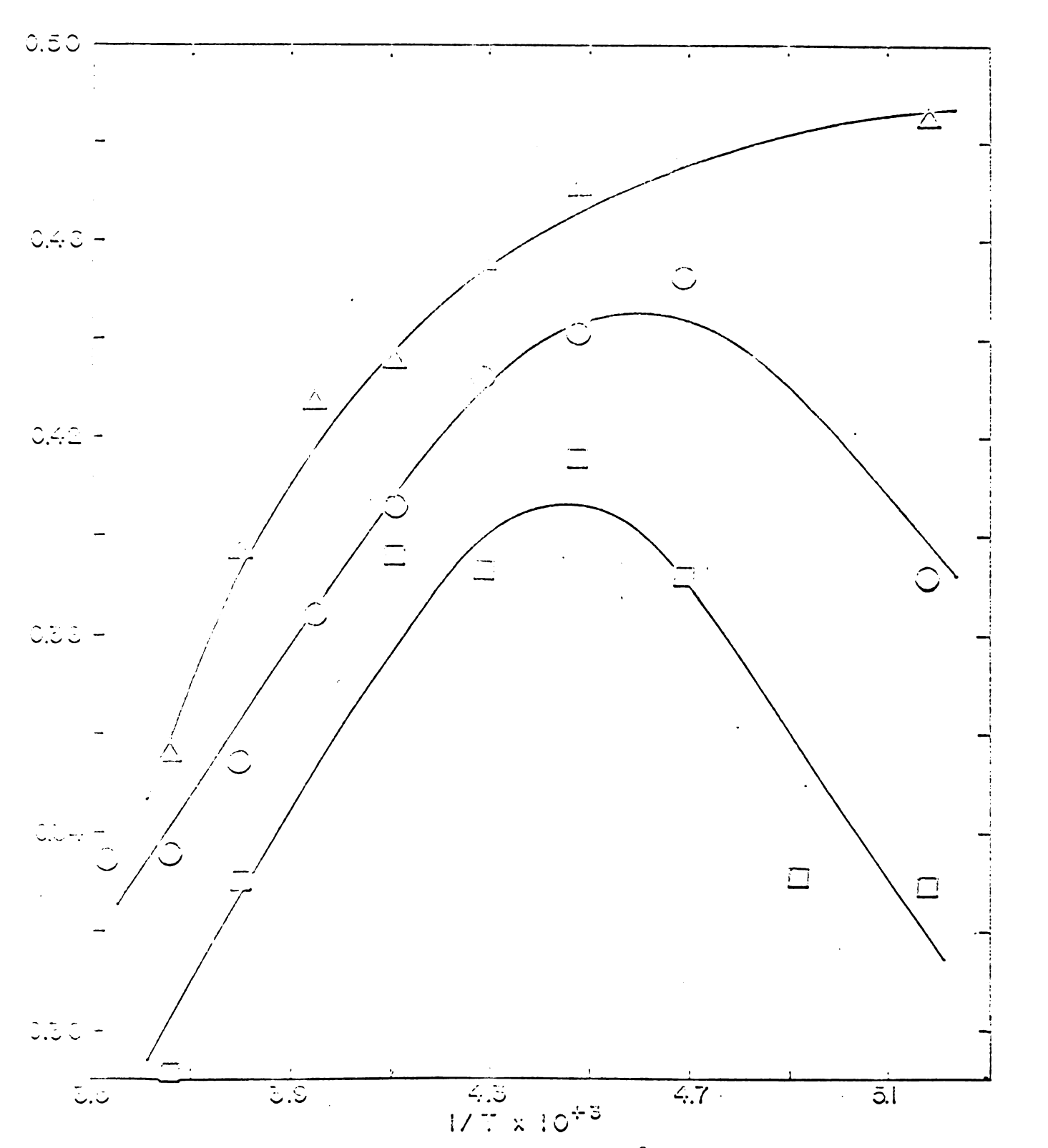


Figure 4c. Variation of the coefficient of ${\rm m_1}^2$ (C₂) with 1/T: Cs in ethylamine. Results are shown for three different sample preparations.

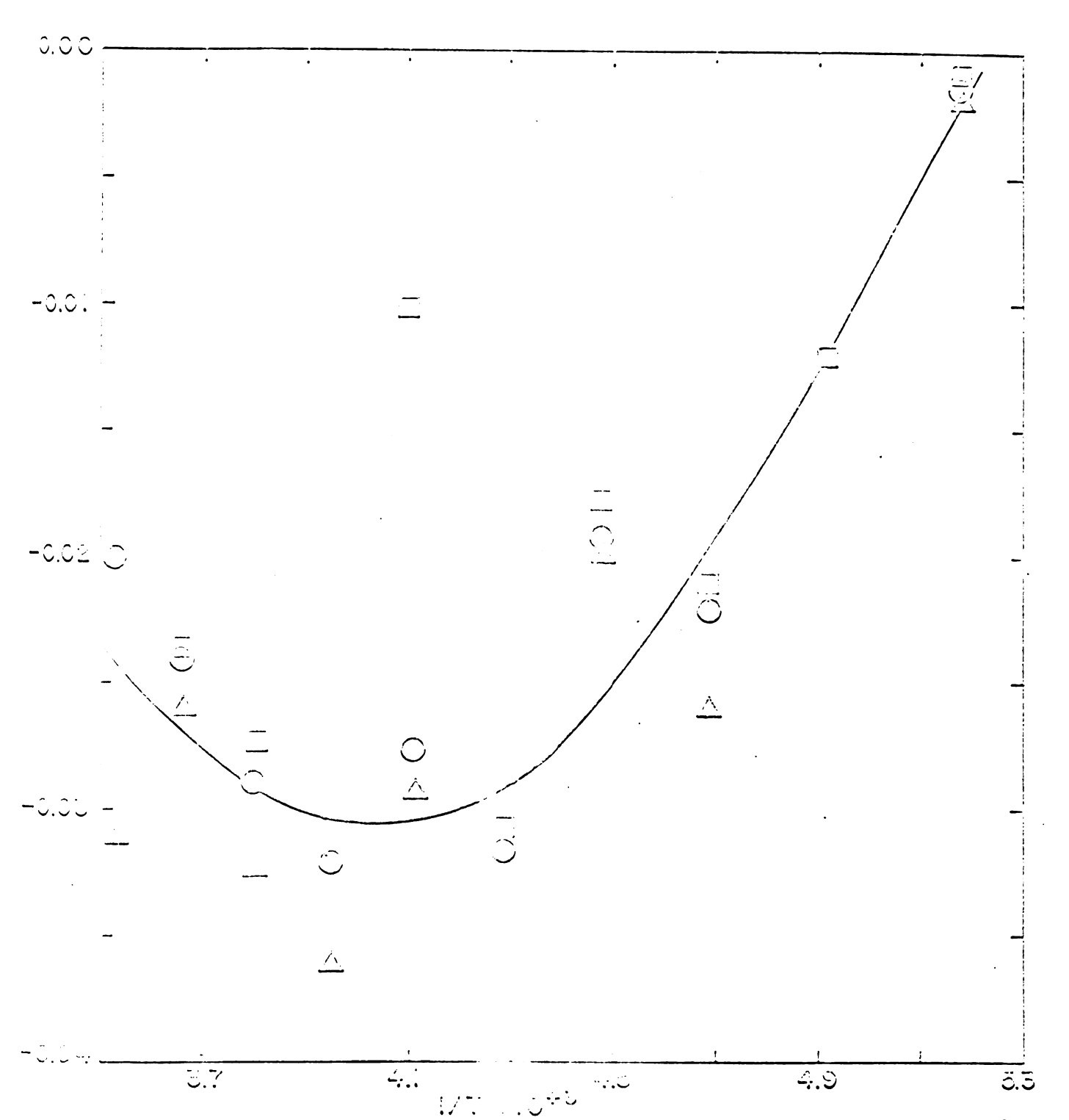


Figure 4d. Variation of the coefficient of $m_1^{-3}(C_3)$ with 1/T: Cs in ethylamine. Results are shown for three different sample preparations.

In addition to examining n₁-dependent relaxation mechanisms, Delten <u>et el</u>. (42) have considered the problem of accounting for the residual linewidth. There exist several mechanisms which must be considered as possible contributors to n₁-independent transverse relaxation in dilute metal-amine and metal-amine-amonds solutions. These are as follows: (a) spin-orbit coupling to solvent molecules and metal ions, (b) molecular hyperfine coupling, (c) anisotropy of the g factor, (d) molecular dipolar interestions, (e) medicar quadrupolar interestions, (f) exchange effects, and (g) effects of finetwating magnetic environment.

These suthers point out that the increase in linewidth with motal emcentration indicates the importance of interactions with other motal nuclei. This interaction may be in the form of hyperfine interaction, quadrupolar interactions, spin exchange, or not shouldn't reactions, with the correlation time of the respective presence determining the relative contributions to linewidths.

The qualitative nature of the spectra indicates that spin embane and chemical equilibria would be expected to be important in determining the observed linewidths. Unfortunately, the large number of species prohibits detailed enclysis of the spin-exchange processes. Even in amonia which shows only a single optical absorption, ions and loose aggregates such as N⁺; o"; N⁺·o",(N); o"·N⁺·o",(N⁻); and (N⁺·o")₂,(N₂) seem to be required to explain the properties of the solutions. In amonia-othylanine mixtures, the infrared absorption had an intensity much larger than could be accounted for by the extra EPR line. This indicates that electron-ion aggregation is even more prodominant in these systems than in amonia. The oppositions of the

visible and red optical absorptions requires two additional species and the nature of the hyperfine interaction appears to require three neutral monomeric species.

The earlier treatment of metal-suine selutions by Bar-Eli and Tuttle (43) was based upon a model restricted to four species. The existence of other species forces one to consider many other chanical and spin exchange processes. To assess the importance of a given precess requires estimation of the rate constants and ecocentrations invelved. The spin concentrations and optical spectra measured in this laboratory permit estimation of the contribution to linewidth of spin exchange processes involving H + H and H + o" and such reactions as H → H+ + e" and 2H → H2. Assuming diffusion-controlled, second--erder processes (which gives the maximum contribution to linewidth), it was concluded that none of these processes can centribute more than 0.1 G to the linewidth. Spin exchange with species as M' and M' would also be without effect at concentrations of these species below 10 %. but could contribute as much as 0.2 G to the linewidth at 10-3 M. The ebserved linewidth (0.5 to 2.5 G) of the hyperfine pattern for petassium in ethylamine-ammenia mixtures appears, therefore, to arise from other processes or reactions.

D. Paramagnetic Relaxation in Alkali Metals

In metals it is the spin-lattice relaxation time T₁ which determines the line width. Several mechanisms for spin-lattice relaxation have been proposed. Overhauser (61) has discussed several interactions of which the one giving rise to the shortest relaxation time is the interaction between the magnetic moment of one electron and the field caused by the translational motion of a second electron. Elliott (62) has discussed a process whoreby the small amount of orbital angular momentum associated with the spin state causes the spin to flip. He obtains the following expression for the spin-lattice relaxation time:

$$T_1 = \alpha r_R / (\Delta g)^2 \quad \alpha \quad 1 / [(\Delta g)^2 \rho]$$
Therefore.

AH
$$\alpha$$
 $(\Delta \epsilon)^2 \rho$

The experiments of Feber and Kip (65) provided the following information about spin-lattice relaxation times in matals:

- 1. Sodimewithe relaxation time is approximately proportional to conductivity from 4°K to 300°K .
- 2. Lithium...The relaxation time is independent of temperature between 40K and 3000K but is longer the more highly purified the samples.

The results in sodium appear to confirm the Elliott-Tafet mechanism of relaxation inasmuch as the linewidth follows the same law as does the resistivity. The data for lithium are a bit confusing since the highest purities obtained have yielded intrinsic relaxation times.

Extension of the measurements to higher temperatures would prewide a better check on the theory especially if the melting points of
the metals could be exceeded, since there the resistivities have discontinuities. Levy (66,67) has carried out measurements on all the
alkali metals to temperatures above their melting points. Resonance
was observed only in sodium and lithium as expected from theory, since
the spin-orbit interactions are too large in the other alkalis to preduce observably narrow lines.

EXPERIMENTAL

A. Glassware Cleaning and Reagent Purification

The cleaning of glassware and purification of reagents has been described previously (42,46,68,69,70). For a more detailed account of the techniques employed them given here the reader is referred to the above references.

- 1. Glassware cleaning. The items were first rinsed briefly with a hydrofluoric acid-detergent cleaning solution (% hydrofluoric acid, 3% concentrated reagent grade mitric acid, 2% acid-columble detergent, and 60% distilled water, by volume), then ten times or more with distilled water. Next, the glassware was filled with fresh aqua regia and heated to beiling, followed by ten more rinses and/or seahings in double-distilled conductance water. After each use and a pre-liminary cleaning, the glassware was heated in an amesling even at 550°C before being cleaned as described above.
- 2. Respent purification. The respents used in this work and their connercial sources are given in Tables IV and V.
- (a) Hotal purification. Sedim and petassium were classed, out, and then degreesed under high vacuum. Repeated vacuum distillations were used to obtain small metal samples in scaled amoules which were used to make up metal sciutions.

The rubidium and comium used in this work came in scaled anpeules. The ampeules were cooled in liquid air, broken, and immedi-

TABLE IV. Alkali Hotals and Solvents Employed and their Commercial Sources

Research Commercial Sources

Lithium Corporation of America

Sedium J. T. Baker

Potassium Mallinokrodt

Reference Chemical Company

Costum Day Chemical Company

Aumonda Matheson, Coleman, and Bell

Hethylamine (MeNH₂) Matheson, Coleman, and Bell

Ethylenine (EtHH₂) Bastman White Label

m-Propylemine (m-Preff.) Matheman, and Bell

ise-Propylamine (i-FrNH2) Matheses, Coleman, and Bell

m-Butylamine (m-BuRH₂) Mathemma Coleman, and Bell

3-Nothern-propylanine (3-PA) Eastman

Ethylemedicaine (EDA) Kathesen, Coleman, and Bell

1,2-Proposediamine (1,2-PDA) Matheon, Coloner, and Bell

1.3-Proponediamine (1.3-PDA) Matheson, Coleman, and Bell

Hexanothylphospheric trianide Eastmon

TABLE IV. Alkali Motals and Solvents Employed and their Commercial Sources

Researt	Commercial Sources			
LA thinns	Lithium Corporation of America			
Sodium	J. T. Baker			
Potassium	Mallinokrodt			
Rubidium	Fairmount Chamical Company			
Coatium	Dow Chemical Company			
Amont a	Matheson, Coleman, and Bell			
Hothylamine (MeNH ₂)	Matheson, Coleman, and Bell			
Ethylenine (EthH ₂)	Eastman White Label			
n-Propylemine (n-Prafig)	Metheson, Coleman, and Bell			
iso-Propylemine (i-PrNH ₂)	Mathesen, Coleman, and Boll			
m-Butylanine (m-BuNH2)	Matheaum, Coloman, and Bell			
3-Metheny-n-propylanine (3-PPA)	Bastnen			
Sthylemedicaine (EDA)	Kathesen, Coleman, and Bell			
1,2-Prepanediamine (1,2-PDA)	Matheann, Coleman, and Bell			
1.3-Prepanediamine (1.3-PDA)	Matheson, Coleman, and Bell			

Eastman

Hexamethylphospheric triamide

TABLE V. Reference standards used for determination of spin concentrations.

Reference			(K)	
Standard	Source	g value	Lorentzian	Gaussian
P doped Si in polyethylene	E. A. Gere, Bell Telephone Laboratories	1.99875 <u>+</u> 0.00010	1.0	0.29
Pitch in KCL (powder)	Varian Associat es Palo Alto, California	2.00280 <u>+</u> 0.00005	0.66	0.19
DPPH in benzene	Eastman Organic Chemicals	2.00354 ± 0.00003	1.6	0.47
DPPH in chloroform	Eastman Organic Chemicals		1.6	0.5
DPPH (powder)	Eastman Organic Chemicals	2.0036 ± 0.0002	1.0	0.29
NO(SO ₃) ₂ = (titrated aqueous NaCO ₃ solution, pH = 10)	Alfa Inorganics, Inc.	2.00550 <u>+</u> 0.00005	1.0	0.29
CuSO ₄ .5H ₂ O (crystal)	Matheson Coleman and Bell (recrystallized from H ₂ 0)		1.0	0.29
K ₃ [Cr(CN) ₅ NO] (aqueous)	H. Kuska, Michigan State Universi	1.99454 <u>+</u> 0.00005 ty	3.5	1.0
VOSO ₄ (aqueous)	Fisher Scientific Company	1.962 <u>+</u> 0.002	1.0	0.29
Mn++ in MgO	Baker and Adamson	2.00774 ± 0.00050	3.5	1.0

immediately transferred to the metal make-up vessel. It was necessary
to cool the samples to avoid excessive exidation of the metal during
transfer. The metal make-up then preceded as described for sedium and
potassium.

The lithium used in the initial phase of this project was cleaned mechanically in a Caemon Hodel 39 dry-box filled with high purity helium (99.7%) which had been passed through an activated silies gol column at liquid mitrogen temperature.

(b) Solvent purification. The solvents used were purified by one of two methods. The first method involved reaction with alkali metals or appropriate drying agents (e.g. a mixture of petassium hydroxide and barium exide), followed by freezing and pumping, several distillations in vacuo, and further reaction with alkali metals. This precedure was followed by a distillation in a mitrogen streen similar to the method described by Describ (71); a final distillation was made in vacuo into a storage flack containing a film of petassium metal. Before use in sample preparation the solvent was then frozen and degassed. Nothylamine, ethylamine, propplanine, iso-propplanine, m-butylamine, tebutylamine, and 3-methoxy-m-propplanine were purified by this method.

A second method involved placing the solvent in a large separatery funnel, slowly freezing it and then melting and discarding the core (69,70). Pre-purified mitrogen was used as a severing gas throughout this precedure. The freeze-melt precedure was repeated at least five times. Following freeze purification the solvent was further purified by the procedure of method 1. Ethylenediculus, 1,2-prepanediculus, and hexamethylphospheric triamide were purified by this method.

- (c) Hitrogen purification. As has been previously mentioned, mitrogen was used in distillations and as a covering gas. It was purified by passing it ever copper turnings in a tube furnace, through an Ascarite column, a dry-ice trap, and finally a silice gel column at 77°K in which some condensation occurred. This nitrogen was then stored in two-liter bulbs on the vacuum line.
- (d) Purification of EPR reference samples. VOSO_h and CuSO_h •5H₂O were purified by recrystallisation from water. Baker NgCl₂ •6H₂O was first souvenged with Mg metal and then precipitated with emmonium hydrixide. The precipitate was washed with distilled water and dried in a controlled-temperature furnace. The other references standards were used without further purification.

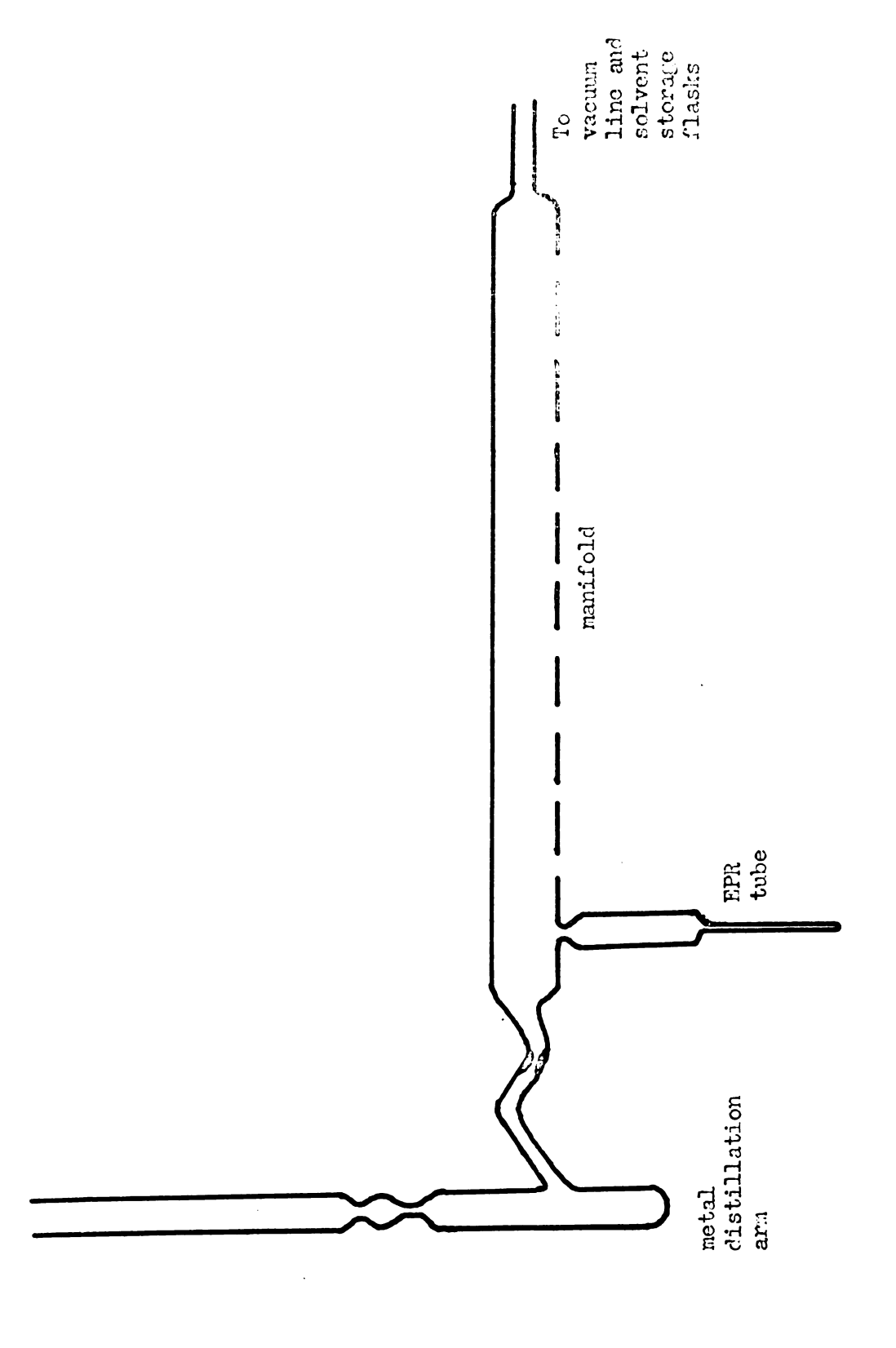
B. Solution Preparation

As one be seen from Table IV a wide range of metal-anime and mixed solvent solutions were studied. Moreover, it was desired to investigate these solutions under a variety of experimental conditions. These factors necessitated the construction and employment of a number of unique solution preparation vessels. These vessels will be discussed in relation to their use.

Prior to actual sample preparation, the following technique was employed to maximise sample stability. After evacuation and flaming, the sample tube was allowed to fill several times with the vapor of the anime under consideration. The anime vapor was then removed to a liquid-mitrogen-cooled trap and the sample tube was evacuated to 10⁻⁵ torr or better.

1. Preparation of metal-amine solutions for EFR measurement. Solutions of sodium, potassium, rubidium, and cesium in the smines listed in Table IV and in mixtures of those amines were prepared using the apparatus shown in Fig. 5. This apparatus was attached to a high yearns system to which the appropriate solvent storage flasks had previcusly been attached. The sealed ampoule containing the alkali metal was frozen with liquid air, broken, and dropped into the distillation arm attached to the manifold shown in Fig. 5. The distillation arm was then capped and the solution preparation apparatus evacuated to at least 5 x 10-6 terr. The metal was subsequently distilled into the EFR sample tubes. After a film of metal had been obtained on the walls of each of the sample tubes, the appropriate suine was distilled into the tube, the solution fresen with liquid nitregun and degessed, and the sample tube scaled off. In order that spin concontration measurements could be extrapolated to samples of infinitesimal sine, the dismeter of the lawer section of the EPR tubes was varied from tube to tube as shown in Fig. 5.

When lithium solutions were desired, the apparatus sheen in Fig. 6 was placed in the dry-box along with a stick of Apienen W wax, a heating only, a imife, and some lithium bars. The dry-box was first evacuated and them filled with high purity belium. The lithium metal was classed mechanically, placed in the selution preparation apparatus, and the apparatus was capped using the W wax and the heating cell. Once sealed the apparatus was removed from the dry-box and attached to the vacuum line containing the storage flasks of the appropriate amine selvents. The solution preparation apparatus was them evacuated and an appropriate amount of solvent was subsequently distilled over the



Vessel used to prepare solutions of sodium, potassium, rubidium, and cesium in amine solvents for EPR measurement. Figure 5.

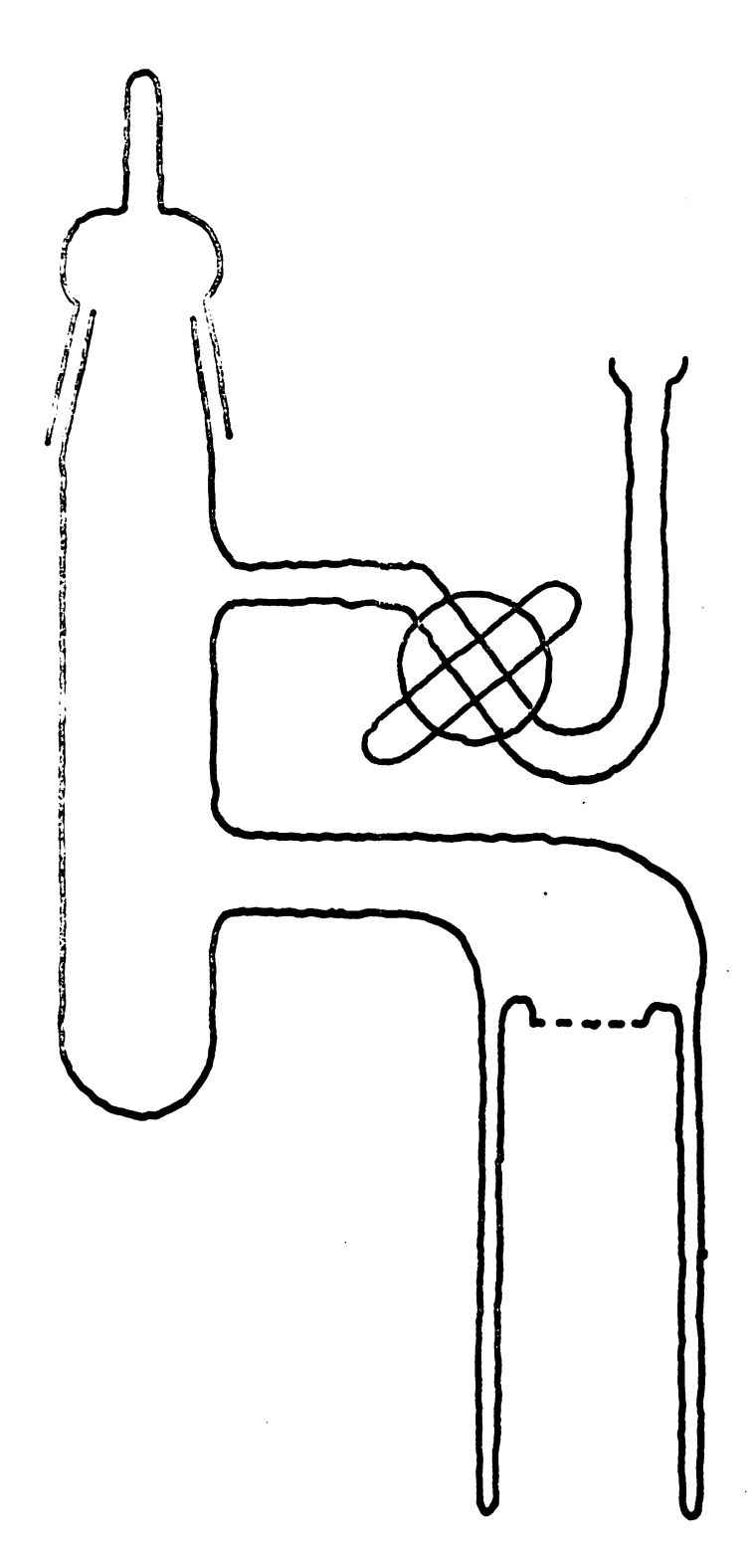


Figure 6. Vessel used to prepare lithium-amine solutions for EPR studies.

lithium. The apparatus was then discommented from the wacum line, the metal-amine solution tipped into the EPR tubes, and the tubes scaled off.

2. Preparation of metal-mixed solvent solutions for EFR measurement. The preparation of potassium-ethylamine-amounts mixtures (42) and continue-thylamine-amounts mixtures (41,42) has been described previously. To measure amounts in small amounts, the volume of the menifold available to vapor was first determined. The amounts reserved; was degreed and held at constant temperature to establish a known pressure of amounts vapor in the menifold. This was then condensed into the sample tube using liquid mitrogen. For higher concentrations of amounts, both liquid volumes were measured directly by determining the liquid height immediately after removal from a dry-doe bath. Hele freetiens were eal-outsted assuming no volume change upon mixing.

After measurements had been completed, the amounts centent was determined using an acrograph Model 90-23 gas chromatograph. Analysis was accomplished by freezing the sample tube in liquid mitrogen, breaking it, and dropping it into a vessel which was quickly scaled off from the atmosphere. The sample was allowed to vaporise and fill the volumetric vessel; the meedle of a volumetric syringe was inserted through an elastic membrane and a sample was removed. The chromatographic column was packed with 155 THEED and 55 tetracthylesspentamine on 60/80 Chromatography (72). The concentration of amounts in those samples was determined by comparing the ratio of the peak areas of amounts and ethylamine in the sample with the ratio of the areas of a number of standards.

Similar methods of preparation and analysis were used for other mixed solvent solutions.

- 3. Preparation of metal-amine and mixed solvent solutions for correlated EPR-optical measurements. When both EPR and optical spectra were desired using the same samples, Aminos cylindrical absorption cells were scaled above the 10-am tubing of the solution make-up apparatus shown in Fig. 5 and the scal-off from the manifold was made on a side tube attached below the absorption cell. In this way the solution could be alternately tipped into the absorption cell and into the EPR sample tube. For absorption spectra, path lengths of 0.1, 0.3, 0.7, and 1.0 mm were used, depending on the expected concentration of the saturated solution.
- 4. Preparation of sedium-ethylenedizatine solutions for correlated EFR-conductance measurements. When conductance measurements were desired in addition to EFR measurements, a series of platinum electrodes was attached to an EFR cell. Dilute solutions of sedium in ethylenedizatine were prepared in an intermediate vessel and forced into the EFR-conductance cell with gaseous nitrogen. The total metal concentration was determined by decomposing a sample of each preparation and measuring the hydrogen liberated by the reaction

5. Proparation of metal-anime solutions for spin concentration measurements. Although this matter will be discussed in greater detail later it is well at this point in the dissertation to describe one of the vessels used. Fig. 7 shows a solution make-up vessel which allowed the EPR reference sample to be placed inside of the metal-anime solution.

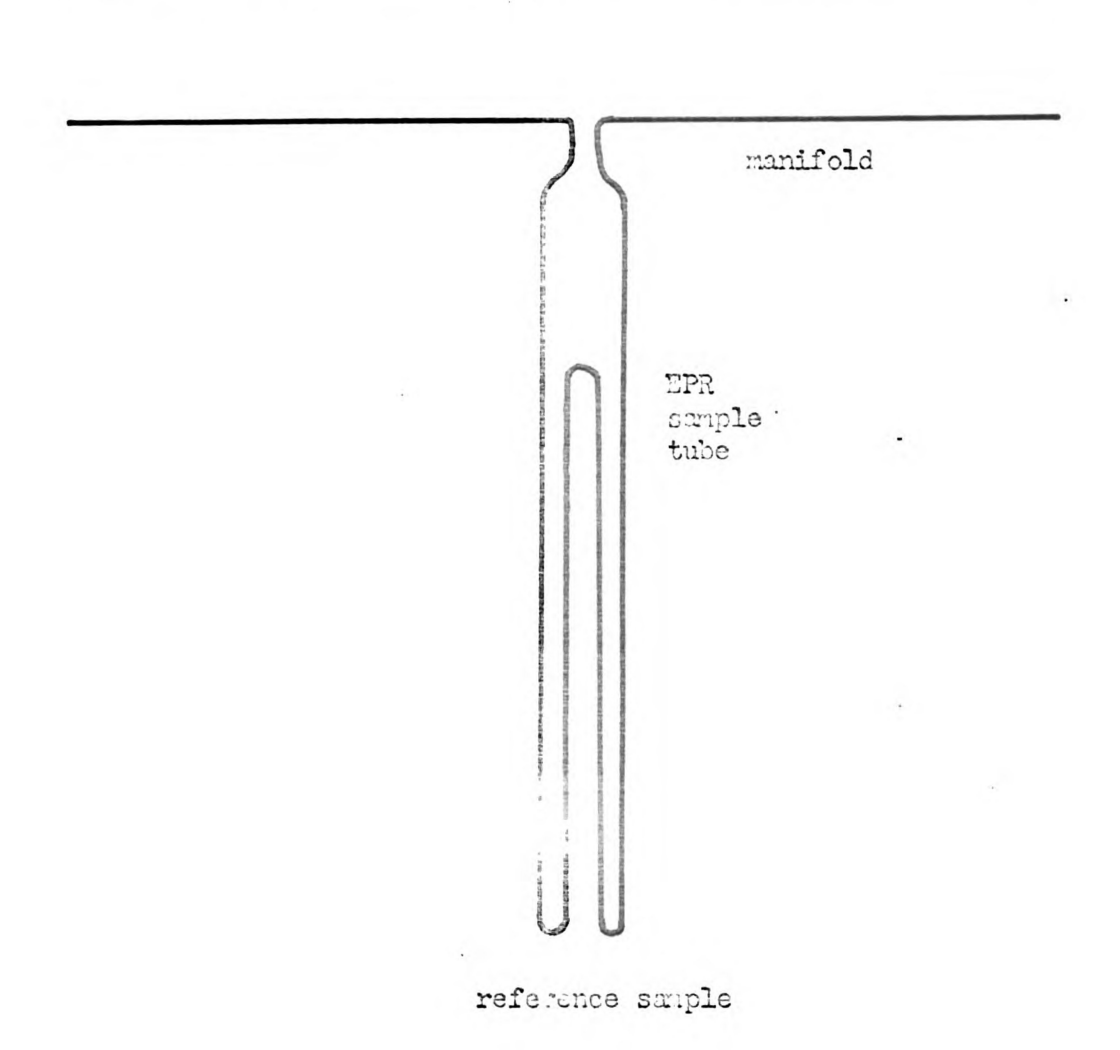


Figure 7. Vessel used to prepare sample for measurement of H₁ inside of metal-amine sample.

This permitted a measurement of the retating magnetic field, R_1 , inside the sample.

6. EPR Measurements at K- and KU-band frequencies. For measurements at the higher frequencies, Pyrex tubing was found to be too glossy; honce, for measurements at these frequencies the EPR cells were constructed of high quality quarts tubing (Engelbard Supresil).

B. EPR Messurements

1. The spectrometer. Four different EPR spectrometers were employed in obtaining the electron paramagnetic resonance data reported in this thesis. The instrument upon which the vest majority of measurements were taken was a Varian Model V-4500-10A X-band EPR spectrometer. The spectra taken using this instrument were recorded on an X-X recorder whose X-axis is proportional to the magnetic field. This is accomplished by use of a Hall probe as a field sensor. This instrument employs 100-ke/sec modulation.

A second EPR spectrometer, located at Stauffer Laboratory for Physical Chemistry, Stauferd, California, was made available to the author by Professor H. M. McConnell of Stanford University. This instrument is a Varian V-A503 35-Ge spectrometer equipped with fielddial and 100-km/see modulation.

The use of a third Varian EPR spectrometer was provided courtesy of Preference C. Elimahi of the Department of Huelour Engineering of the University of Michigan. This spectrometer was equipped with separate, interchangeable klystrons permitting measurements to be made at 17.5, 24.3, and 35.5 kmc/sec. This instrument also employed 100-kc/sec modulation and was equipped with fielddial.

The use of a fourth instrument was authorised by Professor J.

Cowen of the Physics Department of Michigan State University. This

instrument was so equipped as to afford either crystal or superhotoro
dyne detection and permitted the use of several modulation frequencies.

- 2. Temperature regulation. Measurements were made ever a temperature range from 4.2 to 378°K. EPR measurements at 4.2 and 77°K were made using V-4545A and V-4546 liquid helium and liquid mitrogen Dower accessories respectively. For measurements between 90 and 378°K, temperature regulation was achieved using a V-4540 variable temperature central unit. This unit allows the temperature to be selected within a 3°K and maintained within a 1°K. Temperatures were measured during the EPR measurement with a copper-constantan thermoscopie.
- 3. The time averaging computer. The field stability of our I-band spectrometer (better them one part in 10⁵) allowed the use of a Varian C-10²⁴ time averaging computer in studying samples displaying very weak signals.
- A. Heasurement of hyperfine splitting and g-values. Both first and second derivative operations were employed in measuring the spectra. Ryperfine splitting was measured using a Hemlett-Packard Medel 524C Proquency Counter and was checked against the hyperfine splittings of aqueous venedyl sulfate, aqueous K₃Cr(CN)₅NO, and aqueous perceylenine disulphenate which are known to have hyperfine splitting values of 116.13 gauss (42) between the fourth and fifth lines of the eight line pattern, 5.260 gauss (73), and 13.0 gauss (74) respectively. For measurement of peak separations, pips corresponding to measured proton frequencies were placed at 1 to 10 gauss intervals directly on the recorded spectrum by simultaneously recording the second derivative of the EPR and proton signals.

The determination of g-values was carried out using the following formula (75).

g = 0.714489[y (klystrom frequency in megacycles/B (magnetic field in gauss)]
(18)

Hystron frequencies were measured by besting with a harmonic of a Micro-Row Model 101 Frequency Calibrator and tuning the difference frequency with a communications receiver. Under entirem conditions. Accuredies of one part in 105 were obtained. A second method of obtaining gayalues consisted of simultaneously recording the spectre of a metal-suine solution and that of a material whose g-value was previously known. Reference samples included phospherus doped silicon in polyethylene (g = 1.99875), pitch in KCl (g = 2.00280), DPPH in bensene (g = 2.00354), peroxylamine disulphenate (g = 2.00550), and aqueous $K_3Cr(CH)_5NO$ (g = 1.99454). Since near of the hyperfine splittings observed in this work are large, the high field approximation is no lenger rigorously welld. For eases where medicar hyperfine interactions are large, the paramagnetic electron spin operators will not lie along the direction of the applied magnetic field as in the high field appresidention but will rether lie along the resultant of the applied magnetic field and unclear magnetic moment vectors. The perturbation on the Zoomen transition resulting from hyperfine interaction was corrected for as follows:

For g isotropio

$$B_{\bullet} = B_{\bullet}(\mathbf{n}) + A_{\mathbf{F}} \mathbf{n}_{\mathbf{I}} + A_{\mathbf{F}}^{2} [\mathbf{I}(\mathbf{I}+\mathbf{1}) - \mathbf{n}_{\mathbf{I}}^{2}]/2B_{\bullet}(\mathbf{n})$$
 (19)

where B_(m) is the magnetic field position of the EPR line due to the

component n_{χ} of the nuclear magnetic moment I, and A_{χ} is the nuclear hyperfine interaction constant. The derivation of Eq. 19 may be seen as follows:

The spin Hamiltonian appropriate for metal-amine solutions is

m gfB •\$\vec{3} + AI •\$\vec{3}\$ (20)

In the presence of a strong external magnetic field the appropriate representation, in which S_g and I_g are diagonal. The external field defines the s-exis. In this representation the spin Hamiltonian may be divided into a diagonal part

16 = gsB_S_ + AI_S_ and an eff-diagonal part

In order to solve the above Hamiltonian we must recent to perturbation theory. The reader should note that this implies that the resultant magnetic vector is "perturbed" only a slight distance from the magnetic field vector. If the hyperfine interaction is comparable to the applied field, the resultant vector will be considerably removed from the direction of the applied field vector and one obviously cannot treat the problem in terms of the S, I, m_S, m_I representation or by means of perturbation theory.

Applying perturbation theory, we find that the contribution $B_{\phi}(n)$ to the energy is, to second order.

$$W^{(2)}(\mathbf{m}_{S}, \mathbf{m}_{I}) = -\lambda^{2}/4gsB_{\bullet}(\mathbf{n}) \left\{ -\left[3(S+1) - \mathbf{m}_{S}(\mathbf{m}_{S}-1) \right] \times \left[1(I+1) - \mathbf{m}_{I}(\mathbf{m}_{I}+1) \right] \right.$$

$$\times \left. 1 + \sum_{\mathbf{m}=1}^{\infty} \left[\lambda(\mathbf{m}_{S}-\mathbf{m}_{I}-1)/g^{\beta}B_{\bullet}(\mathbf{m}) \right]^{n} + \left[3(S+1) - \mathbf{m}_{S}(\mathbf{m}_{S}+1) \right] \right.$$

$$\times \left[1(I+1) - \mathbf{m}_{I}(\mathbf{m}_{I}-1) \right] \times \left(1 + \sum_{\mathbf{m}=1}^{\infty} (-1)^{n} \left[\lambda(\mathbf{m}_{I}-\mathbf{m}_{S}-1)/g^{\beta}B_{\bullet}(\mathbf{m}) \right]^{n} \right) \right]$$

This is seen to be an expansion in $A[A/gBB_q(n)]^q$. For the purposes of our derivation we need only consider the terms for which q=1, but in order that the reader may receive an idea of the importance of higher order terms we shall consider terms of the expansion through n=2.

$$= gih^{-1}B_{\bullet}(m) + Am_{I} + A^{2}[I(I+1) - m_{I}^{2}]/2gih^{-1}B_{\bullet}(m) + A^{3}[I(I+1) - 3m_{I}^{2}]/4[gih^{-1}B_{\bullet}(m)]^{2} + A^{4}m_{I}[2I(I+1) - 4m_{I}^{2} - \frac{1}{2}]/4[gih^{-1}B_{\bullet}(m)]^{3}$$

It is assumed in this expression that $S = \frac{1}{2}$. This equation can be immediately related to Eq. 19 if one drops the last two terms and notes that $A(sec^{-1}) = gih^{-1}A_{\mu}(gauss)$.

Hery workers prefer to use an approximate form of Eq. 19 by assuming that $B_n(m)=B_n+Am_{n+1}$ thus obtaining

$$B_{\bullet}(\mathbf{n}) = B_{\bullet} - A_{\mathbf{p}}\mathbf{n}_{\mathbf{I}} - A_{\mathbf{p}}^{2}[I(\mathbf{I}+\mathbf{I}) - \mathbf{n}_{\mathbf{I}}^{2}]/2B_{\bullet}$$

If the parametric entity which we are considering on exist in more than one form we must consider dynamic as well as static second—corder effects. Let us assume that the parametric species can exist in two forms, A and B, with splitting constants A_A and A_B . Each form will give rise to its own spectrum, one with frequencies $\omega_A^{\bullet}(n)$ and the ether with frequencies $\omega_B^{\bullet}(n)$. These are obtained from Eq. 19 by replacing the splitting constant A_B with A_A and A_B , respectively.

If rapid interconversion of the two forms takes place, the everage frequencies are obtained: For long correlation times, $(\omega_{\mathbf{e}} \tau)^2 \gg 1$,

and

$$k(\omega_0) = \omega_0^{-1} g(0)$$

= $(\omega_0 r)^{-1} f(0)$

The second-order correction terms in Eq. 21 are replaced by

$$[|\gamma_0|(I^2/2B_0(m)) + \frac{1}{2}k(\omega_0)][I(I+1) - m^2].$$

where now the dynamic shift applies to any type of modulation, not only a two-jump model. In the particular case of the two-jump model we have

$$\frac{1}{2}k(\omega_{0}) = (\gamma_{0}^{2}/2\omega_{0})p_{A}p_{B}(A_{A} - A_{B})^{2}$$

$$= (|\gamma_{0}|/2B_{0}(a)) \langle (\delta A)^{2} \rangle$$

and Eq. 21 is obtained.

An analysis of metal-animo solutions has provided evidence which indicates that Eq. 21 rather than Eq. 19 should be used. Because the assignment of A_A and A_B is not cortain it was folt that the use of Eq. 19 would constitute the most desirable method of obtaining second-order corrections. However, with further refinement of the model of Dalton of A_A (42) Eq. 21 should be used. Because Eq. 19 involves successive reliceration a computer program was written which allowed a Control Data 3600 Computer to perform the mocessary second-order corrections.

Eq. 19 is reasonably accurate for hyperfine splittings up to 150 gauss. Insseveral cosium-suine solutions and in the gas phase, the cosium electron-nuclear hyperfine interaction exceeds 200 gauss. For these cases it is obvious that we must preced from a different framework.

For long correlation times, $(\omega_{\alpha} \tau)^2 \gg 1$,

and

$$k(\omega_0) = \omega_0^{-1}g(0)$$

= $(\omega_0 r)^{-1}f(0)$

The second-order correction terms in Eq. 21 are replaced by

$$[|\gamma_a|(I^2/2B_a(n)) + \frac{1}{2}M(\omega_a)][I(I+1) - n^2].$$

where now the dynamic shift applies to any type of modulation, not only a two-jump model. In the particular case of the two-jump model we have

$$\frac{1}{2}k(\omega_{0}) = (\gamma_{0}^{2}/2\omega_{0})p_{A}p_{B}(A_{A} - A_{B})^{2}$$

$$= (|\gamma_{0}|/2B_{0}(\mathbf{n})) \langle (\delta A)^{2} \rangle$$

and Eq. 21 is obtained.

An analysis of metal-amine solutions has provided evidence which indicates that Eq. 21 rather than Eq. 19 should be used. Because the assignment of A_A and A_B is not cortain it was folt that the use of Eq. 19 would constitute the most desirable method of obtaining second-order corrections. However, with further refinement of the model of Dalton of A_A (42) Eq. 21 should be used. Because Eq. 19 involves successive reiteration a computer program was written which allowed a Control Data 3600 Computer to perform the mecassary second-order corrections.

Eq. 19 is reasonably accurate for hyperfine splittings up to 150 gauss. Inserveral cosium-amine solutions and in the gas phase, the cosium electron-amplear hyperfine interaction exceeds 200 gauss. For these cases it is obvious that we must proceed from a different framework.

.

j sa

i, r

→ ; 1 1

.

In general the mudler interactions of an atom in a magnetic field are the combination of the several interactions of the Hamiltonian.

With several such interactions present simultaneously it is not in general possible to select a priori a representation for which the energy matrix is diagonal. Often it is possible to select a representation in which the largest matrix elements are diagonal, in which case a standard form of porturbation calculation can be used to make corrections for the effect of the non-diagonal matrix elements. Such a precedure was used to derive Eq. 19. In many cases, however, the non-diagonal matrix elements are comparable to the diagonal one, in which case the perturbation is unsatisfactory. In this case the best precedure is to calculate all the matrix elements from the interaction Hamiltonian in any convenient representation. The energy levels of the system may them be obtained by a selution of the corresponding secular equation. An example of the solution of the secular equation for an intermediate coupling problem is the solution of the intermediate field problem given by H. F. Rausey (81). In this case and if the s-axis is taken in the direction of the external field B, the Hamiltenian of the system is

where $d = \mu_X B_{\bullet}/I$ and $c = \mu_S B_{\bullet}/S$

As discussed in Section III of Reference 81, an Fm (where \bar{F} w \bar{I} + \bar{S} and m w $m_{\bar{I}}$ + $m_{\bar{S}}$) representation is most convenient when $B_{\bar{g}}$ is anall and $m_{\bar{I}}m_{\bar{S}}$ representation is most convenient when $B_{\bar{g}}$ is large.

However, in intermediate magnetic fields the matrix is not even approximately diagonal in either representation, so that the secular equation must be solved. As a result it makes little difference which representation is chosen in the calculation of the complete matrix and the secular equation will, of course, be independent of this choice even though the natrices are quite different in form. For the calculation given in Reference 81, Ransey chose the $\mathbf{m_{I}m_{S}}$ representation; a calculation with an Fm representation has been published elsewhere (82). For the case where $S = \frac{1}{2}$, Ransey obtained for the contribution to the energy in the limit of $B_{I} = 0$ (in the Fm representation),

$$W(F,x) = -\Delta W/2(2I + 1) - \mu_I B_x / I \pm \Delta W/2/(1 + 4xx/(2I + 1) + x^2)$$
(22)

with
$$g_I = -\mu_I/I\mu_0$$
 $x = (-\mu_S/S + \mu_I/I)B_0/\Delta W = (g_S - g_I)\mu_0B_0/\Delta W$

where n is the Bohr magneton and g is the electron g-factor.

Bq. 21 was first derived by Breit and Rabi (83). Fessenden and Schuler (84) have simplified the Breit-Rabi equation by expanding the square-root term in the formula. This expansion results in an equation for the various transitions of the form

$$\gamma = g_0 h^{-1} B_0 + m + c_2 a^2 / D + c_3 a^3 / D^2 + c_4 a^4 / D^3 + \dots$$
 (23)

$$D = (g - g_I)\beta h^{-1}B_0,$$

$$C_2 = \frac{1}{2}I(I + 1) - \frac{1}{2}m^2,$$

$$C_3 = m[\frac{1}{2}m^2 + \frac{1}{2} - \frac{1}{2}I(I + 1)],$$

$$C_h = -[I(I + 1) - 6m^2][I(I + 1) - 1] + 5m^4$$

Eqs. 19, 22, and 23 were used when appropriate. As with Eq. 19, Eqs. 22 and 23 should be modified to include the effects of dynamic as well as static shifts.

5. Measurement of spin concentrations. There are two main parts to the problem of determining spin concentration: first, the relation between certain presumably measurable quantities and the actual number of unpaired spins; and second, the accurate measurement of these quantities.

If an EPR absorption line in the absence of saturation satisfice the Hloch equations modified for a linearly polarised field, (85), the static spin susceptibility χ is given by

$$\chi = 2/\pi \omega \int \chi^{\mu} d\omega . \tag{24}$$

where ω is the angular frequency of the rf field of amplitude B_1 , $\omega = \gamma B_0$ is the procession angular frequency, and χ^n is the absorptive part of the total spin susceptibility, χ^n is related to the actual power absorbed by the sample P_a , by $\chi^n = 2P_a/\omega E_1^2$, so that

$$\chi_{\bullet} = \frac{\hbar \gamma}{\pi \omega B_{\bullet}^2} \int_0^{\infty} P_{\bullet} dB_{\bullet}$$
 (25)

However, this relation will be applicable only if the fellowing conditions are not: (1) The spin system must be in thermal equilibrium with its surroundings, i.e., saturation must be absent; (2) The line width must be small compared to H₀ at recommence; (3) The modulation amplitude must be small compared to the linewidth; and (4) skin effects must be absent.

If P_a is small compared to the total power impinging on the sample, the change in crystal detector signal will be directly prepertional to P_a and the necessary data (except for a constant of prepertionality) for performing the required integration would be evailable from a plot of crystal signal versus magnetic field B_a. If a

magnetic field modulation scheme is used in which the modulation amplitude is small compared to the linewidth, a quantity proportional to $dP_{\rm m}/dB_{\rm p}$ is measured so that a double integration is necessary. A susceptibility determination thus depends upon the measurement of four quantities: γ (or the glactor), the microwave frequency ω . $B_{\rm p}$ incide the sample, and $P_{\rm p}$ or $dP_{\rm p}/dB_{\rm p}$ as a function of $B_{\rm p}$. Assuming almost free spine, the spin concentration is then given by the expression

$$H = \chi [3kT/g^2 g^2 s(s+1)]$$
 (26)

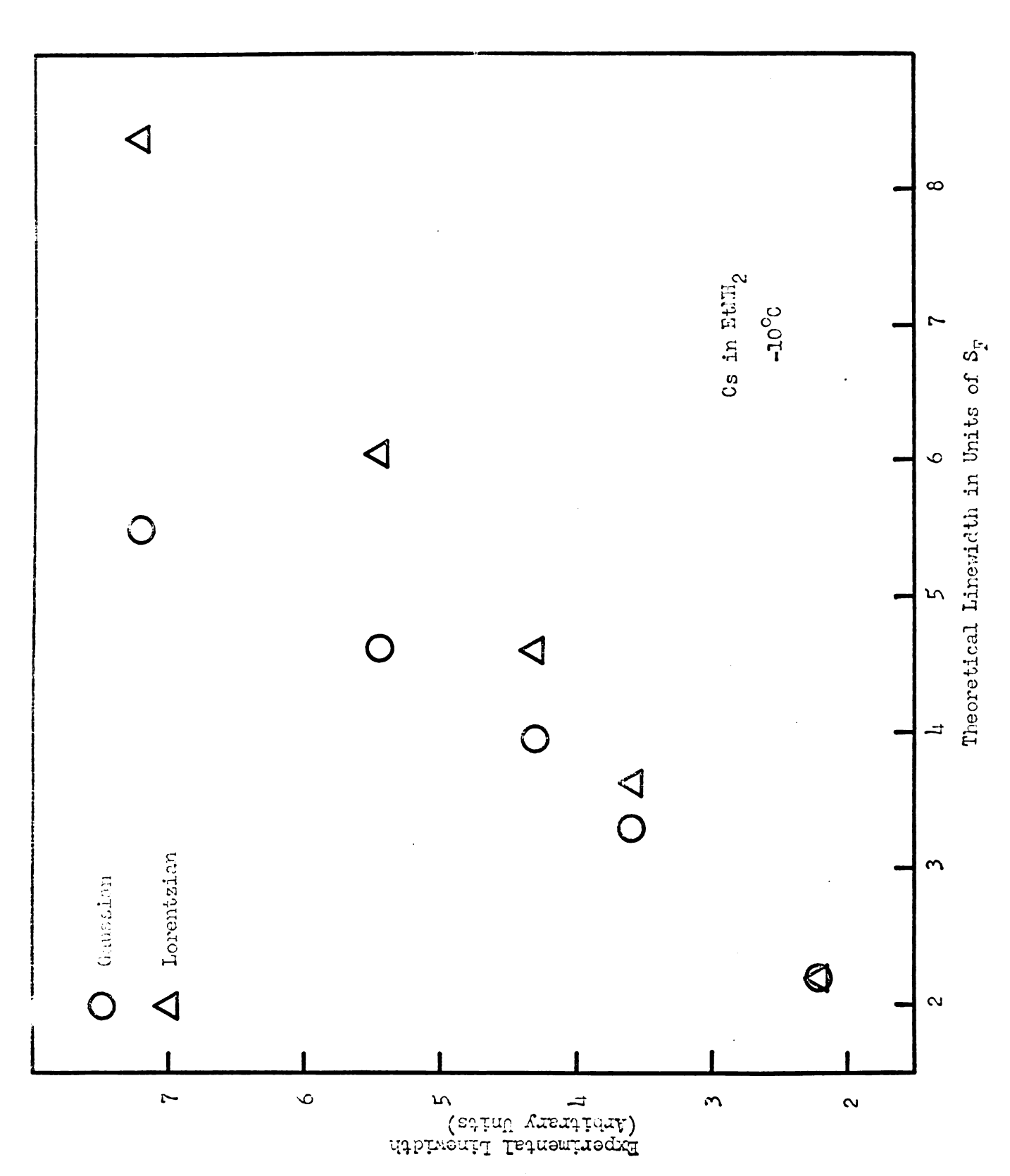
It should be emphasized that the feregoing simple combination of quantities usually measured in an EPR experiment connet, in general, be identified with a static susceptibility. The exact form of the Eremig-Eremore relations (86) applies strictly only to the case where the magnetic field is constant and frequency is the variable. Altabular (87) has attempted to derive similar relations for the case in which frequency is constant and the magnetic field is the variable; however, these relations cannot be obtained in explicit form. Of course, if the EPR line is marrow compared to B₀ at recommon, approximations of the Eremig-Eremore relations lead to the expression (24).

If an EFR curve can be shown to satisfy the medified Elech equations, an increase in both simplicity and accuracy can be achieved in determining the spin concentration. For example, if the EFR curve can be shown to be the first derivative of a Lorentzian curve, the integrated absorption, which is proportional to S_p^2D can be compared directly with a Lorentz-shaped curve for a standard sample of known susceptibility without resorting to numerical integration precedures (88).

The method of line shape analysis used was similar to that used by Singer (89) and by Weidner (90) for an absorption curve. The widths at various fractional heights on the derivative curve were plotted against the corresponding widths for a Gaussian and a Lone entains curve (see Fig. 8). The slape of this line yields a reliable average value for the linewidth $S_{\rm p}$. Line shape analysis were performed on all the curves used to obtain spin concentrations. In the case of metal-amine-amounts solutions of high amounts concentration the high electrical conductance results in a microwave skin depth. As Bloembergen (91) and Feber and Kip (65) have shown, a mixture of χ^0 and χ^0 results when the sample dimensions are comparable to the skin depth. It was found that this effect could be eliminated by using sample tubes of 1.5 mm I.D. or less.

It can be seen from Eq. 25 that χ_0 and thus the spin concentration is inversely proportional to the square of the rf magnetic field amplitude B_1 inside the sample. Because of the difficulty of accurately determining the absolute magnitude of this quantity, a comparison method was used in which only relative values were required. It has been found that the signal from a number of paramagnetic materials comented along side of the notal-cuine sample provides a convenient monitor of B_1 in the cavity.

One complication in any determination of spin concentration is the difference between B₁ inside a sample and B₁ insediately satisfies the sample. Since all naturals have a real part of the dislectric constant greater than unity, the density of the E field and B₁ inside will always be sensulat larger than that immediately satisfies the sample.



ligure 8a. Line shape analysis of a typical spectrum of Cs in EtHH2.

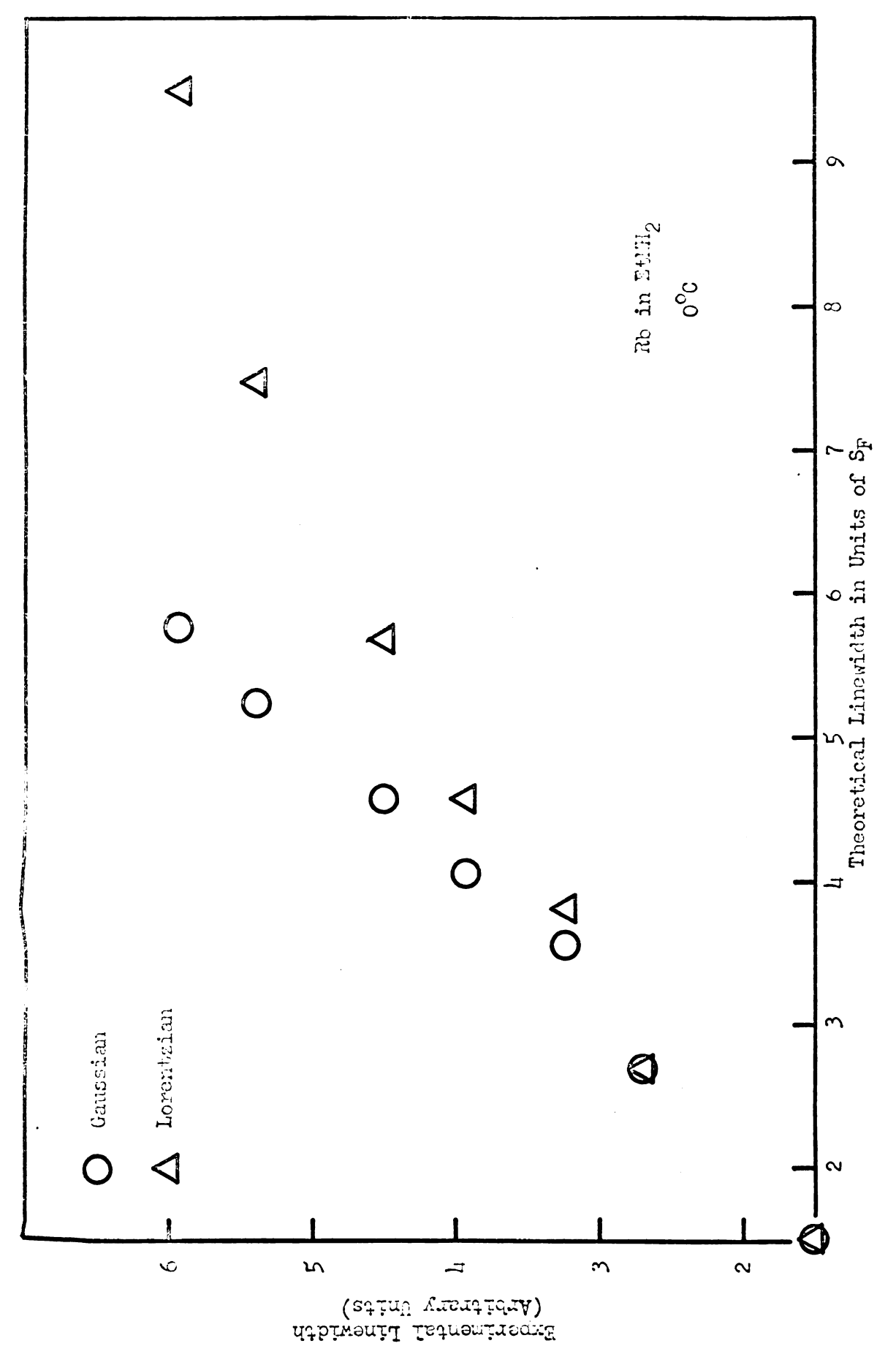


Figure 8b. Line shape analysis of a typical spectrum of Rb in Ethil.

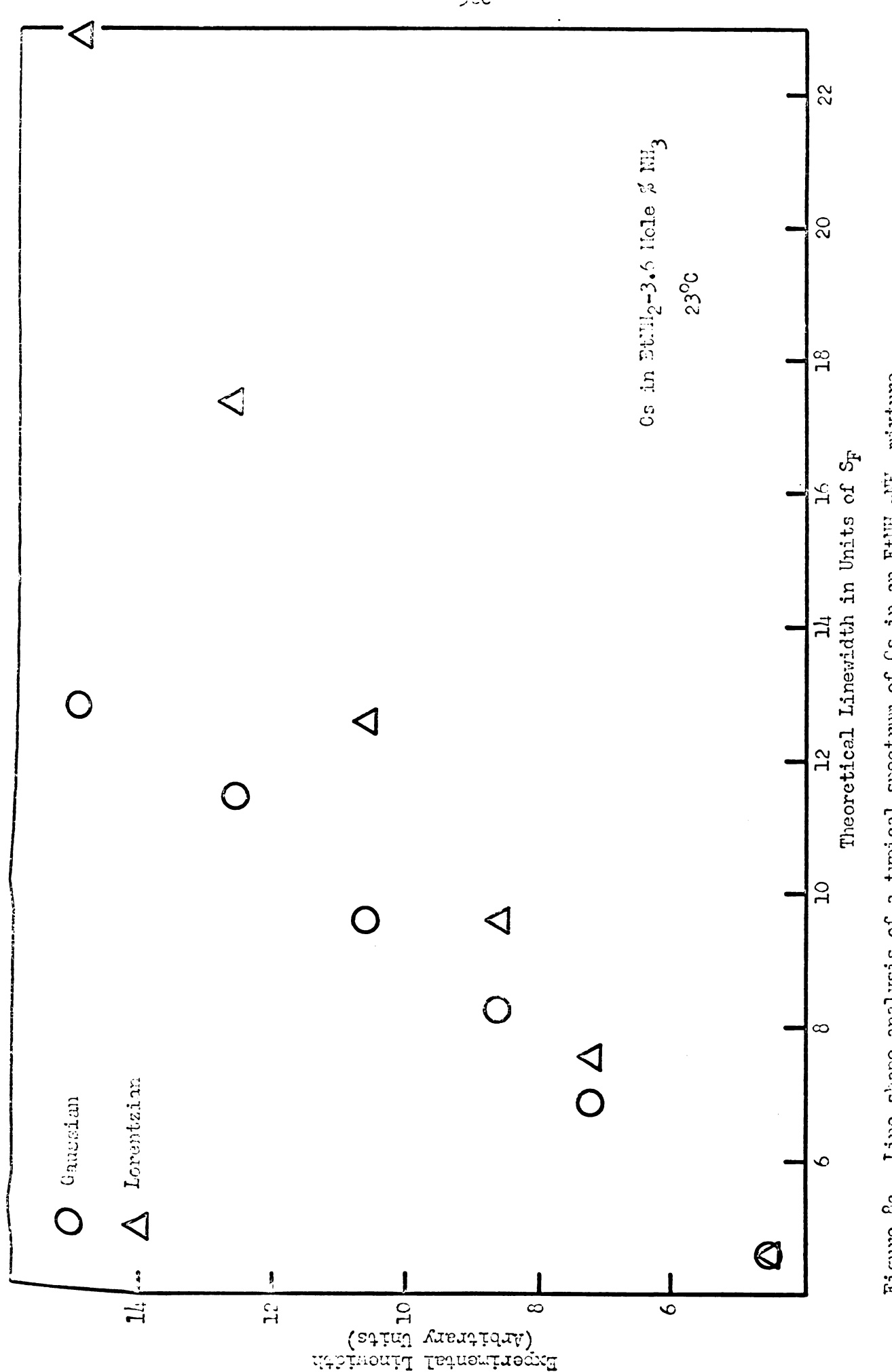
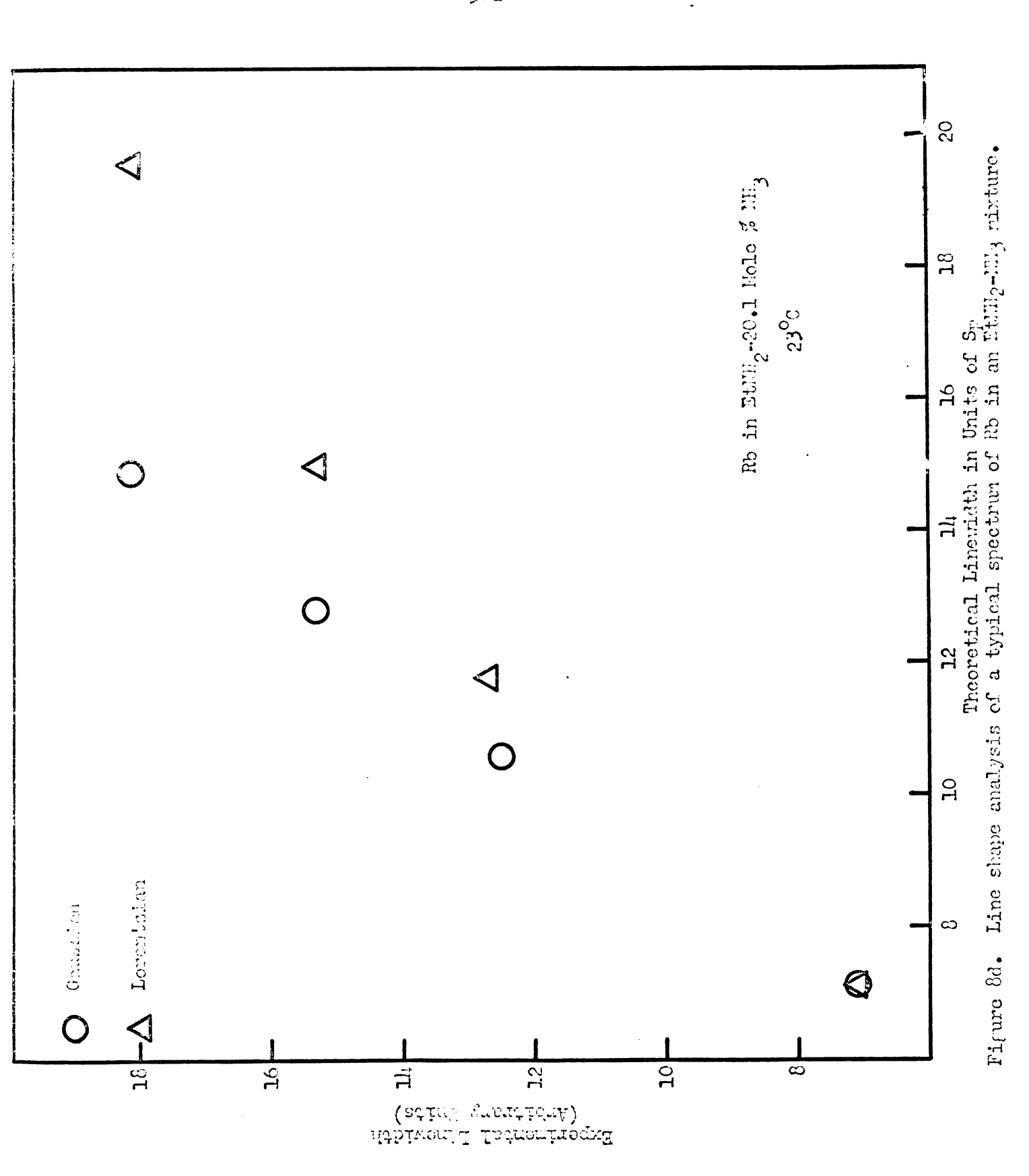


Figure 8c. Line shape analysis of a typical spectrum of Cs in an Ethil - Wit mixture.



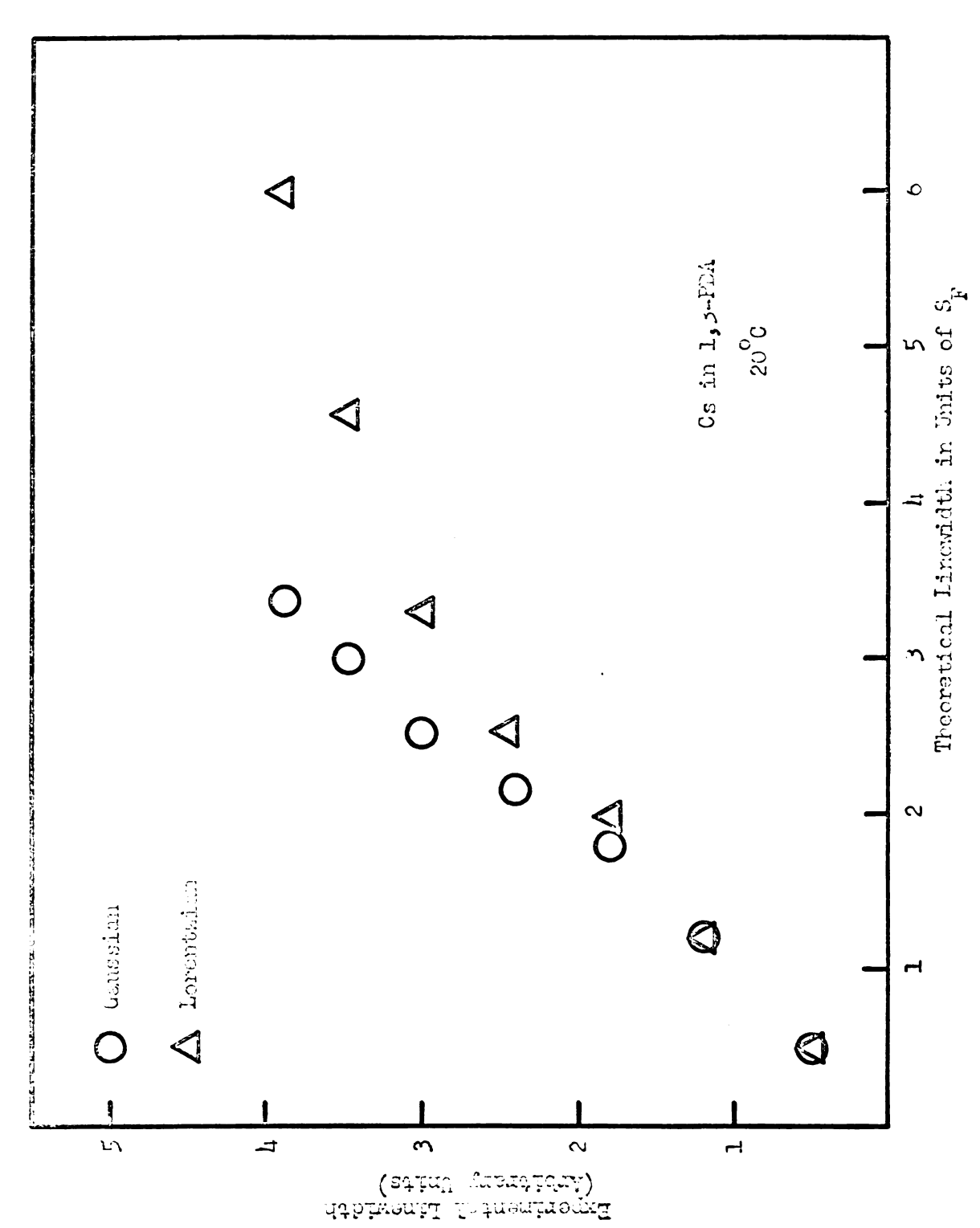


Figure 8e. Line shape analysis of a typical spectrum of 6s in 1,3-FDA.

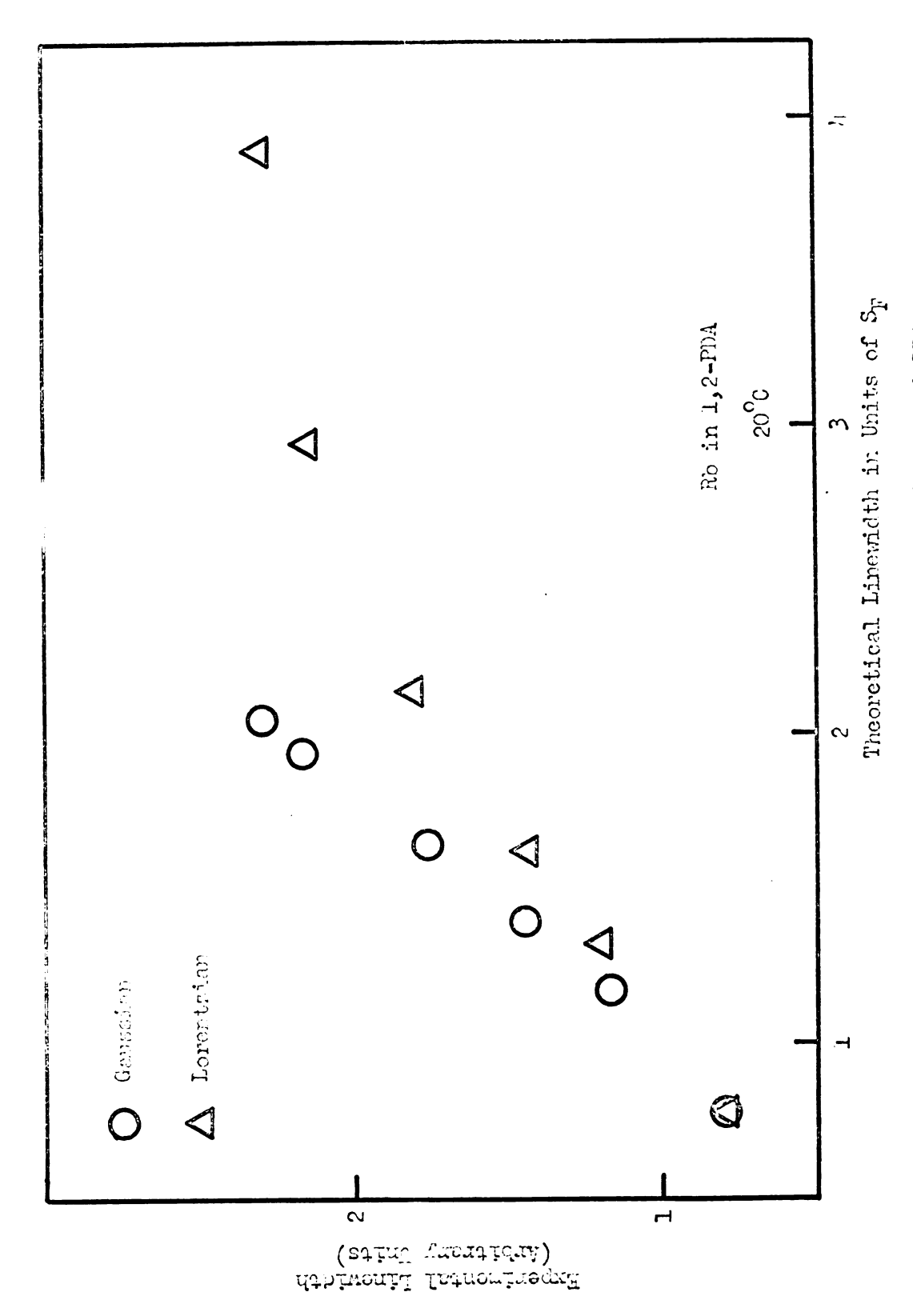


Figure 8f. Line share analysis of a typical spectrum of Rb in 1,2-PDA.

This means that the effective filling factor of the cavity will be considerably enhanced by samples of sizable dislectric constant. One method of correcting for this "sucking in" of the microseve field is to place the reference material inside the sample. This was done by use of the apparatus shown in Fig. 7.

The magnitude of this "sucking in" which of course also depends upon the type and thickness of sample tubes, can be estimated by extrapolating the apparent spin concentration to samples of infinitesimal size. Only a slight size effect was observed for the materials reported here.

As montioned previously, an accurate spin concentration measurement requires the determination of both the signal properties and B_{χ} , in the absence of saturation. Saturation curves (92) were, therefore, run on both reference and sample at the lowest temperatures used and the maximum allowable microwave power level was determined.

When the electrical properties of the sample, conditions for measurement, and the EFR line shape were taken into account as already described, the susceptibility was then calculated from the expression

(27)

 $n/n^{\circ} = \chi_0/\chi_0^{\circ} = K(g/g^{\circ})(D/D^{\circ})(G/G^{\circ})(H_0^{\circ}/H_0^{\circ})(S_p/S_p^{\circ})^2$ in which D is the signal height, G the relative amplifier gain, H_0 the modulation amplitude, and S_p the linewidth. It is a factor dependent upon the line shapes of the reference and the sample. Equating n/n° to χ_0/χ_0° assumes that both systems would obey Curio's law at fixed spin concentrations.

Measurement of I, which relates the line shape of the reference sample to that of the unknown, is required for the evaluation of spin

emocentration. A convenient material to use for the evaluation of I is $CuSO_h$ ' SH_2O in single crystal form. It has a very small Veiss constant so that expression 25 is applicable. Single crystals of convenient size (a few hundred micrograms) can be green, weighed on a microbalance, and then imbedded in paraffin. No change in the EPR properties has been observed for such standard samples over a period of several years. The EPR linewidth and g factor are both orientation dependent; however, the described nothed of determining spin concentrations takes into account both those parameters. The line is very nearly Lorentzian so that the expression 27 could be used accurately for all the measurements reported in this paper. From a signal-to-noise standpoint, it was found worthwhile to rotate the standard sample in the field until a fairly narrow line with S_p approximately 30 gauss was obtained since the signal height D is inversely proportional to S_p^2 .

Neargranate were used on the reference and sample simultaneously. This was done by attaching the reference natorial to the sample in either of two ways. Powdered samples, dispersed in polyothylous or paraffin were out into sleeves that fitted samply around the sample tubes. Reference samples in solution were scaled in tubes of various dismeters and taped to the sample tubes. A summary of the reference samples used along with pertinent information about their proposetion and EPR characteristics is given in Table V. Obviously, not all references were applicable in every case. The references used were solveted to match the spin concentration range of the samples without serious everlap with the lines of the sample. Some of the materials listed were used as checks on secondary reference standards.

6. Heavyrement of paramagnetic relaxation or line widths. There are two reasons for discussing relaxation phenomena in EFR. The first is that the nature of these phenomena must be properly taken into account if one wishes to make a significant measurement of spin susceptibility or spin concentration. The second reason is that relaxation phenomena in themselves can be a valuable indication of the nature of the unpaired spins and their interactions with their surroundings.

Providelly all relaxation phononena can be discussed conveniently by starting with Bloch's phononenelogical description of magnetic recommon (68). Bloch defines a longitudinal or spin-lattice relaxation time T_1 and a transverse or spin-spin relaxation time T_2 and then shows that the imaginary or absorptive part of the susceptimitality is given by

$$\chi^{*} = \frac{1}{2} \chi_{0} \omega_{1}^{2} / [1 + (\omega - \omega_{0})^{2} T_{2}^{2} + (\gamma h_{1})^{2} T_{1}^{2} T_{2}^{2} / 4]$$
where χ^{*} and P_{a} are related by
$$\chi^{*} = 2P_{a} / \omega_{1}^{2}$$
(28)

The payeneters T_1 and T_2 were introduced purely phenomenologically based on a fairly simple model. Therefore, it should be supherised that for the EPR response of any real system, the definition of those parameters and their correspondence to measurable quantities must be closely extended.

The spin-lattice relaxation time T_1 was introduced as the time constant for an assumed first order rate of approach of an excited spin system to equilibrium, i.e. $dn/dt = (n_0 - n)/T_1$ where n is the population difference between the ground and the excited spin states

and n₀ is the equilibrium value of this quantity. The exponential degradation of the energy of a spin system to its immediate surrounding (lattice) has been shown to be a remarkably good approximation even for quite complicated and multilevel systems (94). This does not mean, however, that a single T₁ can adequately describe a system containing different kinds of spins or inhomogeneities in structures.

The significance of T_2 is even less straightforward. For an idealised spin system, the definition of T_2 in terms of a normalised shape function $g(\omega - \omega_0)$, vis. $g(0) = T_2/\pi$, leads to simple relations between T_2 and line width. For example, for a Lorentzian shape function, the half-width at half-height, $(\omega - \omega_0)_{\frac{1}{2}}$, is equal to $1/T_2$, while for a Gaussian shape function this width is given by $(\pi \ln 2)^{\frac{1}{2}}/T_2$ (95). In these cases, both T_1 and T_2 in Eq. 28 can thus be related simply to experiment.

For many paramagnetic materials, such simple correspondences do not exist. As Portis (96) has shown in his detailed study of spin relaxation of F-conters, the different interaction mechanisms which give rise to line breadening can cause drastic differences in the EPR behavior which do not permit the direct application of Eq. 28. The basis for these differences is most easily discussed by defining two types of breadening, homogeneous and inhomogeneous, which depend upon how fast these interactions are varying relative to the time of a spin transition. Pertis (96) lists a number of sources of homogeneous breadening in which the interactions of the spins enong themselves and with their surroundings are so fast that all the spins can be conveniently characterised by time-averaged interaction parameters. For these situations, Eq. 28 will be applicable.

In the case of inhomogeneous broadening, Portis (96) lists several interactions which vary slowly ever the time required for a spin transition. As a result of these "inhomogeneous" interactions, the EPR signal will appear as the envelope of a number of spin packets as is shown in Fig. 9. The parameter T_2^{\bullet} is now defined for the envelope distribution $h(\omega = \omega_0)$ by $h(0) = T_2^{\bullet}/\pi$. It should be emphasized that T_2^{\bullet} cannot in general be related to a line width since not only can the line shape deviate substantially from Lorentzian or Gaussian but it can also be asymmetric.

Portis (96) has also shown that the EPR saturation behavior of homogeneously and inhomogeneously broadened lines is quite different. As expression 28 indicates, the line width increases with microwave power (preportional to B_1^2); whereas in the inhomogeneously breadened case, the line shape is independent of the extent of saturation. The behavior of the peak absorption intensity for the two cases also indicates that one can clearly differentiate between the two types of line breadening by earsful saturation studies.

Considerable contien must be exercised in the use of Portie's simplified Eq. 19, however. It is strictly applicable only to the case illustrated in Fig. 9 where the ever-all broadening is large compared to the width of the spin packets and T₁ is identical for all the spin packets.

The preceding paragraphs emphasize that any analysis of paramagnetic relaxation must be performed with great care. For any analysis to be meaningful we must always establish the applicability of any mathematical relationship which we desire to use.

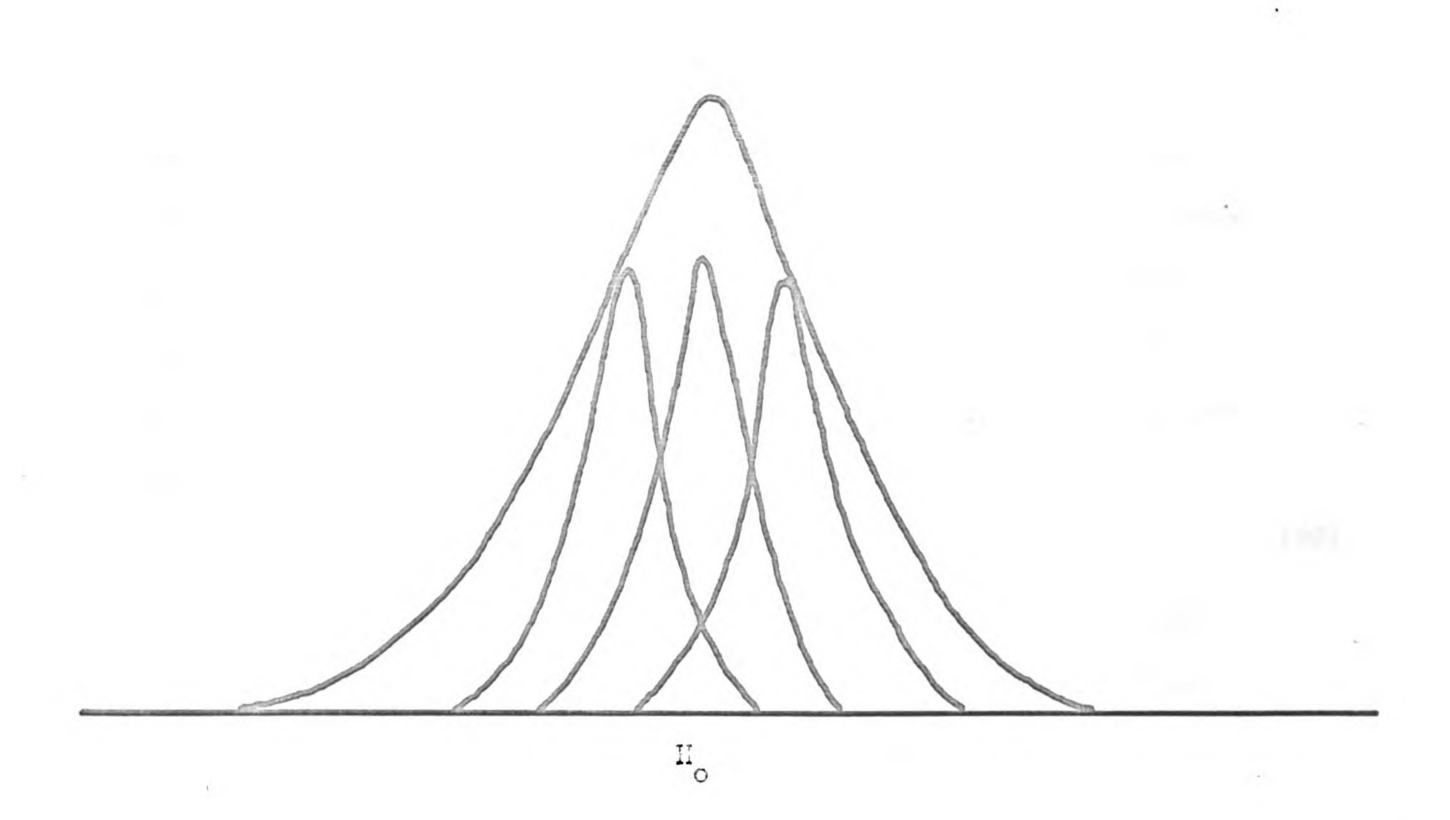


Figure 9. Inhomogeneously broadened resonance line.

As is also clear from the preceding paragraphs, the same considerations must be kept in mind when measuring T_1 and T_2 as when measuring spin concentrations. Let us first discuss the measurement of the spin-spin relaxation time T_2 . To accomplish this we must be able to relate the measured line shape to the Lorentzian or Gaussian shape function. If we are able to do this T_2 can be calculated from the two simple relationships already given. There are two experimental factors which must be carefully considered if one is to avoid distorting the true EPR line shape and thereby obtaining an erroneous measure of the half-width. The first of those is the modulational amplitude, particularly if high-frequency modulation is used (97).

E. R. Andrew (98) has shown that the second measure is related to the amplitude of the field modulation by

$$S_2$$
 (observed) = S_2 (intrinsic) + $\frac{1}{4}H_2^2$ (29)

It has been found by experience in this laboratory that the range of modulation 2 H_m may be set at about a quarter of the line width without introducing appropriable error. The line width, defined as the interval between maximum and minimum of the first derivative, is usually about twice the rms width (rest second moment). From Eq. 29 it is seen that an error of about 2 percent is thus incorred in the second moment.

The second experimental factor which must be closely menitored is the scenning speed. Perticularly with semples having very short relaxation times, scenning too fast can have the effect of distorting line shapes and widths. To guard against this possibility, line shapes were examined as a function of scenning speed.

There are a number of experimental methods which can be used to obtain I, . The particular method chosen depends upon both the absolute and relative magnitudes of T_q and T_{2*} . A number of pulse techniques have been used (99), but these schemes are sementat elaberate and may become exceedingly difficult for the shorter relaxation times. The saturation method is experimentally fairly simple but again requires the proof or assumption of certain characteristics of the EPR signal before I, can be determined. One simple way of obtaining absorption intensities as a function of microwave power is by using two attemptors, at least one of them calibrated. Known ensunts of attemption can be inserted in front of the cavity and identical amounts removed immediately before the detector. One can in this way insure a constant sensitivity of the system with change in microwave power. A single crystal of DPPH, for which T, and To are known ($T_1 = T_2 = 6 \times 10^{-9}$ sec), on conveniently serve as a calibration material. If two attempaters are not available, one can also memiter H, in the cavity with one of the reference samples as described for the measurement of spin concentrations. Although the methods described above were employed by the author it may also be mentioned that Suddt (100) has used a method for determining B, which involves a direct measurement of the cavity Q.

An example of the results of saturation experiments on some motal-anime samples is shown in Fig. 10. The quantity $D/D_{\rm e}$ is the extreme deflection on the derivative curve normalised to unity at some microscope power. If Eq. 28 is applicable, the modulation frequency is not too large, and T_2 is known, a T_1 for each sample can be exlculated from the expression

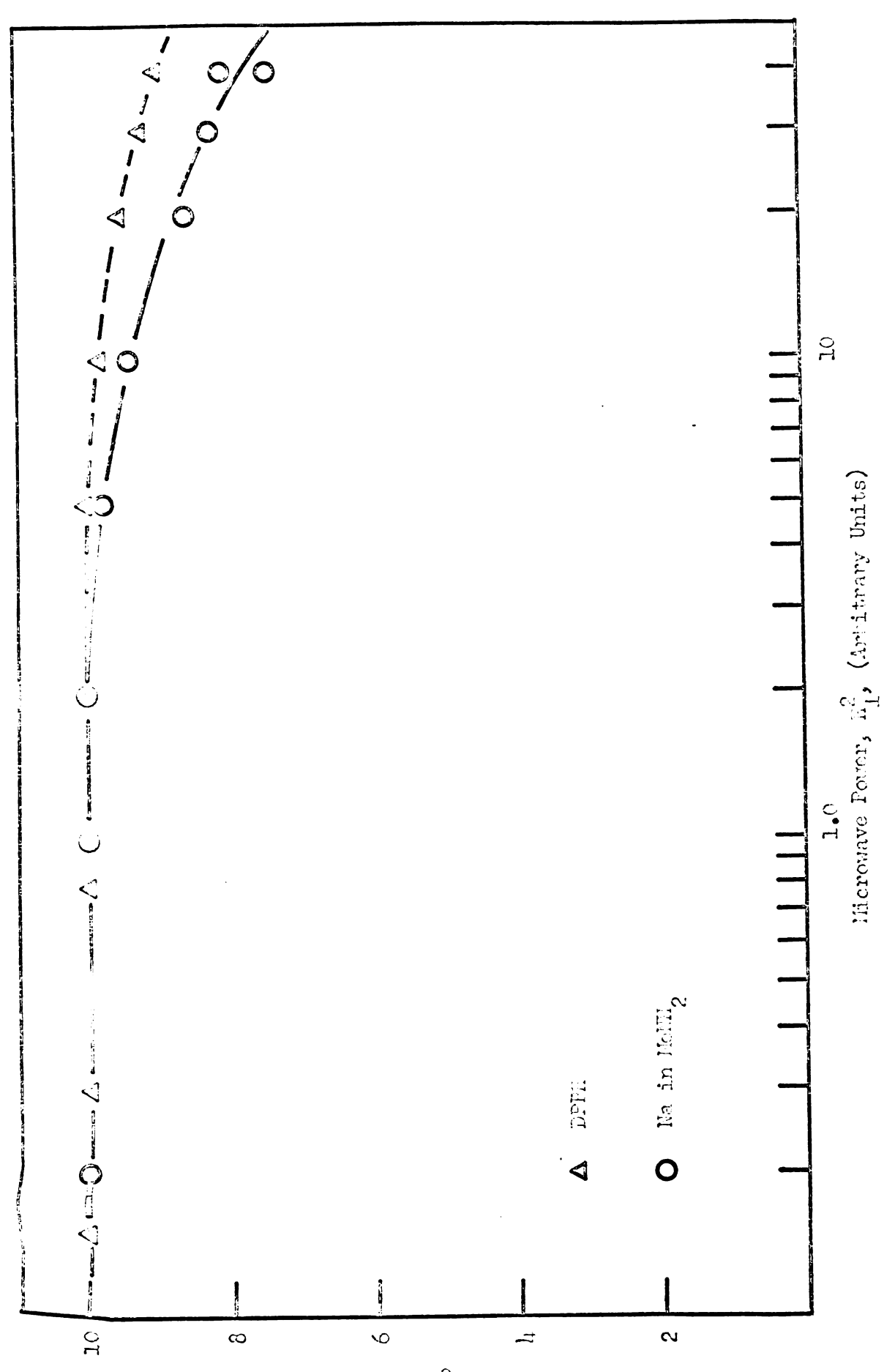


Figure 10. Saturation curve for a typical metal-maine sample and hydrazyl.

$$T_1 = (B_{1_{DEPH}}^2/B_1^2)T_{1_{DEPH}}^2T_2^{-1}$$
 (30)

evaluated at the same percent of saturation.

In addition to the measurement of T_1 and T_2 we were faced in this work with the analysis of the anisotropic relaxation of hyperfine components. To insure that we were not measuring intermolocular spin-spin exchange effects only-solutions dilute in notal were considered. Analysis showed that the integrated intensities (101) of the hyperfine lines of potassium, rubidium, and cosium solutions when normalised to unity are equal to within experimental accuracy. The absolute linewidth was determined from the $m_1 = -3/2$ line and the relative widths so determined agreed with these obtained by direct linewidth measurements.

The analysis of the n_1 -dependent relaxation observed in metalaxine solutions was carried out by evaluating the coefficients of T_2^{-1} to various powers of n_1 .

C. Optical Measurements

Two optical systems were employed in taking the optical measurements reported in this thesis. When Amines cylindrical absorption calls were attached to the EPR tubes optical spectra in the range 500 to 2000 mm were taken using a Beckmann DK-2 recording spectraphotometer. Temperature regulation was provided by a thermostat which has been providually described (102) and permitted control to a 200.

Heasurements at reem temperature and in EPR tubes were taken employing a rapid semming optical system constructed by Dye and Foldman (103). With the appropriate source and detector this instrument is mable ever a range from 200 to 2500 mm. Recently, Rymbrandt and

Dye have modified this system so that a Varian V-4540 variable temperature control unit can be used to achieve temperature variation and regulation.

D. Conductance Measurements

Conductance measurements were attempted on sedium-ethylemediamine selutions using an EPR tube with conductance cell attached and employing a Wayne Kerr conductance bridge. The technique employed was similar to that used by Dowald (104).

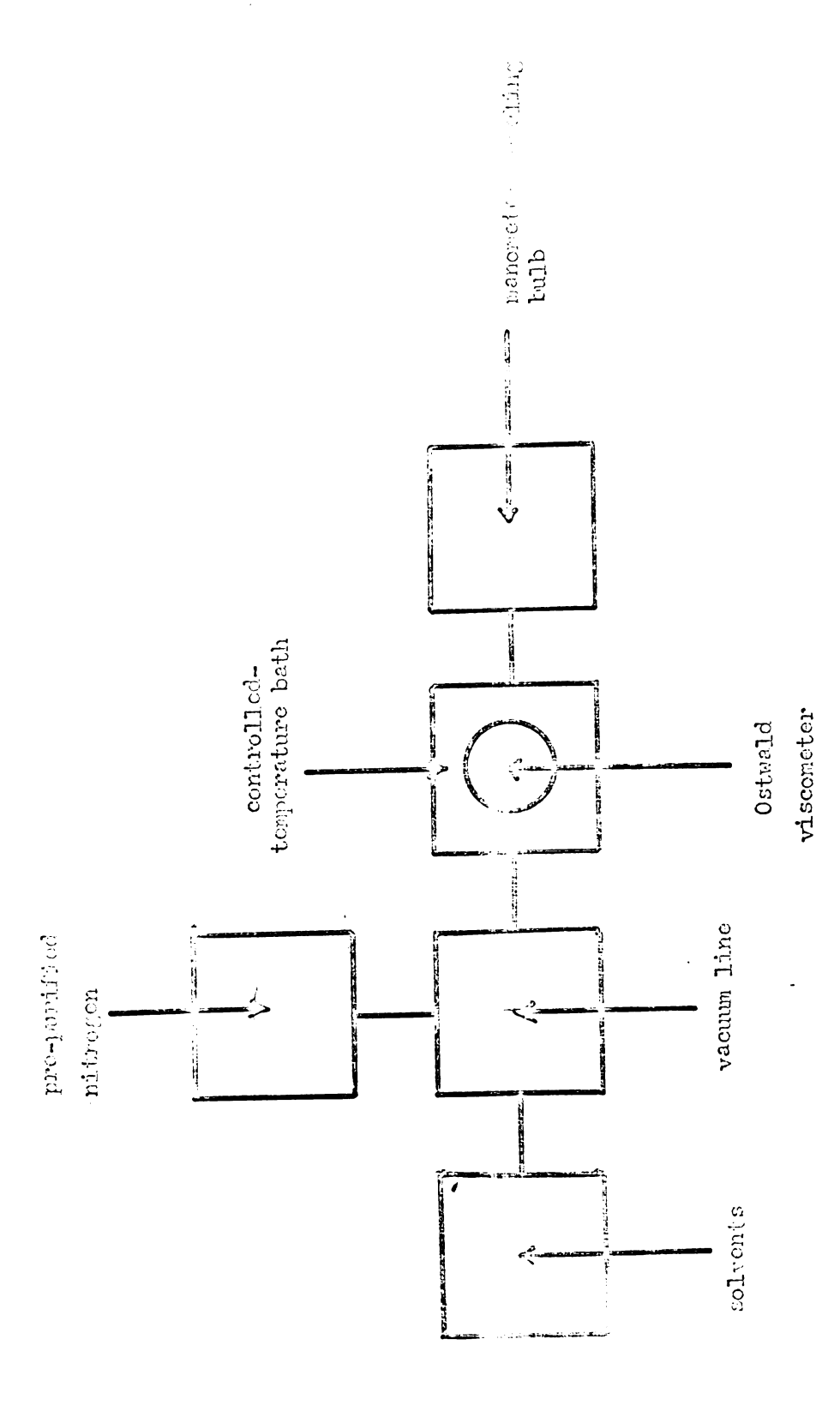
E. Viscosity Measurements

The viscosities of methylamine and ethylamine were determined using the Ostanic viscometer arrangement shown in Fig. 11. The arrangement was so constructed that a solvent could be purified using high vectom techniques, distilled into the viscometer, covered with preparation nitrogen, membraled by means of a mercury leveling bulb, its viscosity measured, and finally distilled out to make way for another solvent. Temperature regulation was achieved by use of an evacuated Downy filled with 2-propagal and cooled by the addition of dry-Los.

The viscometer was first calibrated using acctone and then the viscosities of methylemine and ethylemine were determined using the equation

$$\eta = \rho * \eta' / \rho^* *$$
 (31)

where η is the viscosity; ρ is the density; and t is the time in seconds required for the liquid to flow through the viscometer. The starred quantities refer to acctone.



Block diagram of apparatus used to obtain the viscosities of methylamine and ethylamine as a function of temperature. Figure 11.

RESULTS

A. EPR Measurements on Metal-Amine Solutions (Magnetic Parameters)

The qualitative observation of electron paramagnetic resonance in the metal-amine systems studied by the author are summarized in Table VI. In discussing these systems in detail we shall in general group them according to particular EPR characteristics; hence, our subheadings shall be the characteristic EPR absorptions or species.

1. The monomeric species. The characteristic EFR absorption of most potassium, rubidium, and cesium-amine solutions (also observed for some sodium solutions) is a hyperfine pattern arising from the interaction of a paramagnetic electron with a single alkali metal nucleus. The magnitude of this interaction is always less than the "free atom" value and is very sensitive to solvent as shown in Table VII. In general the hyperfine splitting increases as the ratio of alkyl character increases. This can also be viewed as the hyperfine interaction increasing as the solvating power of the solvent decreases.

Studies on dilute solutions show that the hyperfine splitting is independent of metal concentration.

Perhaps the most startling aspect of the hyperfine interaction is its marked dependence upon temperature. As seen in Table VIII, the hyperfine splitting may change by a factor of 4 over a one hundred degree temperature range. As can also be seen from Table VIII and from Fig. 12,

TABLE VI. Qualitative Nature of the Electron Paramagnetic Resonance Spectra of Hetal-Amine Solutions

Solvent			Hotal		
	Lithium	Sodium	Potaestum	Rubfidtum	Continu
m3	Single 11med	Single linecod	Single linecod	Single line	Single line
IID.3	Single Man	Single 11mb,d	Single 1ino ⁰ Single 1ino ^{b,d}	He from metal muteusbedef: Single linebed	He from metal muleusb.d.f; Single lineb.d
HeIM2/III3	Not studied	Not studied	Not studied	He from metal meleus ^b ; Single line; Broad extra line ^b	He from metal moleus ^b ; Single line; Eroad extra lineb
Hamp/Mo ₂ hh	He from h equiv. nitrogens;				
Etm2	Hfs from h Bequiv. mitrogens be single line bie.def	No spectra bes	He from metal macleus ^{b, h} , ^e , Single line ^{b,h}	He from notel melensboli Angle Masbol	He from metal modeusbal, Single lineba
ethi2m3	Hrs from h equiv. mitrogens h	Not studied	M's from metal. moleus ^b ; Broad extra line ^b	Me from metal moleus ^b	Hrs from motal mucleus ^b ; Broad extra line ^b

TATLE VI. Continued

Solvent			Notel.		
	1.1 thim	Sedium	Potaestina	Pablidium	Condum
Bung/henn2	Single line	life from metal moderneby Single line	He from sotal madense	Fot studied	Not studied
etm_/na	Sot studied	not studied	He from metal mediensky Single tinek	Fot studied	Not studied
2 2 3 3 3 3 3 3 3 3 3 3	Not stadied	Not staffed	He from metal modeusbehr Engle 11meh	He from metal ancloses	He from metal modersh Magic Mash
14P #fff ₂	Fot studied	Not studied	He from metal medensbab, Angle Hash	He from patel ancloses by	He from metal modens ^{b, k} , Magle line
etmyl-prinz			He from metal modern's		
FUA	Single line	Single lineden	Magle Madda	Single line don	Single line
1.2 PDA	Sot studied	Not studied	He from metal modeus ^b ; Single line	life from metal modens ⁵ : b Magle 11m	He from metal medeus ^b ; single line
1.3 PDA	Not stadied	Not staffed	He from metal medieneby Single 14me	He from metal mediens ^b ;	He from metal medicus ^b ; Single 15m

TAIRE VI. Continued

Solvent				Metal		
	11thdu	8	Sodium Sodium	Potassium	Publed un	Condina
3-1PA	Not studied	ndted	Not studied	His from metal madeus ^{bolt} bel	He from petal moleus ³⁰¹ s, Single line ^b el	He from metal moleus ^{bel} i Single line ^{be} l
1.2 PDA/34"PA Bot studied	Bot stu	rd1od	Not studied	Hfs from metal moleus ^b ; Mngle line ^b	Not studied	Not studied
Buille	not at	not stadied	Fot studied	He from metal macleusbeh; Magle linoh	lifs from metal moleus ^b el	
a-Pully still fot studied	Sot at	potpo	Not studied	He from metal macleash; Single limeh	Not studied	Not stadied
liexanethyl. phosphorie tri arkie	tot studied	perpa	Fot studied	Complex spectre Rot studied	hot studied	Not studied
1,2-Masthory- Not studied othere	- Not st	pe ipu	No signal has	fo eignel ⁿ	No stgnal	Not studied
Fis (2-(2-methoxy- ethoxy)ethyl) Not ether	hony. Not studied	361 64	not studied	್ಟಿಂ ಆಗ್ಲೆಲಾಖ್	Single line	Not studied

Only the characteristic absorptions are given.

This work.

References 6 and 7.

dasferences 37 and 69.

Reference 43.

factorence 115.

Esotium does not appear to be soluble in ethylanine.

References 51 and 52.

Reference 115.

Although no electron paramagnetic resonance spectra have bean taken, the author has observed this asine to form the characteristic blue solution upon dissolution of lithium.

Kolution was metastable.

1 Solution was very unstable.

Raforence A.

Reference 29.

Osodium-potassium alloy was used.

TABLE VII. The Hyperfine Splitting, Am, of the Menomeric Species as a Function of the Metal and Solvent Employed.

		A _M (Gauss) ^b				
Solvent	23 _{Na}	39 _K	85 _{Rb}	133 _{Cs}		
MenH ₂			25.60 ± 0.3 (23°C)	55.89 ± 0.8 (23°C)		
ELNH ₂		13.00 ± 0.1 (50°C)	64.06 ± 0.3 (23 ⁶ C)	127.6 ± 0.6 (23 ⁸ C)		
Ethe2/Menh2	5.79 ± 0.1 (23°C)					
n-Priff ₂		14.00 ± 0.1 (23 ⁸ C)	83.91 ± 0.4 (23°C)	171.5 ± 2.0 (23°C)		
1-Priii		18.25 ± 0.1 (23 ⁰ C)	99.2 ± 3.0 (0 ⁸ C)	240.7 ± 5.0 (20 ⁸ C)		
3- 1 /PA		5.17 ± 0.3 (-16 ⁰ C)	59.19 ± 2.6 (23 ⁸ C)	71.46 ± 1.0 (-40°C)		
1,2-PDA		2.82 ± 0.3 (0°C)	30.55 ± 0.3 (20°C)	67.30 ± 0.6 (26°C)		
3-194/1, 2-PDA (1/1)		5.45 ± 0.2 (10 ⁰ C)				
1.3-PDA		2.74 ± 0.3 (-10°c)	30.81 ± 0.3 (20°C)	67.47 ± 0.6 (20°C)		

Only values obtained by the author or by the author and V. A. Hiesly are reported.

It is often convenient to express hyperfine splittings as percent free stem splitting. This is accomplished by dividing the observed splitting by the free stem splitting. The free atom splittings for the alkali metals are as follows: $A_{14} = 143$ G; $A_{8a} = 316$ G; $A_{8} = 82.5$ G; $A_{8b} = 363$ G; $A_{Ca} = 818$ G.

TABLE VIII. The Hyperfine Splitting, $A_{\hat{H}^0}$ of the Homeneric Species as a Function of Temperature.

			dvlemine Hum (⁸⁵ Rb)		
T(°C)	A _M (Gauss)	T(°C)	A _M (Gauss)	T(°C)	A _H (Ganes)
90	36.8	43	27.8	- 5	18.0
85	35.9	40	25.6	-20	15.0
80	34.6	25	24.0	-25	15.0
70	33.0	23	25.6	-30	13.6
60	31.1	19	23.2	40	10.0
<i>5</i> 7	30.0	10	21.5	-45	11.2
50	28.6	-3	20.0	-75	6.1
		Coatx	m (¹³³ Ce)		
T(*C)	A _M (Genes)	T(*C)	A _H (Genes)	T(°C)	A _K (Games)
75	84.2	22	55.7	5 0	20.6
70	83.5	22	52.8	-60	18.3
6 8	78.2	7	44.3	-73	15.2
60	75.0	6	45.0	-75	15.0
50	70.2	~5	39.0	-3.00	12.9
40	63.7	-12	35.8	-100	14.3
30	58.2	-21	33.4		
23	52.9	-35	26.0		

			derlacine dina (⁸⁵ Nb)		
T([©] C)	A _M (Gazes)	T(°C)	A _M (Genes)	T(°C)	A _M (Ganes)
50	78.8	9.0	49.6	-80	55 -1 4
40	72.8	0	43.9	-80	<i>5</i> 4,63
35	69.8	-10	43.5	-80	55.78
30	66.5	-20	37.8	-9 0	50.71
23	64.1	-30	34.1	-9 0	50.71
23	65.0	ئ ە	25,4	-9 0	50.69
20	61.0	-50	20.0	-100	46.21
15	57.5	-70	99.28	-100	49.02
10	55.0	-70	59.35		
5	52.0	-70	59.15		
		Cost	ma (133cs)		
T(°C)	A _M	T(°C)	A _M (Gause)	T(°C)	A _H (Ganes)
85	205	10	118.8	-30	83.25
80	197	10	117.8	-30	82.93
70	185	10	117.8	40	77-30
60	173	0	109.6	-40	76.90
50	161.8	0	107.5	-40	77.71
40	149.6	0	108.6	-5 0	71.64
40	150.2	-30	98.59	~5 0	71.55
30	138.7	-20	90.46	-50	70.34
M 0	138.7	-20	89.87	-60	64.61
20	127.8	-20	90.67	-60	64.86
20	127.7	-30	82.81	-60	65.06

			envlamine enium (³⁹ K)		
7(°C)	A _N (Gauss)	T(°C)	A _M (Ganss)	T(*C)	A _H (Genes)
80	21.8	30	14.6	-10	9.4
70	20.3	23	14.0	-20	8.3
60	18.9	20	13.2	-30	7.2
50	17.5	10	11.9	-35	6.6
40	15.9	0	10.5		
		Rubidi	lam (⁸⁵ Rb)		
T(°C)	A _N (Games)	T(°C)	A _H (Ganse)	T(*C)	A _H (Ganes)
40	91.5	29	86.5	10	79-1
36	91.0	25	85.7	0	75.0
35	89.0	23	83.9	-10	70.5
32	88.0	20	83.0		
		Contr	m (¹³³ cs)		
7(°C)	A _M (Gauss)	T(°C)	An (Ganse)	T(*C)	A _M (Gause)
50	204	30	180	-10	135
45	197	23	172	20	125
40	193	10	1.57	-30	116
35	186	0	145		
		Isom	continue		
		Potas	rism (³⁹ K)		
T(°C)	A _H (Ganss)	T(* C)	A _H (Genes)	T(°C)	A _H (Gense)
30	19.4	23	18.3	15	16.9
25	18.5	20	17.5	0	14.1

TABLE VIII. Continued.

			ronvlanine um (¹³³ cs)				
?(* C)	Ag(Genes)	T(* C)	A _H (Genes)	T(*C)	A _M (Gense)		
20	241	10	231	0	220		
			mm (¹³³ cs)				
7(*c)	A _N (Games)	T(* C)	Ag(Genes)	T(°C)	A _N (Games)		
-20	82.0	30	77.8	-42	69.1		
-25	80.3	-40	71.5	45	69.5		
1.2-Prepanadianina Potassium (³⁹ K)							
7(°C)	A _H (Ganes)	T(OC)	A _N (Ganas)	T([©] C)	A _K (Gause)		
50	5.91	10	3.82	-20	2.75		
40	5-35	0	3.25	-20	2.55		
30	4.55	0	2.81				
20	4.42	-10	2.75				
Rubidium (⁸⁵ Rb)							
1(°C)	Ag(Games)	T(* C)	An (Genes)	T(*C)	A _M (Games)		
60	38.6	25	30.5	0	66.6		
50	37.0	20	30.6	-10	23.9		
40	34.1	15	29.2	-20	21.9		
30	32.4	10	27.7				

			namedianine m (¹³³ Cs)				
T(*C)	A _K (Genss)	T(* C)	Ag(Genes)	T(OC)	A _N (Games)		
60	83,5	30	72.7	-10	57.5		
50	82.0	20	67.3	-20	54.2		
45	76.7	10	63.1	-30	50.5		
40	75-5	0	60.8				
	3-Methers	-n-mant en	ine/ 1.2-Proper	edicates			
		Potess	dum (³⁹ K)				
T(°C)	A _M (Genss)	T([©] C)	A _M (Ganes)	7(*C)	A _H (Gmass)		
10	5.45	5	5.16	0	4.94		
1.3-Propanedianine							
Potassium (³⁹ K)							
T(°C)	Ag(Ganes)	T(°C)	A _K (Gause)	T(°C)	A _H (Games)		
50	5.90	10	3.80	-20	2.83		
40	5-35	0	3.40	-20	2.63		
30	4.75	-10	2.72				
20	4.25	-20	2.48				
		Rebidi	mm (⁸⁵ Rb)				
T(°C)	A _K (Gense)	T(°C)	A _H (Games)	T(*C)	A _H (Gâmes)		
45	35.0	30	2.1	15	28.6		
40	34.0	20	30.8	0	23.6		
35	33.0						

TABLE VIII. Continued.

			penediamine ium (¹³³ Cs)		
T(°C)	A _H (Games)	T(°C)	A _H (Gazes)	T(° C)	Ag(Gense)
60	82.4	10	64 .6	-20	52.7
40	74.4	0	60.5	-30	50.3
20	67.5	-11	54.3		

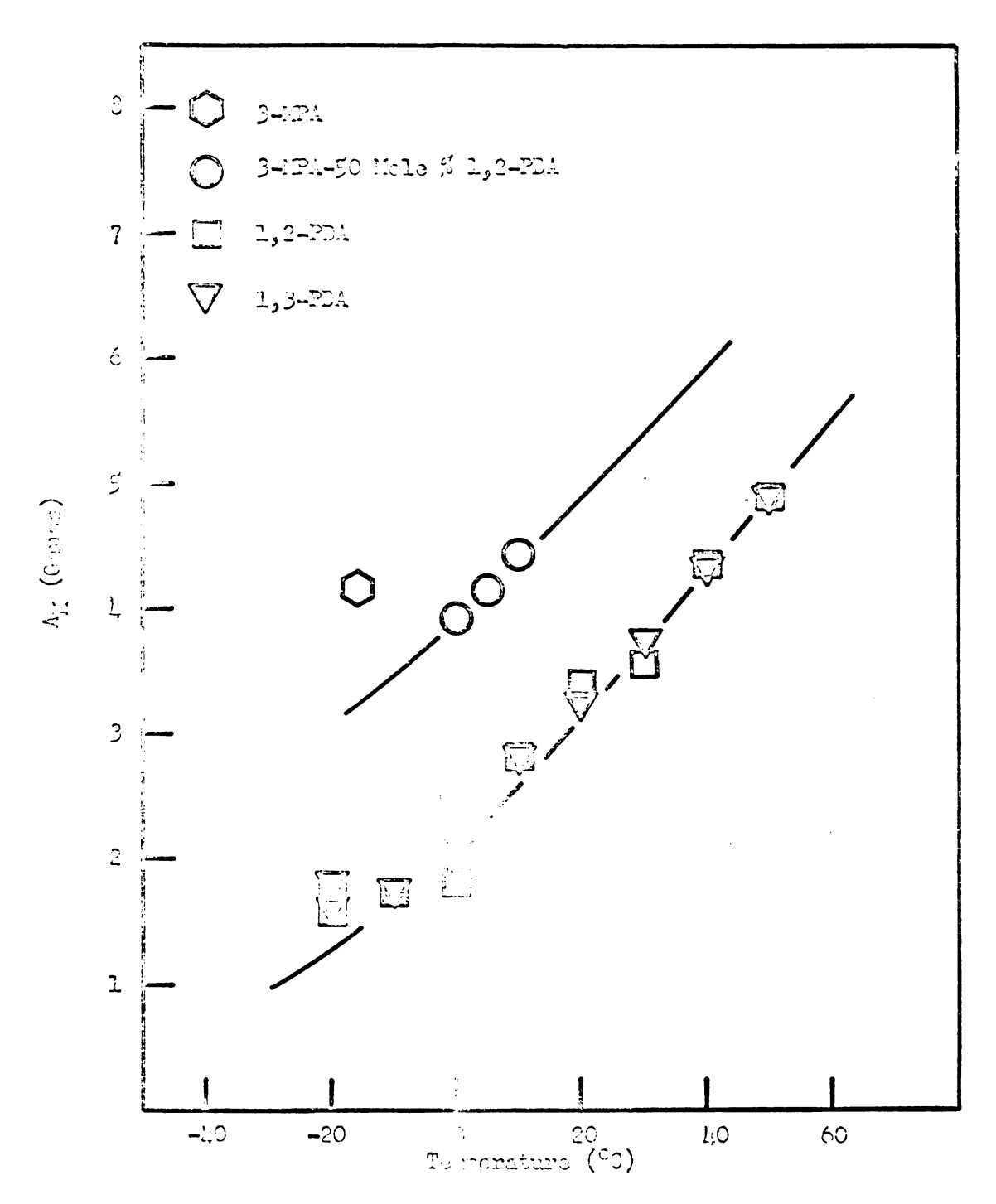


Figure 12a. Hyperfine collections for some potassium solutions as a function of solvent and temperature.

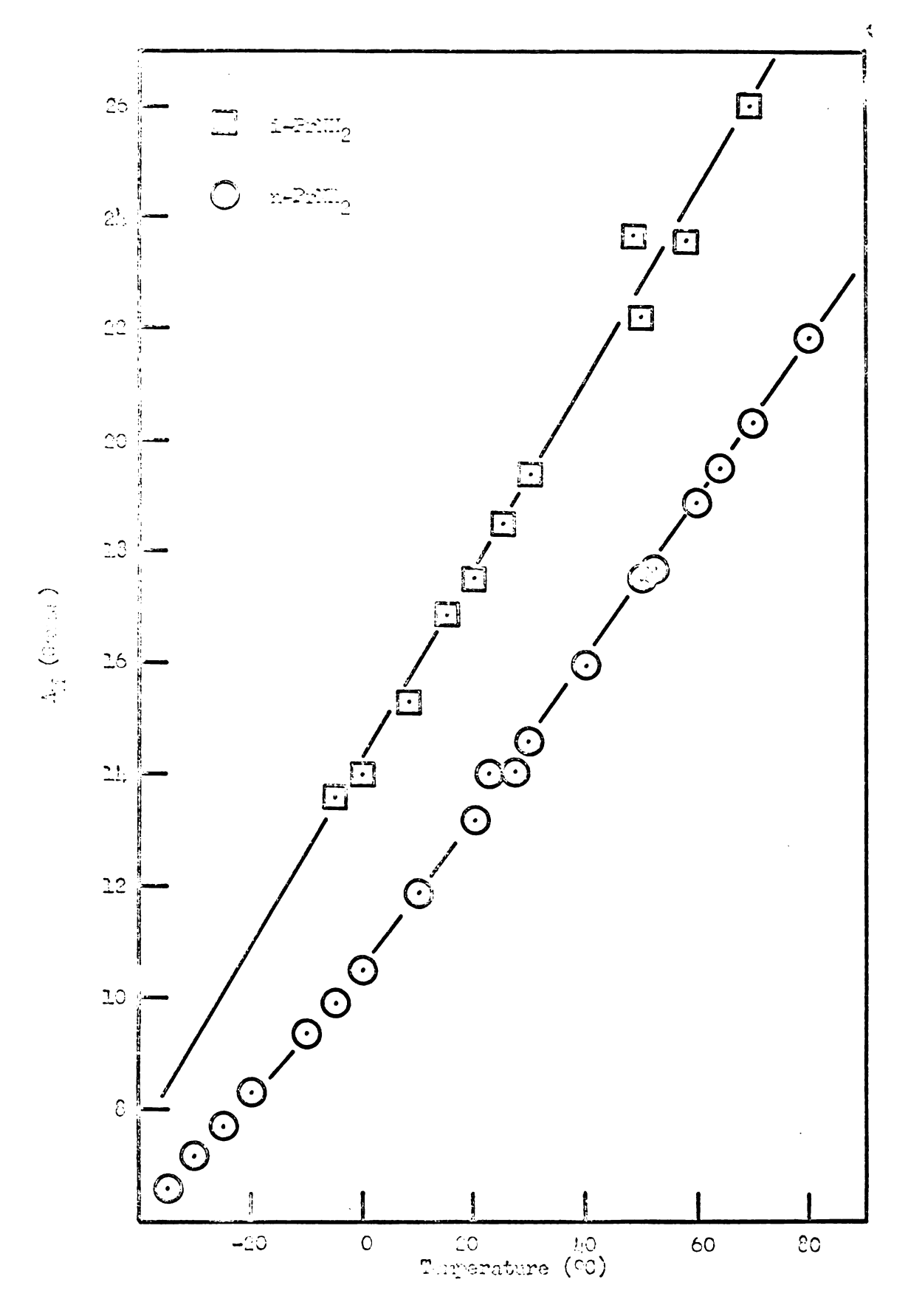
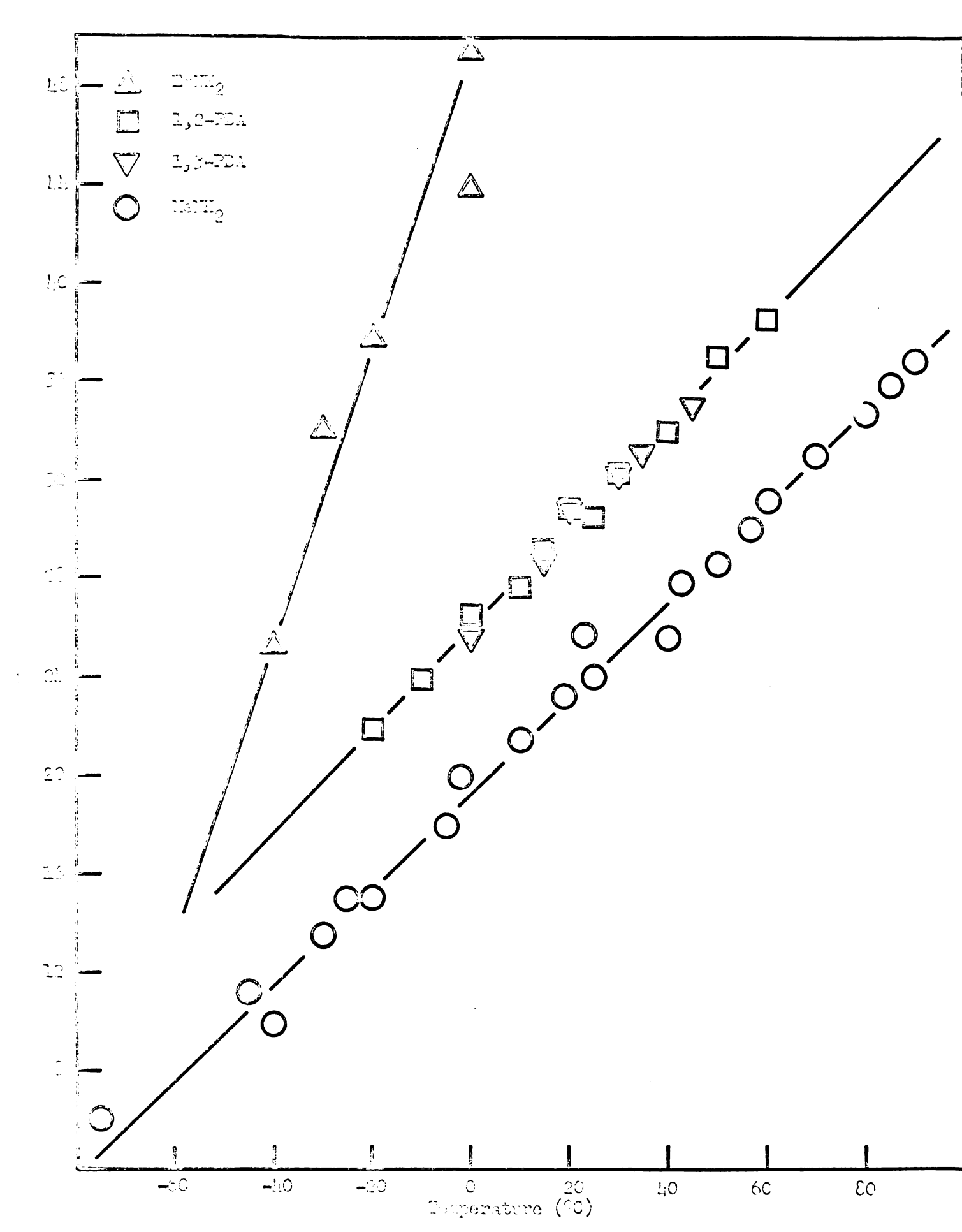


Figure 12b. Hyperfine splitting for some potassium solutions as a function of solvent and temperature.



Pagure 12c. Experdine splitting for some rubidium (85Rb) solutions as a functio of solvent and temperature.

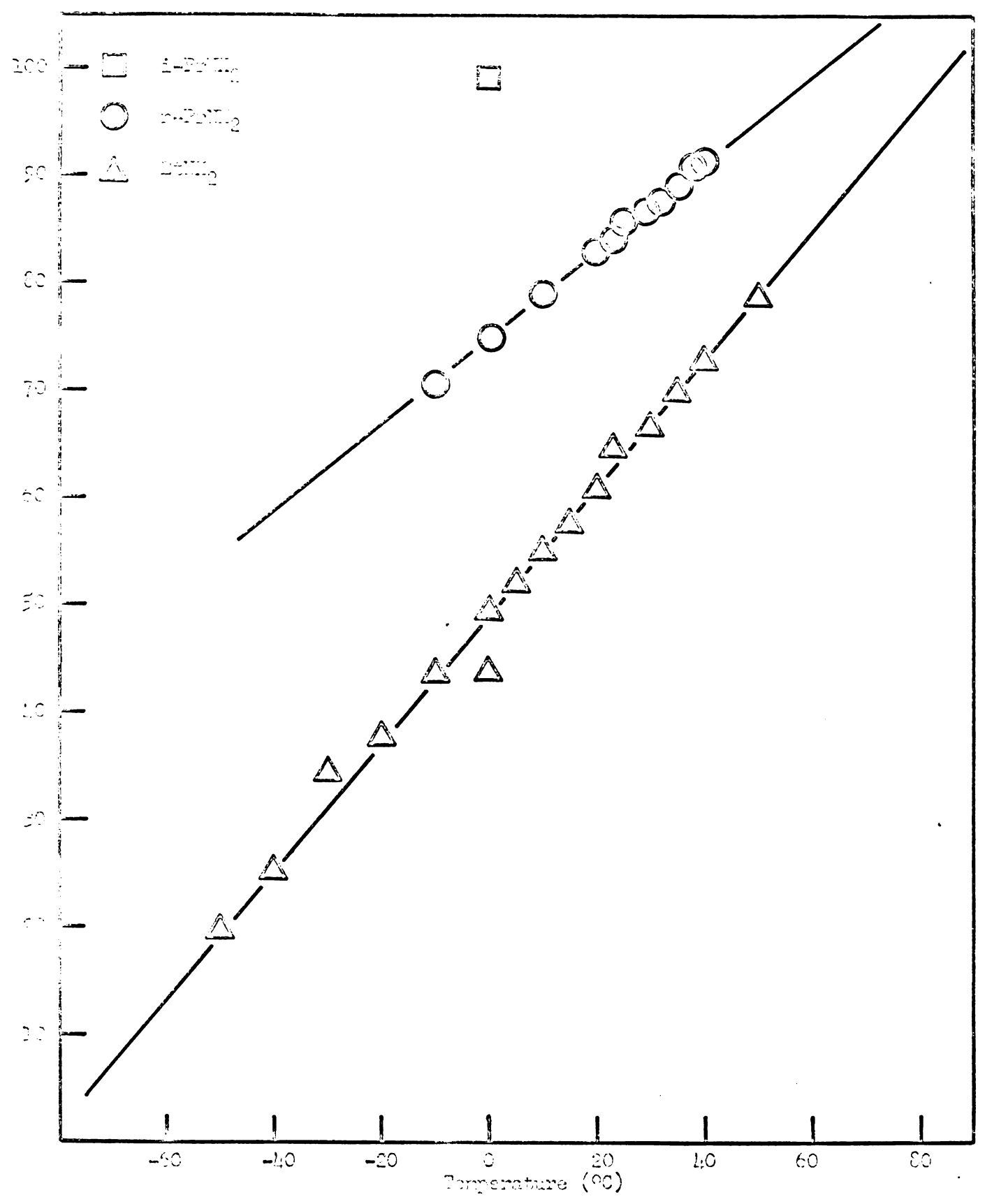


Figure 12d. Hyperfine splitting for some rubidium (85Rb) solutions as a function of solvent and temperature.

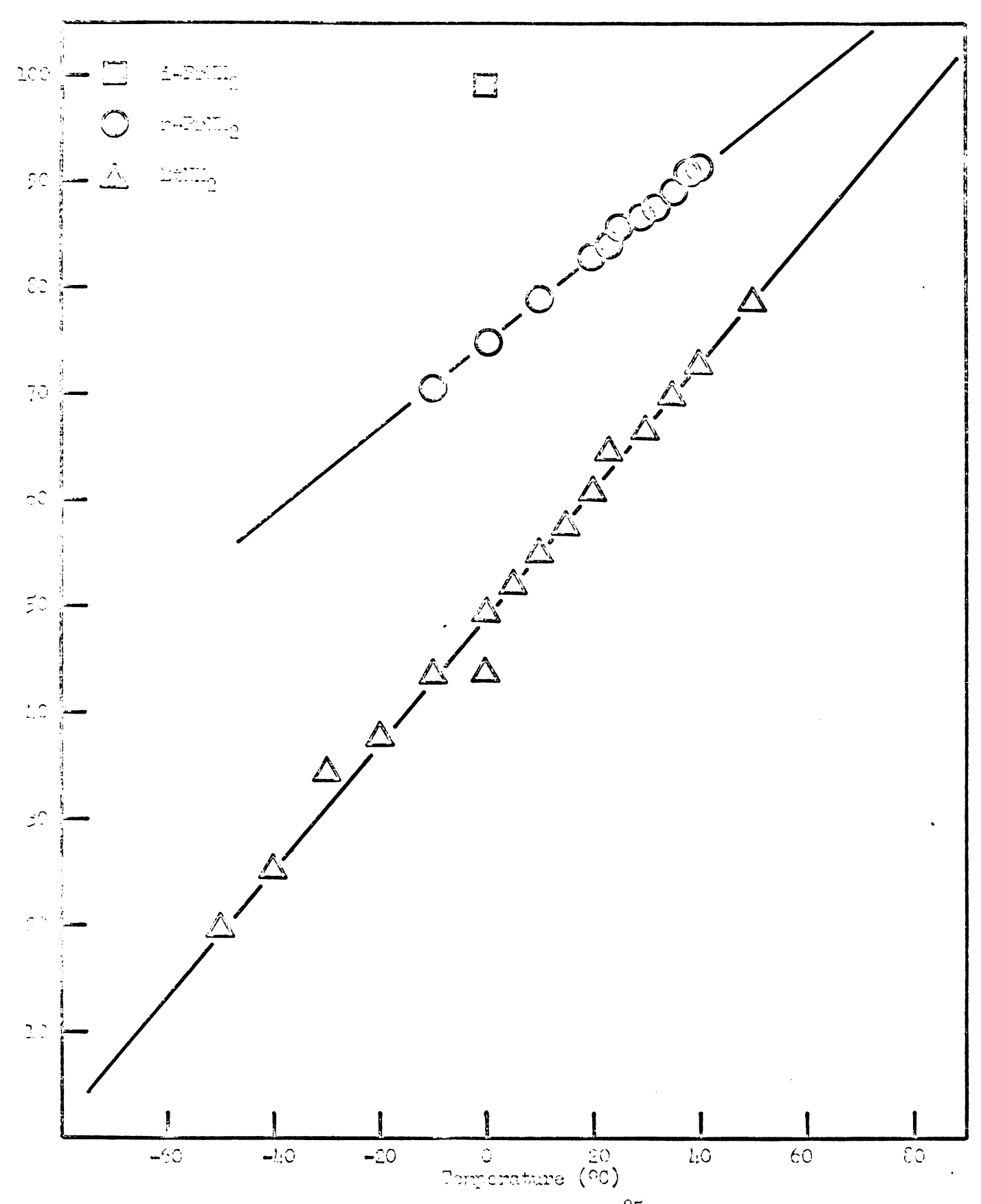
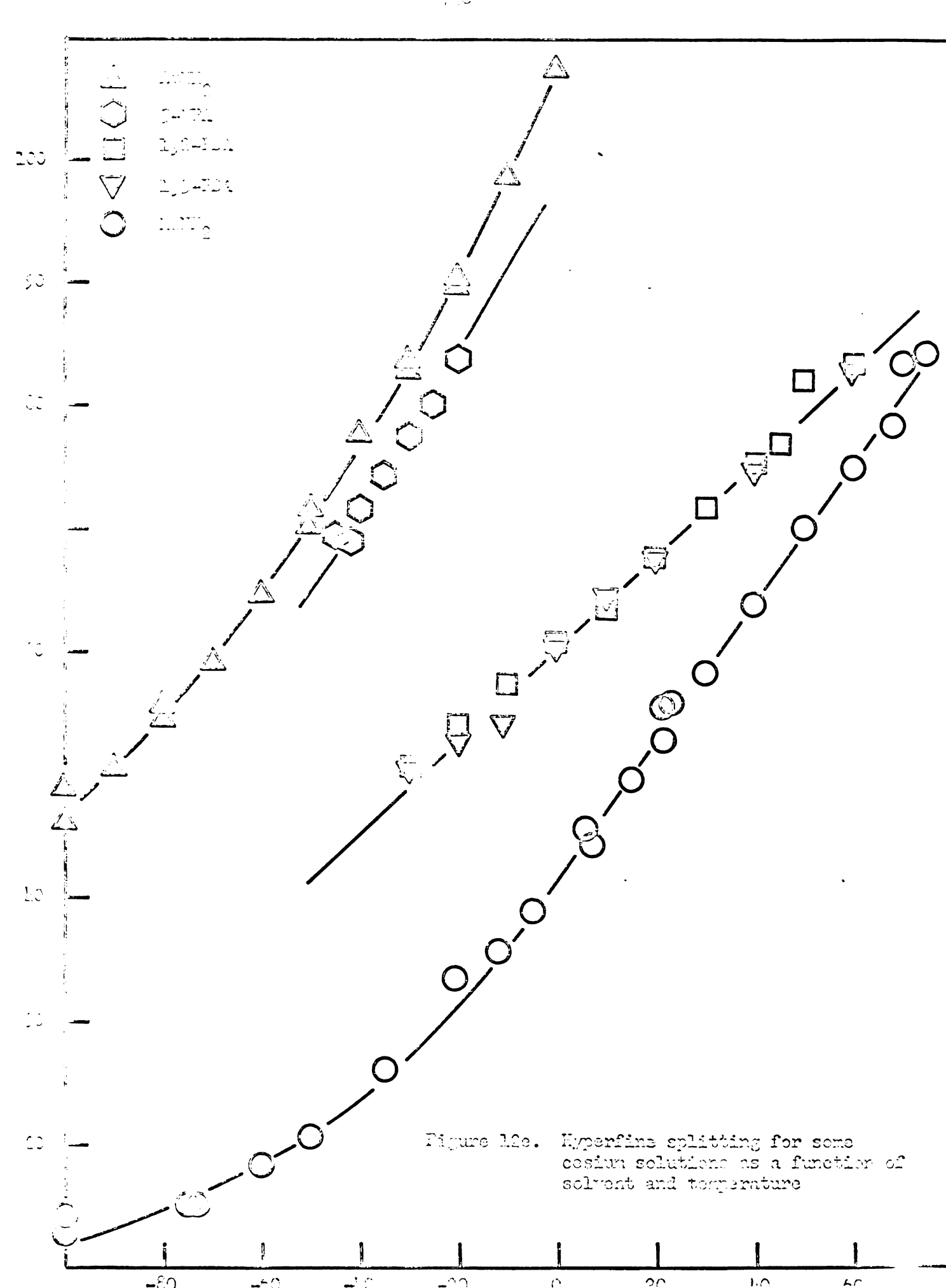


Figure 12d. Hyperfine splitting for some rubidium (^{85}Rb) solutions as a function of solvent and temperature.



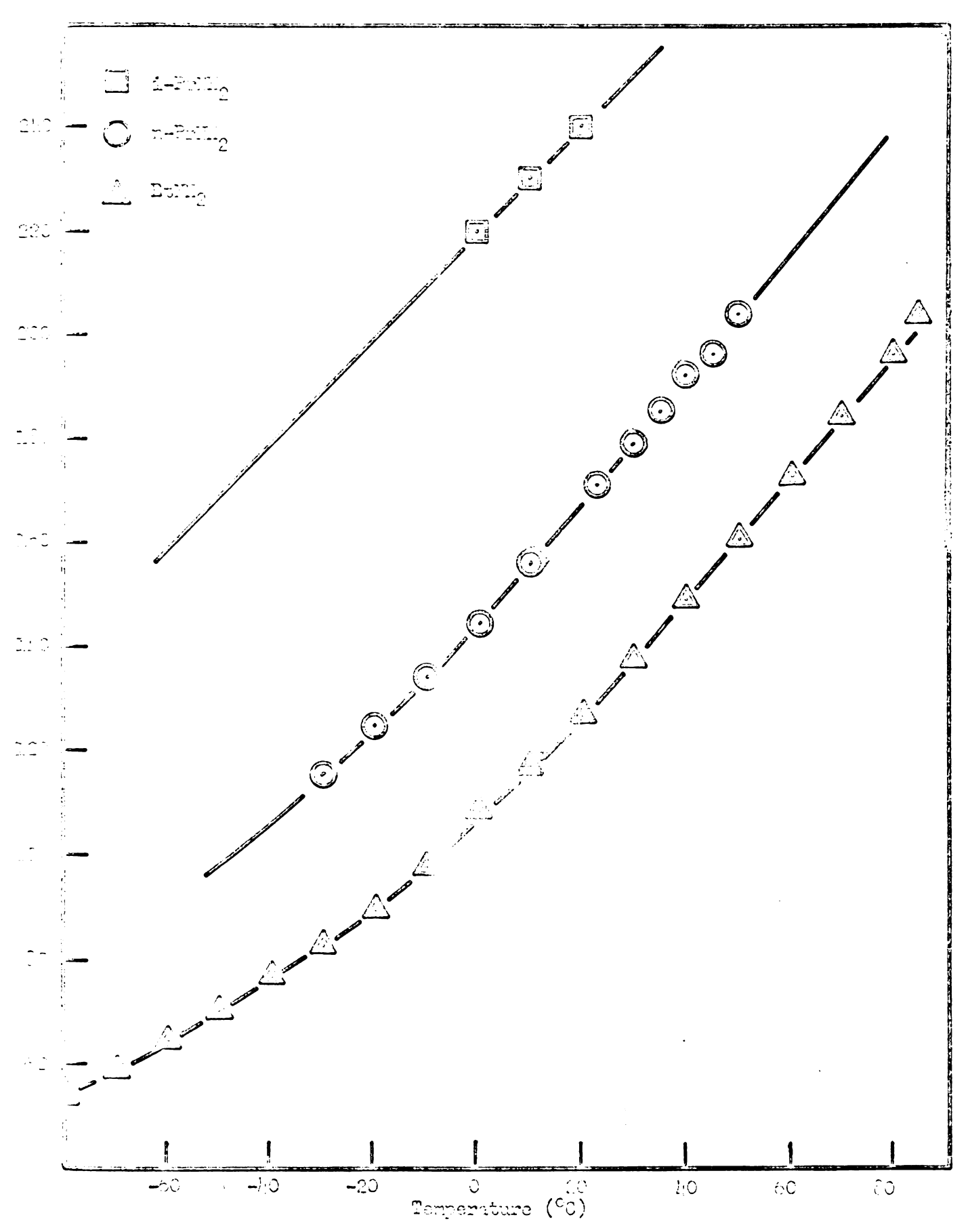


Figure 121. Typerfine splitting for some design solutions as a function of colvent and temperature.

the functional dependence of $A_{\underline{M}}$ upon temperature is not always the same. However, in ne instance has the hyperfine interaction been observed to increase with decreasing temperature.

As can be observed from Table VII and Fig. 13, the effect of mixing two amines or of mixing ammonia with an amine is to yield a value of A_M intermediate between the values for the metal dissolved in the pure solvents. However, the temperature dependence of A_M for the mixed solvent may or may not be the same as for the pure solvents as can be seen from Fig. 14.

The g-value of the monomeric species as can be noted from Table IX appears to be nearly independent of the solvent used but appears to be a strong function of the alkali metal investigated.

The temperature dependence of the g-value also varied from metal to metal as can be seen from Fig. 15 and Table X. For solutions of potassium in the smines, g_M is nearly independent of temperature while the g-value for rubidium and ossium solutions decreases markedly with increasing temperature over the range from -100° C to room temperature. The scatter of the data prevents the establishment of a definite pattern for rubidium and cesium solutions above room temperature.

The g-value of the monomeric species is independent of metal concentration and is only slightly affected by the addition of ammonia er a second amine to the solution under investigation.

The spin concentration of the monomeric species in saturated metal-amine solutions as a function of metal and solvent used is given in Table II. The concentration of the monomeric species is observed to decrease as the temperature is decreased. The relative magnitude of this decrease is similar to that reported in Ref. 42.

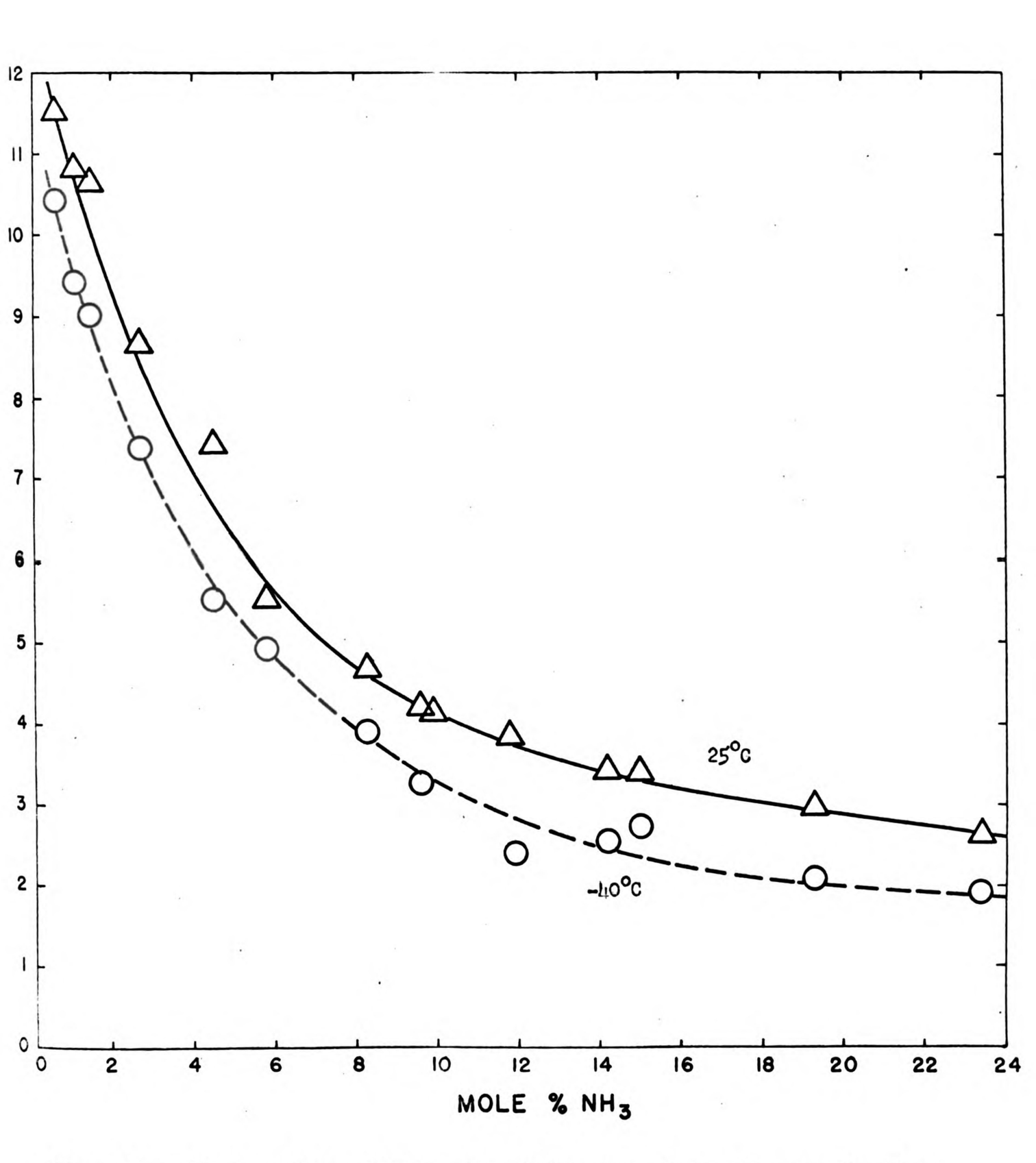
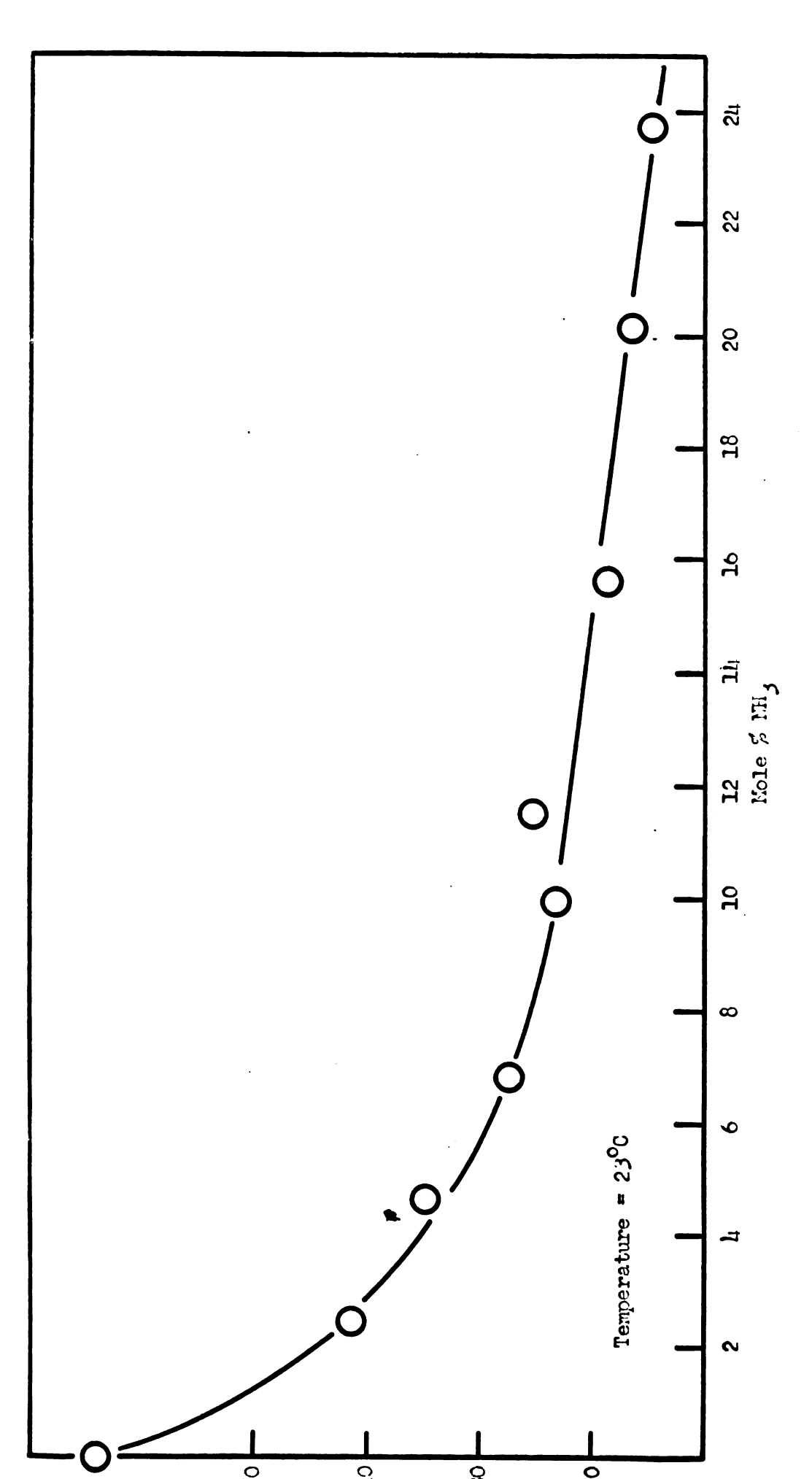


Figure 13a. The hyperfine splitting, Am, of the monomeric species as a function of ammonia concentration for some potassium-ethylamine solutions.



The hyperfine splitting, $A_{\rm M}$, of the monomeric species as a function of armonia concentration for some rubidium (M5Rb) solutions. Figure 135.

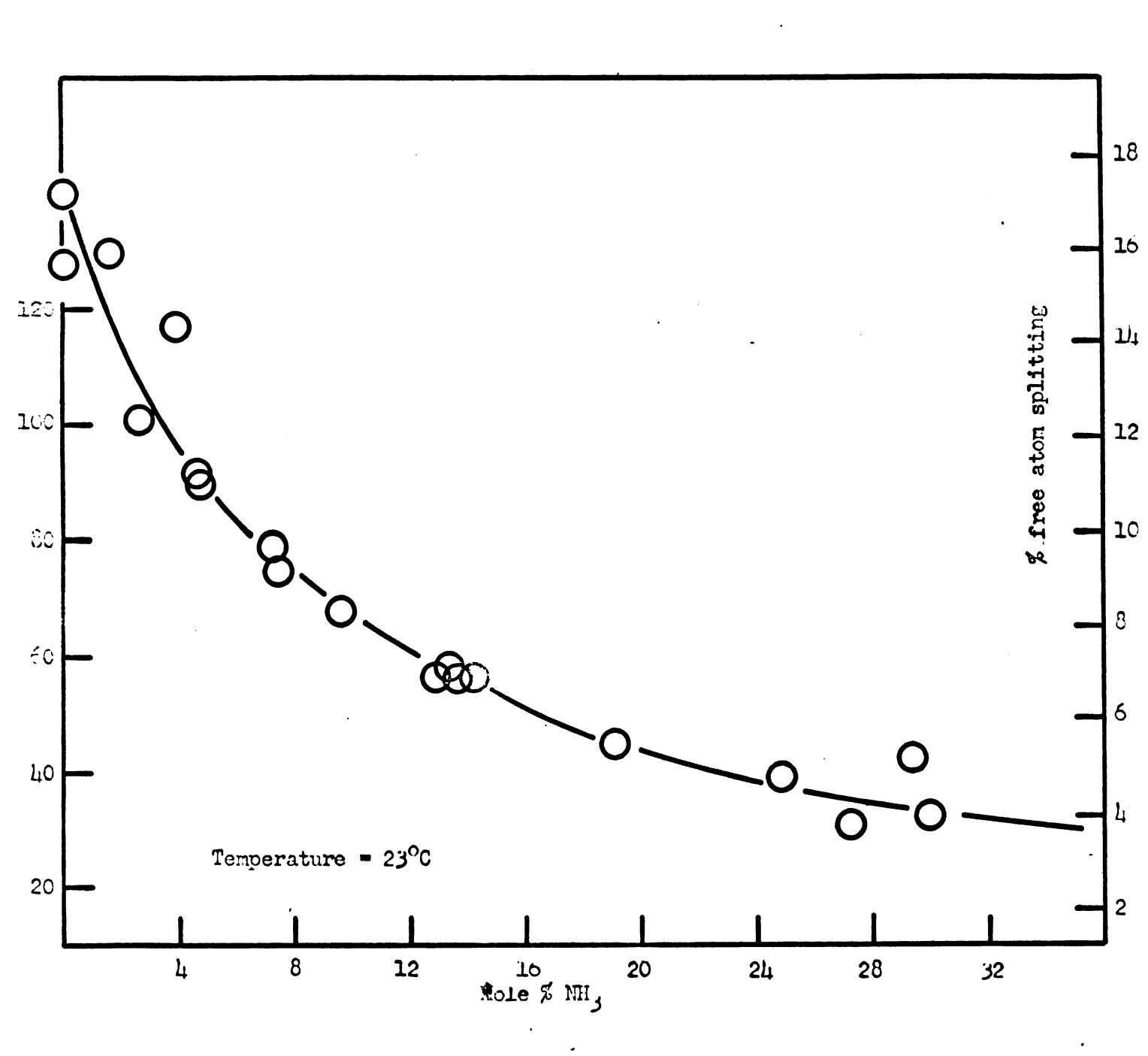
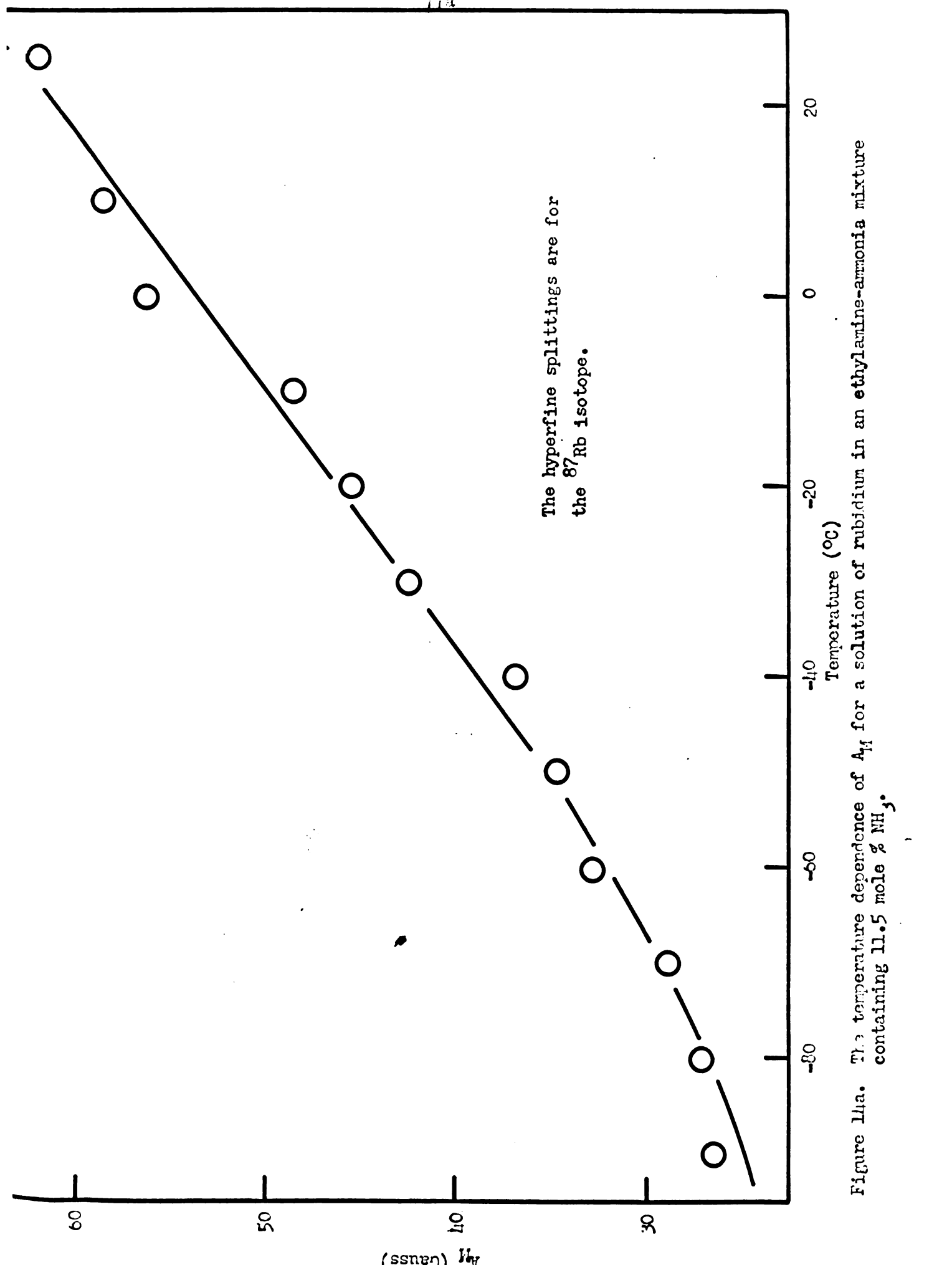


Figure 13c. The hyperfine splitting, $A_{\rm M}$, of the monomeric species as a function of ammonia concentration for some cesium-ethylamine solutions.



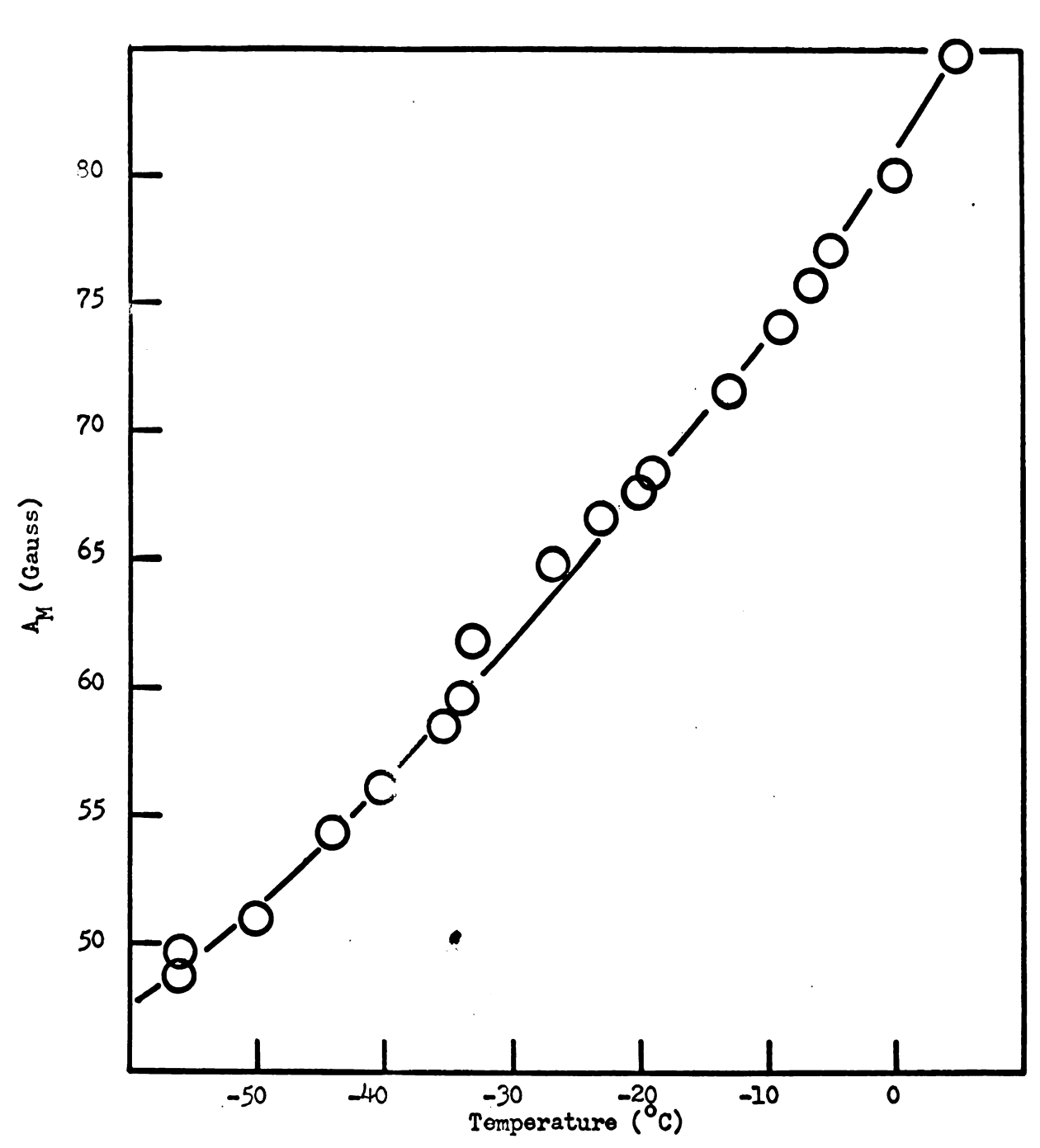


Figure 14b. The temperature dependence of A_M for a solution of cesium in an ethylamine-ammonia mixture containing 3.6 mole % NH₃.

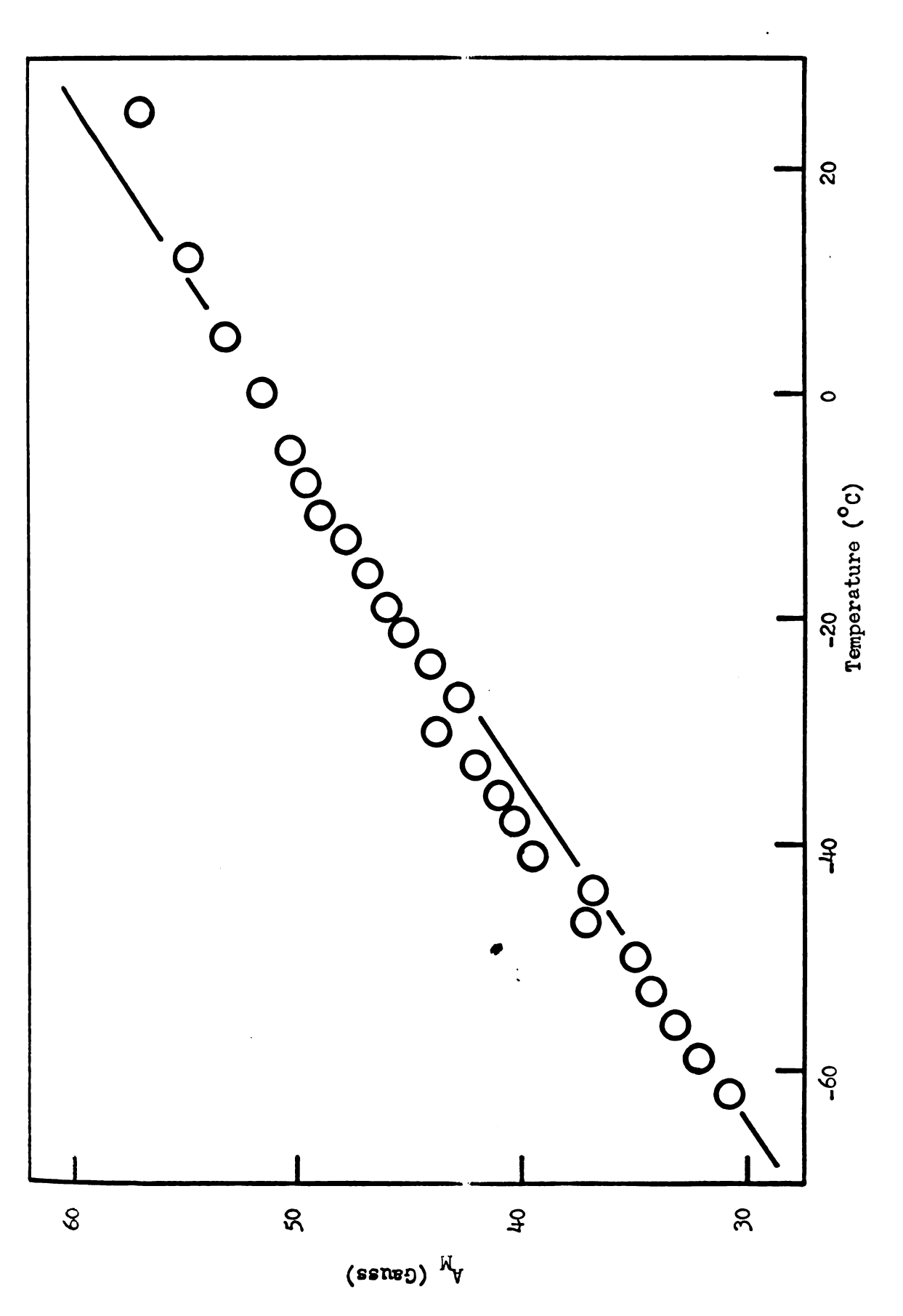


Figure 14c. The temperature dependence of A, for a solution of cesium in an ethylamine-ammonia mixture containing $14.3~\mathrm{mole}$ % NH_3 .

TABLE IX. The g-value, g_H of the Monomerie Species as a Function of Alkali Metal and Solvent for a Number of Metal-Amine Solutions.

Solvent			Hotel	
	23,14	≫ _K	85 _{Rb}	133 _{Ce}
MARIA 2			1.99986 ± 0.0005 (23°C)	1.99481 4 0.0007 (23°C)
enh ²		2.00140 ± 0.0002 (0°C)	1.99982 ± 0.0002 (23°C)	1.99484 ± 0.0002 (23°C)
HH2/	2.00149 ± 0.0002 (23°C)			
-Pran		2.0015 ± 0.0002	1.99979 ±	1.99479 4
Priii		(23°c) 2.0013 ± 0.0002 (23°c)	(23°c) 1.9998 a 0.0006 (0°c)	(23°C) 1.99¼6 ± 0.0008 (20°C)
→ PA		2.0013 ± 0.0005 (-16°C)	(0 0)	1.997 ± 0.002 (_40°c)
, 2 PDA				1.996 ± 0.001 (20°C)
,3-PDA				1.996 ± 0.001 (20°C)

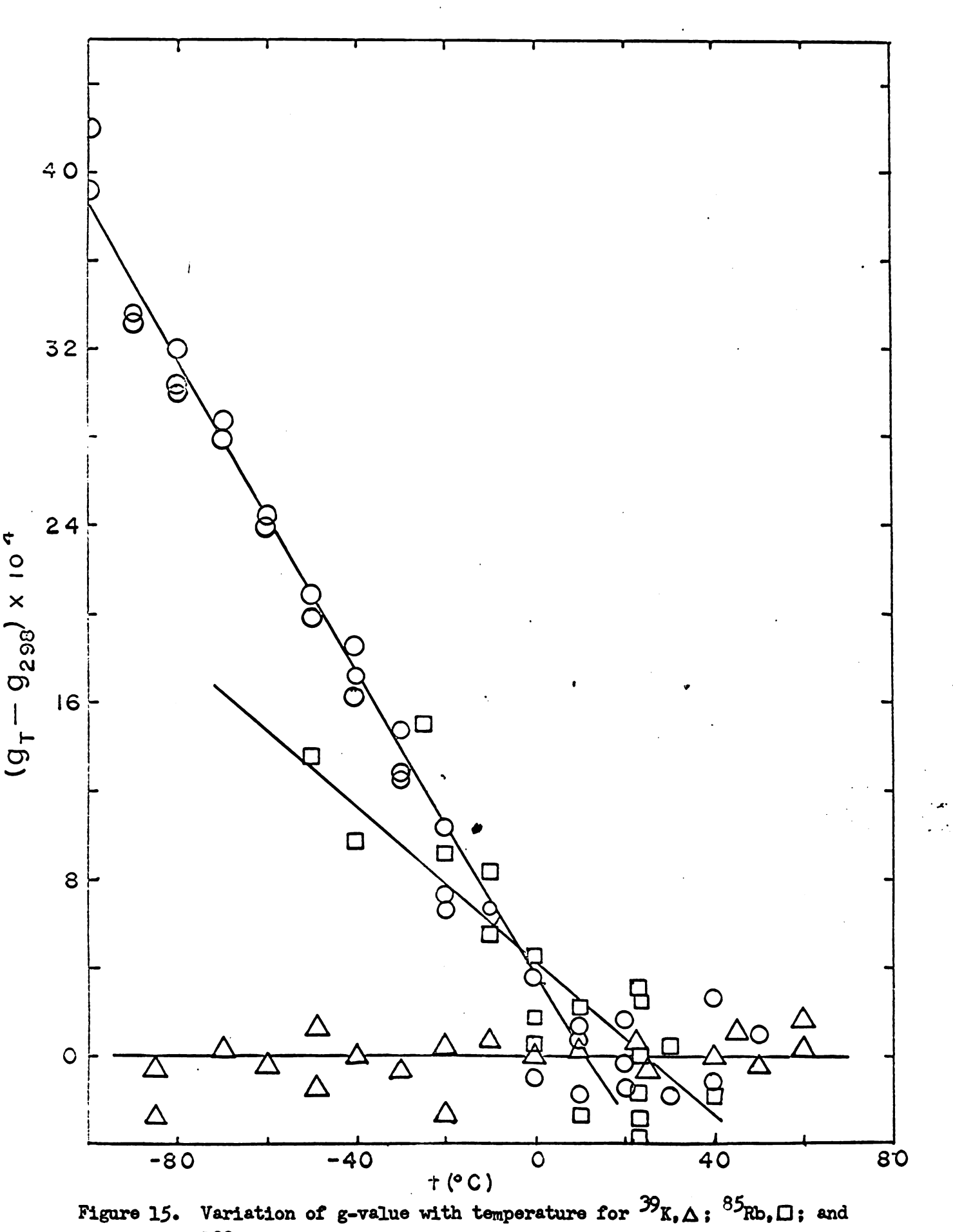


TABLE I. The g-value, $\mathbf{g}_{\mathbf{M}^0}$ of the Monomeria species as a Function of Temperature.

2.00157 50 2.00002 2.00154 55 1.99986 2.00156 40 2.00000 2.00156 20 1.99989 2.00156 20 1.99982 0 2.00156 0 1.99875 0 2.00158 0 1.99985 0 2.00150 -30 1.99992 0 2.00150 -30 1.99992 0 2.00150 -30 1.99995 0 2.00152 -50 2.00080 5 2.00165 -50 2.00082 Cestus Column Colum			[thvi sains		
2.00157 50 2.00002 2.00154 55 1.99906 2.00156 40 2.00000 2.00156 20 1.99989 23 2.00156 23 1.99982 00 2.00150 0 1.99875 20 2.00152 20 1.99902 20 2.00156 20 1.99935 20 2.00156 20 1.99935 20 2.00156 20 1.99935 20 2.00156 20 2.00080 25 2.00165 40 2.00080 25 2.00165 20 1.99970 20 1.99501 20 1.99502 20 1.99501 20 1.99502 20 1.99507 10 1.99500		Potessium		Rubidism	
2.00144 b5 1.99986 2.00136 b0 2.00000 2.00140 30 1.99989 23 2.00146 23 1.99982 0 2.00140 0 1.99874 0 2.00148 0 1.99885 0 2.00148 0 1.99985 0 2.00112 -20 1.99902 0 2.00140 -30 1.99921 0 2.0015 -30 1.99935 0 2.00165 -40 2.00080 2.00165 -40 2.00082 Continue Continue Continue Continue Continue Continue 1.99495 0 1.99511 20 1.99502 0 1.99497 10 1.99490	T(°C)	g-value	T(*c)	e-value	
2.00136 40 2.00000 0 2.00140 30 1.99989 23 2.00146 23 1.99982 0 2.00148 0 1.99885 20 2.00148 0 1.99985 20 2.00140 -30 1.99902 20 2.00140 -30 1.99921 20 2.00142 -40 2.00080 20 2.00142 -40 2.00080 20 2.00165 -40 2.00082 Continue Continue Continue Continue 1.99495 20 1.99470 0 1.99501 20 1.99502 0 1.99497 10 1.99490	60	2-00157	50	2.00002	
2.00140 30 1.99989 23 2.00146 23 1.99982 0 2.00140 0 1.99874 20 2.00148 0 1.99885 20 2.00140 -30 1.99902 20 2.00140 -30 1.99921 20 2.00140 -30 1.99935 20 2.00142 -40 2.00080 25 2.00165 -40 2.00082 Cestus Costus 1.99495 20 1.99470 20 1.99502 20 1.99502 20 1.99481 20 1.99490	60	2-00144	45	1.99986	
23 2.00146 23 1.99982 0 2.00140 0 1.99874 20 2.00148 0 1.99685 20 2.00112 -20 1.99902 20 2.00140 -30 1.99921 20 2.00156 -30 1.99935 20 2.00165 -40 2.00080 25 2.00165 -40 2.00082 Costum Costum Costum 1.99495 20 1.99470 0 1.99511 20 1.99481 0 1.99477 10 1.99490	50	2.00136	40	2.00000	
0 2.00140 0 1.99874 0 2.00148 0 1.99885 0 2.00112 -20 1.99902 0 2.00140 -30 1.99921 0 2.00142 -40 2.00080 5 2.00165 -40 2.00082 Costum Costum Costum 1.99495 20 1.99470 0 1.99511 20 1.99502 0 1.99477 10 1.99490	40	2.00140	30	1.99989	
2.00112	23	2,00146	23	1.97982	
2.00112	0	2.00140	0	1.99874	
2.001% -30 1.99921 0 2.001% -30 1.99935 0 2.001% -30 2.00080 2.001% -30 2.00082 Costum Costum 1.99495 20 1.99490 0 1.99511 20 1.99502 0 1.99497 20 1.99491	-20	2.00148	•	1.99685	
2.001/6 -30 1.99935 0 2.001/2 -40 2.00080 5 2.001/5 -40 2.00082 Continu Continu 1.99495 20 1.99470 0 1.99511 20 1.99502 0 1.99477 20 1.99481	-20	2.00112	-20	1.99902	
2.001/12	-to	2.001/30	-30	1.99921	
Continue Continue Continue T(°C) g-value 1.99495 20 1.99470 20 1.99502 20 1.99481 20 1.99481	-60	2.00136	-30	1.99935	
Costus (C) g-value (C) g-valu	-70	2.001/2	مائد.	2.00080	
ec) e-value T(°C) e-value 1.99495 20 1.99470 0 1.99511 20 1.99502 0 1.99473 20 1.99481 0 1.99477 10 1.99490	-75	2.00165	-h0	2.00082	
1.99 ¹ / ₁ 95 20 1.99 ¹ / ₁ 90 1.99511 20 1.99502 1.99 ¹ / ₁ 73 20 1.99 ¹ / ₂ 81 1.99 ¹ / ₁ 77 10 1.99 ¹ / ₂ 90			Costus		
1.99511 20 1.99502 0 1.99473 20 1.99481 0 1.99477 10 1.99490	T(°C)	g-value	T(°C)	g-value	
20 1.99 ¹ /73 20 1.99 ¹ /81 20 1.99 ¹ /90	50	1.99495	20	1.99470	
1.99 ^h 77 10 1.99 ^h 90	40	1.99511	20	1.99502	
	40	1.99473	20	1.99481	
1.99466 10 1.99467	30	1.99477	10	1.99490	
	30	1.99466	10	1.99467	

TATLE X. Continued.

		Costum	
T(*C)	6-vejue	T(°C)	g-value
10	1.99497	-5 0	1.99683
0	1.99474	-60	1.99725
0	1.99521	-60	1.97729
-10	1.99551	-60	1.99721
-20	1.99583	-70	1.99773
-20	1.99553	-70	1.99764
-20	1.99551	-70	1.99767
-30	1.99612	-80	1.99805
-30	1.97609	- 20	1.99790
-30	1.99632	-80	1.99784
⊸ 40	1.99657	-9 0	1.99821
40	1.9769	90	1.99816
710	1.9964	-100	1.99878
-50	1.99604	-100	1.99905
-50	1.99692		

TABLE XI. The Spin Concentration (at 23°C) of the Honomeric Species as a Function of Metal and Solvent for a Number of Saturated Metal-Amine Solutions.

Solvent	Spin Concentration			
	Sedium	Potassium	Rubidiva	Cestum
Helling.			1 × 10 ⁻³ M	8 x 10 ⁻³ M
ELNE ₂		1 = 10-6 _H	6 x 10 ⁻⁵ n	5 x 10 ⁻¹ H
BtnH ₂ / MenH ₂	2 x 10 ⁻⁶ H			
a-Parit		9 × 10 ⁻⁷ m	8 x 10-6	2 = 10 ⁻¹ M
1-Prim2		$7 = 10^{-7} \text{M}$	5 x 10-6	1 × 10-4
3-MPA		$1 \times 10^{-7} \text{M}$	5 = 10 ⁻⁷ M	5 × 10-6
1,2_PDA		6 x 10 ⁻⁵ H	1 = 10 ⁻⁵ H	1 × 10 ⁻³ H
1,3-PDA		9 × 10 ⁻⁵ #	4 x 10 ⁻⁵ M	2 x 10 ⁻³ H

The encentration of the saturated solution appears to be consitive to the method of solvent purification used. This may cause as much as a ten-fold variation in the measured spin encentration.

2. The solvated electron. To distinguish this absorption from the broad extra absorption detected by computer analysis we shall mean by the electron absorption the line located at $g=2.00190\pm0.0002$ and of linewidth comparable to that of the hyperfine pattern. The spin concentration of this species and the ratio of its concentration to that of the monomeric species varies from solvent to solvent and from metal to metal as can be seen from Table XII. In general one can say that this species is favored by polarizable or ionizing solvents such as methylamine or the dismines. The temperature dependence of the spin concentration of the solvated electron varies markedly from one metal solution to the next.

In solutions of potassium in the amines the concentration of the solvated electron is observed to decrease slightly with decreasing temperature. On the other hand, the absorption due to the solvated electron is observed to increase with decreasing temperature for solutions of rubidium and cesium in the smines. The behavior of the extra line in solution of lithium in ethylamine and ethylamine-ammonia mixtures will be discussed later.

In general it has been found that the electron absorption is favored by conditions indicative of decomposition, e.g., standing at room temperature or above for prelonged periods of time. This could however be because equilibrium is attained very slowly in these solutions.

The addition of ammonia has the effect of suppressing the solvated electron absorption relative to the monomer absorption.

The g-value of the solvated electron is independent of metal and solvent used, metal concentration, and temperature as can be seen from Table XII.

TABLE XII. The Spin Concentration (at 23°C) and g-value of the Solveted Electron for a Number of Ketal-Amine Systems.

Solvent			S.	
	Sodium	Potassium	Rubidium	Costun
Yell 2			2.0018 ± 0.0002	2.0018 ± 0.0002
			1 × 10 ⁻⁵ H	8 x 20 ⁻³ k
rem ₂	·	2.0019 ± 0.0002	2.0019 ± 0.0002	2.0019 ±
		5 = 10 ⁻⁷ H	5 = 10 ⁻⁷ H	1 × 10-6
eter ₂ /	2.0019 ± 0.0002			
Meliti ₂	2 x 10 ⁻⁶ H			
3-KPA		2.0019 ± 0.0002	_	2.0019 ± 0.0002
		1 × 10 ⁻⁷ M	5 x 10 ⁻⁷ H	1 × 10 M
1,2-PDA		_		2.0019 ± 0.0002
		1 × 10 ⁻⁶ H	5 × 10 ⁻⁵ M	1 = 10 ⁻³ n
1.3-PDA				2.0019 ± 0.0002
		1 × 10-6	7 × 10 ⁻⁵ x	2 × 10 ⁻³ 4

- 3. Extra absorption detected by computer analysis. Computer analysis of potassium-ethylamine-ammonia solutions showed the building in of an additional broad absorption at higher ammonia concentrations (42). The results of this analysis on a typical spectrum are shown in Fig. 16 and the parameters of the extra absorption for potassium-ethylamine-ammonia solution are shown in Table XIII. As can also be seen from Fig. 16, this absorption is also present in other amine-ammonia solutions. At the time of this writing computer analysis had not been performed upon these solutions.
- 4. Lithium-ethylemine and lithium-ethylemine-ammonia solutions.

 Several aspects of the behavior of lithium-ethylemine and ethylemine-ammonia solutions are unique; hence, these solutions will be discussed apart from other metal-amine solutions.

Lithium dissolves in ethylemine to give highly concentrated solutions which can not be studied because of their deleterious effect on the cavity Q. Resonances have been observed from diluted samples of these solutions.

The range of metal and solvent compositions which we studied are summarised in Table XIV. The qualitative nature of these spectra can be seen in Fig. 17.

At room temperature the resonance of a moderately dilute solution of lithium in pure ethylemine is a single line at g=2.0019 ± 0.0002 of width 0.3 gauss. The width of this line increases monotonically with decreasing temperature until at -80° C it measures 2.5 G. A precipitous drop in the line width to 0.1 G and a ten-fold decrease in the spin concentration occurs as the solution freezes just below -80° C.

TABLE XIII, EPR parameters of hfs pattern and extra absorption as obtained by computer analysis

5.8 Mole percent ammonia

Sample K-12

Sample K-12		3.0 More percent	anmonia	
Temp.	A _F	s _F (hfs)	S _F (extra absorption)	n _{extra} /n _{hfs}
(°C)	(gauss)	(gauss)	(gauss)	
- 38	5.08 ^b	1.25 ^b		
- 72	4.24 ^b	1.17 ^b		
Sample K-11	9.	6 Mole percent amm	onia	
- 7	3.76 ^b	2.11 ^b	12.1 ^b	2.31 ^b
-15	3.66	2.18	10.3	1.28
	3.66 ^b	2.18 ^b	10.2 ^b -	1.27 ^b
-41	3.24	1.76	12.7	4.94
	3.23 ^b	1.84 ^b	11.8 ^b	3.35 ^b
Sample K-25	9.9	Mole percent ammor	nia	
-8	3.52	2.63	9.27	1.74
	3.52 ^b	2.64 ^b	2.24 ^b	1.70 ^b
- 35	3.39	2.54	8.83	1.78
-68	2.97	2.24	7.87	1.88
	2.97 ^b	2.24 ^b	7.85 ^b	1.73 ^b
Sample K-10	11.	8 Mole percent amm	onia	
-12	2.74	2.31	6.83	4.81
-42	2.36	1.97	5.95	6.45
- 75	1.89	1.48	4.69	7.78

TABLE XIII. (continued)

Sample K-9

14.2 Mole percent ammonia

Temp	A _F	Sp (hfs)	Sr(extra absorption)	n _{extra} /n _{hfs}
<u>(°C)</u>	(gauss)	(gauss)	(gauss)	***************************************
-10	2.94	2.50	7.45	4.77
-41	2.54	2.16	6.51	4.31
- 69	2.21	1.77	5.68	3.19

aspectra were fit by the superposition of two absorption patterns. One of these was the Gaussian hyperfine pattern arising from electronic interaction with the ³⁹K and ⁴¹K nuclei. The other was a single absorption of Gaussian shape. The routine alternately adjusted the parameters for both of these patterns. Except as noted, initial adjustment was made on the single absorption.

bThe hyperfine pattern was adjusted first.

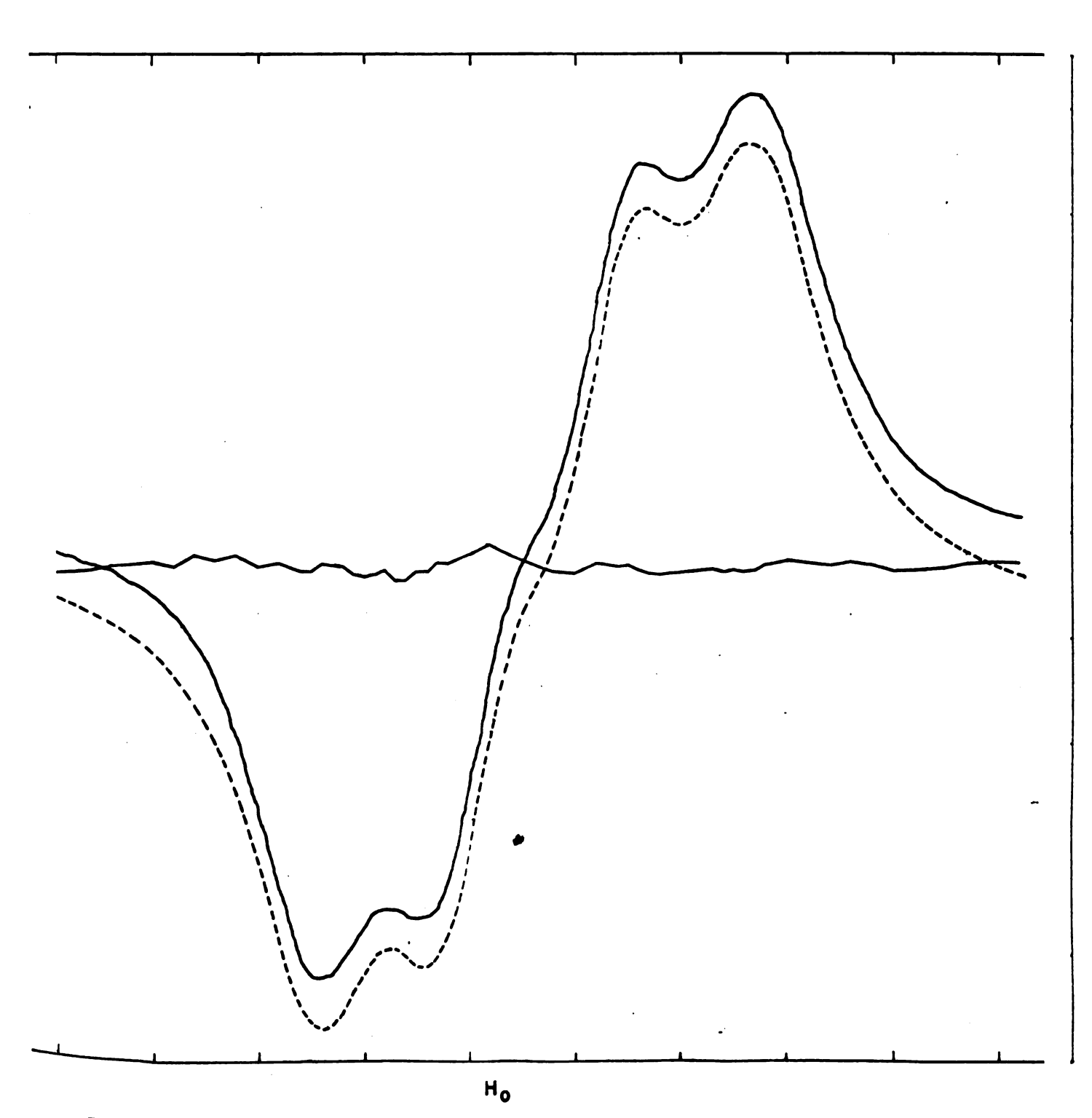


Figure 16. A potassium-ethylamine-ammonia solution showing the presence of the extra absorption

TABLE XIV. Summary of EPR Results for Lithium in Ethylamine-Aumonia Mixtures.

Sample	Mole Percent Ammonia	Estimated Hetal Concentration Moles/liter	RPR Spectre
1	0.0	10 ⁻³ to 10 ⁻⁴	Single line
2	0.5	10 ⁻⁵ to 10 ⁻⁶	Fine line hfs + single line
3	1.3	10 ⁻⁶ to 10 ⁻⁵	Rine line hfs + single line
4	2.1	20 ⁻³ to 20 ⁻⁴	Single line
5	4.3	10 ⁻⁶ to 10 ⁻⁵	Wine line hfs + single line
6	5.2	10 ⁻⁵ to 10 ⁻⁶	Hime line hfe

LITHIUM

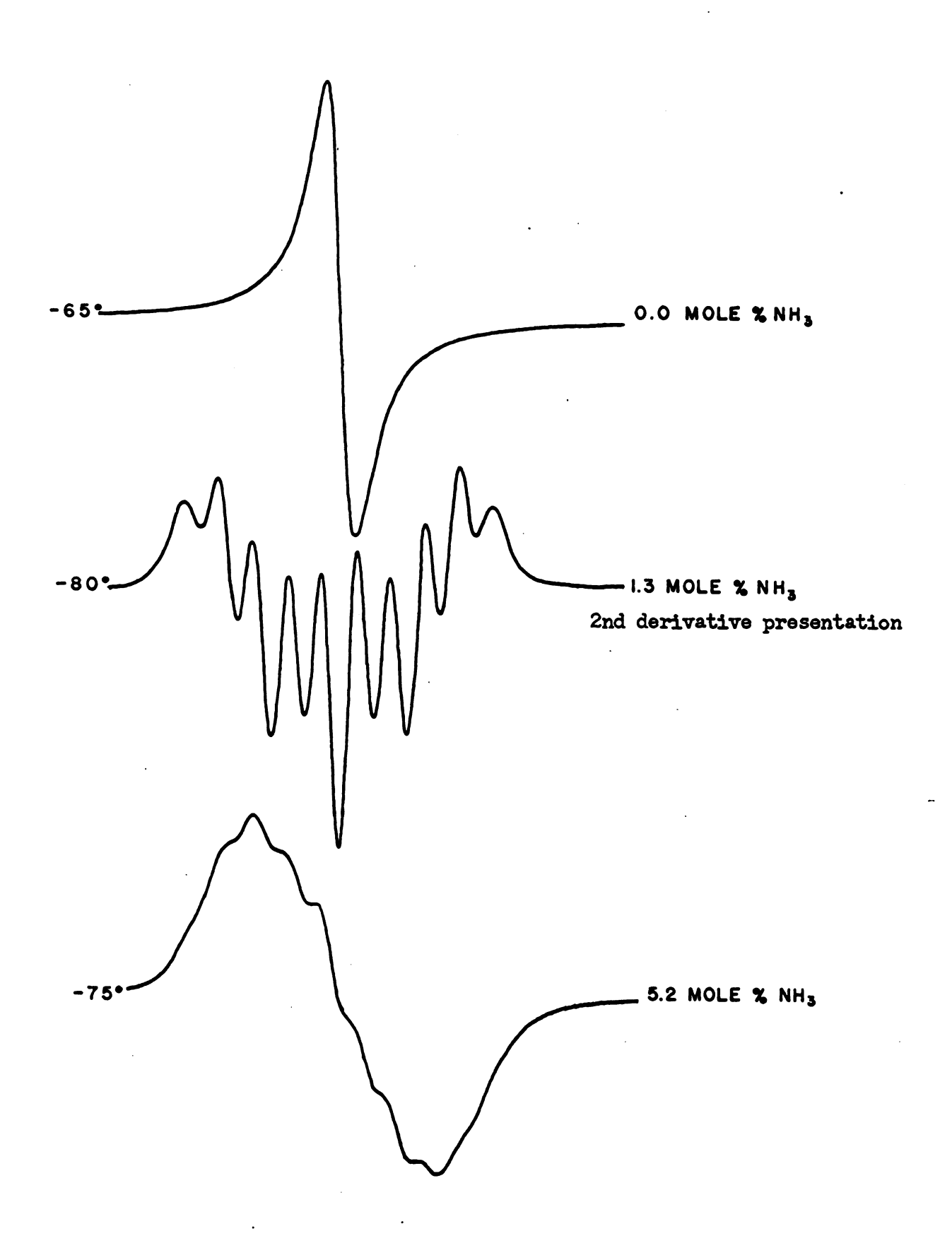


Figure 17. EPR spectra of lithium in some ethylamine-ammonia mixtures.

Below -90°C the line width increases as the temperature decreases; the spin concentration decreases over this same region.

In a more dilute solution of lithium in an ethylamine-ammonia mixture the author observed a spectrum consisting of nine lines spaced at intervals of 2.45 ± 0.1 G. The relative intensity of the eight outer lines indicate that the hyperfine splitting arises from interaction of a paramagnetic electron with four equivalent nitrogens. The central line is much more prominent than any of the others indicating the presence of an extra absorption. Careful analysis showed the g-value of these two patterns to be the same; namely, $g_{H} = g_{a} = 2.0019$. The g-values of the two species and the hyperfine interaction, $A_{\mu\nu}$ are independent of temperature over a range from -50° to -98°C. At -80°C the line width of the hyperfine components is observed to be 1.84 G. The line width of the extra line appears to be slightly less than this. Both increasing temperature and increasing concentration have the effect of broadening the individual hyperfine lines and the extra line, the line width of the extra line being more sensitive to changes in these parameters. The addition of summania appears to result in a slight increase in the line width of these two species. Increasing the concentration of metal also has the effect of reducing the amplitude of the central line with respect to the hyperfine pattern. In the most dilute solutions the extra line was the predominant species. Upon freezing, the hyperfine pattern and extra line collapse to a single line ($S_p = 4.52 G; g = 2.0019$) at $-98^{\circ}C$. Upon further cooling the line width increases ($\bullet.g., S_p = 10.98$ G at -120° C) with decreasing temperature. Below -130°C it is clear that the spectrum consists of a single narrow absorption superimposed upon a broad absorption.

The broad absorption appears to consist of unresolved hyperfine splitting. The signal intensity decreases markedly at -98°C and continues to decrease as the temperature decreases. The low spin concentration made resolution below -150°C difficult. Upon warming, the single line reverts back to the hyperfine pattern and extra line at -85 to -87°C. Further warming results in smearing of the hyperfine pattern and extra line so that at -35°C only a single absorption with broad tails is observed. Above 0°C the line width of the absorption decreases very slightly. However it appears that unresolved hyperfine splitting may be present up to +50°C.

The stability of our samples was much greater than that reported by other workers(43). The samples prepared by the author were stable for over a week. During this time they were stored at room temperature and were heated intermittently to temperatures as high as +50°C.

5. Absorption of sodium in methylamine and the alkali metals in ethylenediamine. When only a single absorption is observed one is not justified in assigning this a <u>priori</u> to the monomer, solvated electron, or any other paramagnetic species. Thus we will group these spectra together until further evidence can be presented meriting their assignment to any given species. The g-values of several single absorptions are given in Table IV.

Solutions of sodium in methylamine give a weak signal (approximately 5×10^{-6} H) and display a g-value of 2.0017 ± 0.0002 and a line width of 1.45 G. The g-value is found to be independent of temperature. Above the melting point of the solution the linewidth increases with increasing temperature; moreover, below the melting point the linewidth was observed to decrease with decreasing temperature. There is however

TABLE IV. g-walues of Solutions Exhibiting only a Single Line.

Solvent			Hotal		
	lithium	Sodium	Potassium	Rubidium	Conium
KII ³	2.001 ±	2.0012 ±	2.0012 ±	2.0003 ±	
•	0.001	0.0002b	0.0002b	0.0002	
	(23°C)	(23°C)	(23°C)	(23°C)	
Menii,	2,0019 ±	2.0017 ±	2.0017 ±		
-	0.0002ª	0.0002	0.0002		
	(23°C)	(23°C)	(23°C)		
EDA	2.0023 ±	2.0017 ±	2.0018 ±	2.0017 ±	1.998 ±
	0.0002	0.0002	0.00024	0.0005	0.003
•	(23°C)	(23°C)	(23°C)	(23°c)	(23°C)

AReference 68.

bReference 6.

This work.

a discontinuity in the behavior of linewidth as a function of temperature at the melting point. As can be seen from Table IVI, the present data are in excellent agreement with those obtained previously by Vos (68).

The addition of ethylamine has the effect of broadening this line. At sufficiently high ethylamine concentrations, a composite pattern appears, consisting of a single narrow line superimposed upon what appears to be a four-line hyperfine pattern. The hyperfine splitting arising from the interaction of a single paramagnetic electron with a ²³Na nucleus is given in Table VII. The g-values of the hyperfine species and of the solvated electron are given in Tables IX and XII respectively. At room temperature the concentration of the monomeric species and the solvated electron were approximately the same.

6. Kinetics of decomposition as studied by EFR. With the exceptions of isopropylamine, n-butylamine, and 3-methoxy-n-propylamine the solutions of the alkali metals in amines prepared in this laboratory exhibited extremely good stability. Some of the solutions have been stable for as long as two years. The stability of the solutions appears to depend upon the metal. Lithium and cesium solutions were found to be considerably more unstable than potassium and rubidium solutions.

In general when a metal-amine solution was observed to decompose, the monomeric species exhibited a first-order decay.

The decomposition of cesium solutions is particularly interesting. Freshly prepared solutions of cesium in ethylamine and the higher alkylamines show only the eight-line hyperfine pattern due to the cesium monomer. When decomposition begins, as indicated by the decrease in the spin concentration of the cesium monomer, the building in of a single line (due presumably to the solvated electron) is observed. The electron

TABLE IVI. Limewidth of Sodium-Bothylamine Solutions.

Temperature (*C)	S _p (Genss)	T ₂ × 10 ⁷ (***)	T ₁ x 10 ⁷ (see)
-140	1.72 ^b	1.75	
-1.35	1.77ª	1.70	
-1.30	1.81	1.66	
-120	1.894	1.59	
- 70	1.18 ^b	2.54	
 60	1.23 ^b	2.44	
- 60	1.20ª	2.50	
- 50	1.244	2,42	
- 43	1.24 ^b	2,42	
- 40	1.274	2,46	
- 30	1.30 ^a	2.31	
• 22	1.34 ^b	2.24	
- 10	1.36 ^a	2.21	
0	1.394	2.16	2.17
+ 14	1.43 ^b	2.10	
+ 22	1.48°b	2.03	2.05
+ 40	1.544	1.95	

a This work.

bRaference 68.

absorption continues to increase as the hyperfine pattern decreases in intensity until the hyperfine pattern can no longer be detected. At that point the electron absorption begins to decay. This process is shown in Fig. 18 for a solution of cosium in ethylamine.

B. EPR Measurements on Metal-Amine Solutions (Paramagnetic Relaxation)

Measurement of T_1 and T_2 by the saturation method indicates that $T_1 = T_2$, at least in the vicinity of room temperature.

We shall now proceed to discuss the linewidth behavior of the bread extra line, the species in lithium-ethylamine-amonia solutions, and of sodium in methylamine-ethylamine solutions has already been given.

1. The monomeric species. One of the most fascinating features of the EFR hyperfine spectra of metal-smine solutions is the dependence of the line width upon hyperfine component. This madear spin-dependent relaxation appears to be present in all solutions studied in this laboratory except for solutions of sodium in methylamine-ethylamine mixtures. It may well be present in these solutions but be obscured by other relaxation phenomena such as chemical or spin exchange processes. The effect is most pronounced in sesium solutions and becomes increasingly less prenounced as one goes to the lighter alkali metals. The effect appears to be slightly more in evidence in the higher alkylamines than in methylamine. (It is difficult to ascertain this with certainty since the apparent effect may in reality be a result of different metal concentrations.) The dependence upon the muclear spin quantum number is definitely most pronounced in the dismines as can be seen by comparing Fig. 19 to Fig. 3. Unfortunately very little quantitative analysis of

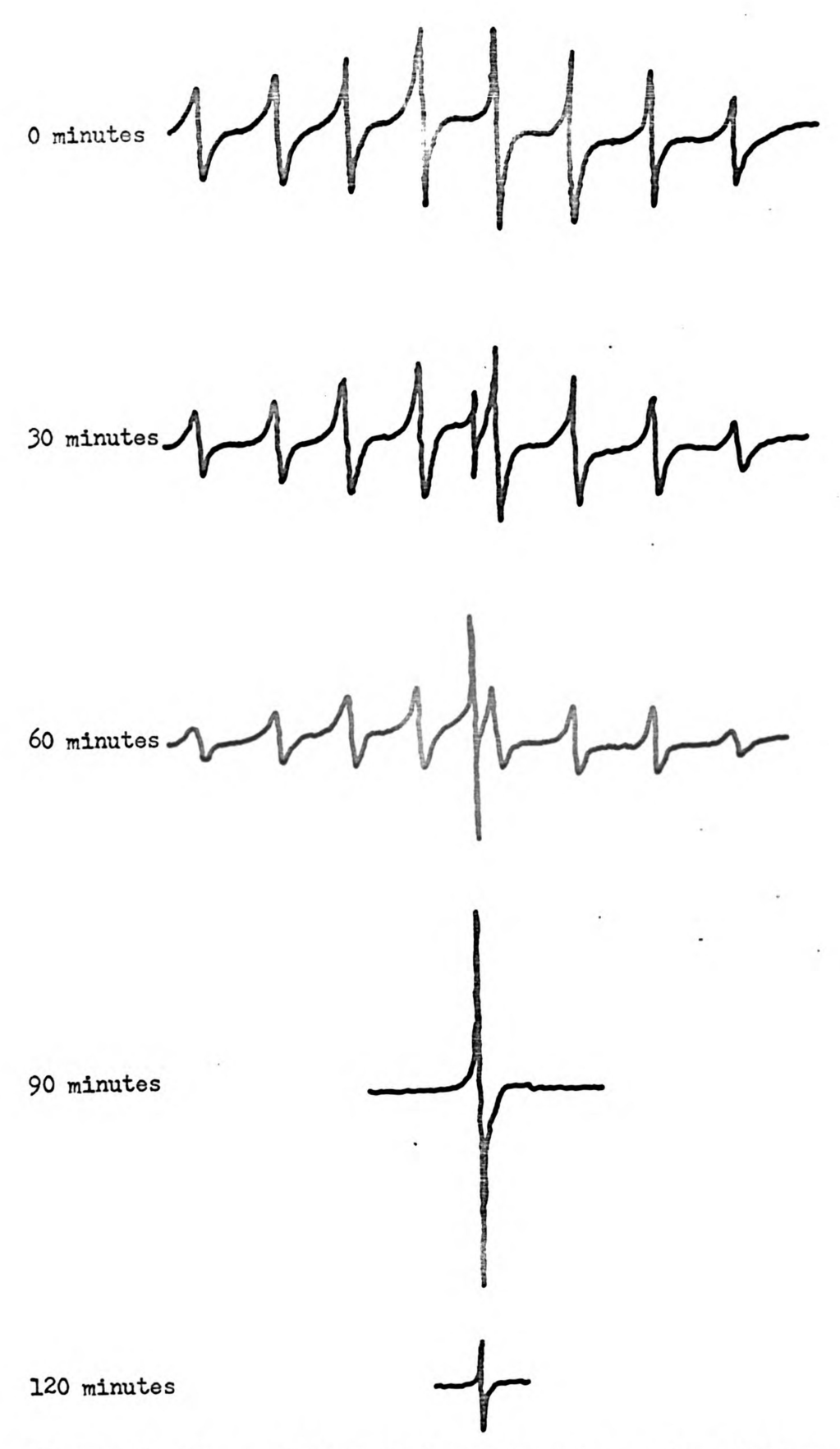


Figure 18. Decay of the EPR absorption of a cesium-ethylamine solution.

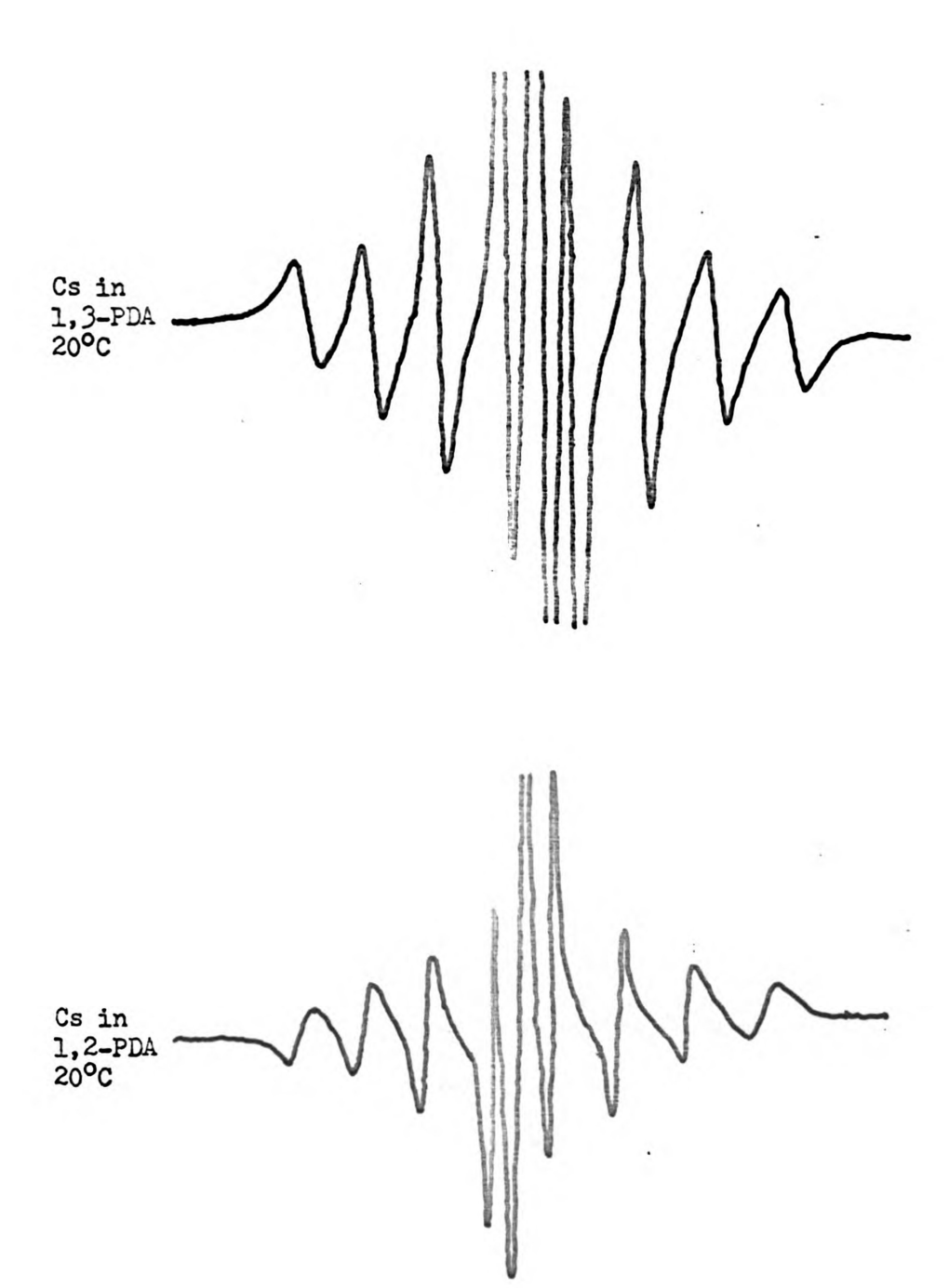


Figure 19. Cesium in 1,2- and 1,3-propanediamine.

this m_-dependent relaxation has been performed to date. The experimentally determined values of the coefficients of the expression

$$T_2^{-1} = c_0 + c_1 m_1 + c_2 m_1^2 + c_3 m_1^3$$

are given in Table XVII for those solutions upon which such an analysis has been applied.

The predominant coefficients appear to be C_0 and C_2 . The dependence upon \mathbf{n}_{I} through third order is real but the deviations from a symmetric pattern are so small it is difficult to measure the coefficients of the first and third-order terms.

The addition of amonia to ethylemine solutions of the metals broadens the lines and reduces the apparent dependence upon $\mathbf{m_{I}}$. Since most of the studies were made on saturated solutions and the solubility is increased markedly upon addition of amonia, it is difficult to separate contributions to the linewidth caused by $\mathbf{m_{I}}$ -dependent relaxation processes and from those due to exchange reactions. Indeed, the linewidth of samples with appreciable amonia content was less for the unsaturated than for the saturated solutions.

The temperature dependence of the C_0 coefficient varies markedly from metal to metal. For potassium solutions C_0 is nearly independent of temperature while for cosium solutions it is a strong function of temperature.

2. The solvated electron. The behavior of the line width of the single absorption due to the solvated electron varies markedly from metal to metal. For solutions of lithium, rubidium, and cosium in the smines and dismines the line width increases with increasing temperature as can be seen from Table XVIII. As can also be seen from Table XVIII,

TABLE XVII. Analysis of Ruclear-Spin Dependent Relaxation for Several Metal-Amine and Metal-Amine-Amine-Amine-Solutions.

Costum in Et	hylamine			
Tamperature OC	C _O Gauss	Gauss	C2 Gauss	C ₃
10	7.42	0.235	0.335	-0.021
0	6.75	0.323	0.336	-0.024
-10	5.73	0.322	0.354	-0.029
-20	5.16	0.311	0.384	-0.032
-30	4.95	0.327	0.406	-0.028
40	4.53	0.299	0.433	-0.032
- 50	4.42	0.221	0.442	-0.019
-60	5.12	0.198	0.453	-0.022
-80	4.57	0.006	0.392	-0.001
Cosium in Et	hylanine-(5.6	Mole & Ammonie		
Temperature OC	C _O	C ₁ Gauss	C ₂	C ₃
-45	10.79	0.287	0.608	-0.056
- 50	9.94	0.075	0.617	~0. 006
~55	9.87	0.082	0.436	-0.015
Rubidium in	Ethylanine			
Temperature °C	C ₀	C ₁ Gauss	C ₂ Gauss	C ₃
23	3-57	0.014	0.161	0.000

TABLE IVIII. Linewidths of the Solveted Electron.

Solution	Sye Ganes
Cosium in Nothylamine	40 (0°C) 20 (_40°C)
Potessium in Ethylamine	0.2 (25°c) 0.4 (-35°c)
Rubidium in Ethylerine	3.1 (0°c)
Cosium in Ethylemine	6.98 (10°c) 6.45 (0°c)
Comium in Armonia/Ethylamine (1/5)	6.6 (23°c)
Robidium in 1,2-Propensdismine	5.1 (10°c)
Cesium in 1,2-Propenediamine	11.8 (20°c)
Cesium in 1,3-Propenedismine	21.0 (20°C)

the line width of the extra line decreases with increasing temperature for solutions of potassium in the smines.

At the time of this writing the dependence of the width of the extra line upon metal concentration had not been ascertained.

C. Optical Measurements on Metal-Amine Solutions

The results of qualitative optical spectra taken in this laberatory and elsewhere are summarised in Table III.

The temperature and summais dependence of the visible, red, and infrared bands for solutions of rubidium and cosium in ethylamine-assenta mixtures are similar to those observed for potassium solutions (42).

D. Conductance Measurements on Sodium--Ethylenediamine Solutions

Because of experimental difficulties only one successful conductance measurement was obtained. This value is given in Table II along with the values observed by Dewald (71).

E. Viscosity Measurements on Anhydrous

Methylsmine and Ethylsmine

The viscosities of methylemine and ethylemine are given as functions of temperature in Table III.

TARK ALK.	ä	AND UPCACHE SPORTS OF ROCAL-STRO ON ROCAL-STRONGS SOUNTERED.	Track of Moter.	ANTEN AND MAKE		Klene.
Selven	Solvent Rotal	Temperature Oc	Abeerption Haz. (mm)	Aberrhance	Cell Path Langth (mm)	Reference
m ₃	=	8	1500	2,43	0.1	(1)
	•	23.	202	2.57	1.0	3
	M	Ę	1480		1.0	3
	8		1,900			
			1500			
'enn ₂	77	-55	28	0.73	0.1	3
	ដ		170 1500			(a)
	71	-75	88			(5)
	ជ	2	650			(3)
	1.1	8	680, In-			(9)
		23	690			(2)
	•	Ŗ	655	54.0	1.0	3
		Q.	659			(3)
	4	٤-	8 8			9 3

Cell Puth Reference Length (m) 3 3 ව ව 3 7,00 2.24 2.24 \$ \$ \$ \$ \$ \$ \$ \$ \$ g + 402 MT3 NA 7

TAME IIX. Continued.

TARES XIX.	TANK XIX. Continued.					
Solvent	Heta	Tesperature Oc	Bearpties Hex. (mm)	Deschase	Cell Path Langth (sm)	Refreesco
Beatt,	#		600			(4)
	4		039			(4)
	1 44	9	0 -9			(2)
	b id	\$	650	39%		(3)
	M	ស	675	1.2	10	(8)
	ē	ឆ	88 88			(2)
	£	ຄ	638 938	1.6	201	(9)
	£	R	650		10	(8)
	8	ស	310.60 1,300 1,300			(2)
	8	ଧ	720 1300 1300	8.0	222	£€£
	8	0	873 840 840			(2,8) (2,8)
+ 10% mm3 K	м	r	223 230 1340			222

2 E 2 E E E E 8 8 8 6 6 0.1 0.0 1.2 0.0 0.03 1.5 **2**2 1500 1250 1500 1500 Ω \mathfrak{P} 8 PARKE XIX. Continued. + 50% 7813 184

 * Absorption
 Absorbance
 Call Path
 Reference

 670
 1.0
 0.1
 (1)

 670
 1.0
 0.2
 (1)

 670
 1.0
 0.3
 (12)

 690
 1.0
 0.5
 (10)

 690
 1.3
 0.1
 (12)

 700
 1.5
 0.1
 (12)

 700
 0.5
 0.1
 (12)

 700
 0.5
 0.1
 (12)

 700
 0.5
 0.1
 (12)

 1270
 1.23
 0.1
 (10)

 600
 1.23
 0.1
 (10)

 670
 670
 (11)
 (11)
 Ø TAILS AIX. Confirmed.

TAME MIX. Continued.

- · Strong absorption in IR region.
- (1) Reference 26.
- (2) This work.
- (3) Reference 116.
- (4) Reference 117.
- (5) Reference 118. (6) Reference 36.
- (7) Reference 119.
- (8) Reference 40.
- (9) References 51,52.
- (10) Reference 71.
- (12) Raference A.

(11) Reference 30.

TABLE XI. Conductance of Sedium im Ethylenediamine.

c ¹ = 10 ²	Equivalent conductance
4.96	25•5 ⁶
4.86	25.5 ⁴
3.65	25.8 ^b
3,23	25 . 9 ^{&}
1.56	26.3ª

Reference 71.

bals work.

TABLE III. Viscosities of Hethylanine and Ethylanine.

Temperature	Methylemine	Ethylemine
• <u>K</u>	eentipoise	oentipoise
296.4		0.250
296.4		0.259
289.2		0.276
283.2		0.299
273.2	0.236	0.328
263.2	0.285	0.343
263.2	0.291	0.370
258.8	0.300	
253.2	0.331	0.415
243.2	0.372	0.467
239.7		0.437
238.3	0.400	
233.2	0.422	0.588
223,2	0-480	0.780
223,2		0.671
217.5		0.800
213.5	0.552	
203.5	0.665	
293.2	0.829	

CONCLUSIONS

A. The Assignment of the Optical Absorptions

1. The infrared band. The work of Dalton, Dye, Fielden and Hart (46) leaves little doubt as to the correctness of the assignment by Dye and Davald (33) of the infrared band to the solvated electron and aggregates.

A comparison of the spin concentration of the EPR singlet attributed to the solvated electron with the absorbance of the infrared band indicates that in many metal-smine solutions the electron exists largely in dismagnetic aggregates.

2. The red band. If we assume that the equilibrium constant for the reaction $2M \rightleftharpoons M_2$ is the same in solution as it is in the gas phase, we can predict the concentration of M_2 from the measured spin concentration of the monomeric species M_1 . The predicted concentration of M_2 is given in Table XXII for a number of metal-smine solutions. The agreement with experiment as can be seen by comparing Tables XXII and XIX is surprisingly good. Indeed it might have been expected that the equilibrium constant would have been significantly shifted as a result of differences of solvation between M_2 .

If, as pointed out by workers in this laboratory (42), the red band must be assigned to the $\frac{1}{n}$ \leftarrow $\frac{1}{E}$ transition of the dimer an interesting question arises; namely, "where does the $\frac{1}{E}$ \leftarrow $\frac{1}{E}$ transition occur?" By comparison with the higher energy transition it might

TABLE IIII. Concentration of the Solvated Diner Predicted from Monomor Spin Concentration Measurement by Use of Gas Phase Equilibrium Constant.

Solvent		Dise	r Concentration.	moles/liter
	Sodium	Potassium	Rubidium	Costum
eer,			6 x 10 ⁻³	2.7 × 10 ⁻²
Stati ₂		1 × 10 ⁻⁵	3.6 x 20-4	1.6 x 10 ⁻³
rung/	4 x 10 ⁻⁴			
ionn ₂		_	_	
-Pysii		9 × 10 ⁻⁶	4.8 x 10 ⁻⁵	6.7 x 10 ⁻⁴
-Prilling		7 × 10-6	3 × 10 ⁻⁵	3.3 × 10-4
HIPA -		1 × 10 ⁻⁶	3 × 10 ⁻⁶	1.6 × 10 ⁻⁵
L, 2-PDA		6 x 10 ⁻⁴	6 x 10 ⁻⁵	3.3 × 10 ⁻³
L. 3-PDA		9 = 10 ⁻⁴	2.4 x 10 -4	6.7 x 10 ⁻³

be expected that the $\frac{1}{L_{pl}^{+}} \leftarrow \frac{1}{L_{g}^{+}}$ transition will be shifted into the infrared region. There now appears to be some experimental evidence to substantiate this. As has been pointed out to the author (105), the normalised infrared absorption tails more when the red band is present than when it is absent. If one argues that this is due merely to everlap with the $\frac{1}{L_{g}^{+}} \leftarrow \frac{1}{L_{g}^{+}}$ transition it can be pointed out that such everlap would actually result in less tailing of the normalised infrared absorption.

3. The visible band. This work further confirms the argument of Dalton et al. (42) that the visible band is not due to the monomeric species responsible for hyperfine splitting. A comparison of Tables II and III indicates a complete lack of correlation between the species responsible for these phenomena.

Unfortunately the work reported in this thesis throws little light upon the nature of the visible species. The only thing that is certain is that the species which gives rise to the visible band cannot also give rise to a sharp EPR signal. This does not exclude the possibility that the visible species gives rise to a broad EPR absorption.

If the visible absorption is the M_2^+ -e⁻ species as postulated by Dye and Devald (33), two possible paramagnetic absorptions could result. The first of these is a triplet absorption resulting from the interaction of the paramagnetic electron of the M_2^+ core with the electron trapped in the field of the M_2^+ ion. Eivelson (56) has shown that the line width of a triplet state absorption is given by

$$T_2^{-1} = \gamma_0(3/10) \, \mu^2(4s^2 + 4s - 3) \left[(3/2) + (5/2)/(1 + \omega_0^2 \xi_0^2) + 1/(1 + 4\omega_0^2 \xi_0^2) \right]$$

where

$$\mu^2 = (1/5) [|D_{aa}|^2 + (16/3) (|D_{aa}|^2 + |D_{aa}|^2)]$$

and D is the fine structure tensor. To give the reader an idea of the magnitude of triplet state line widths we note that for the case of maphthalene diluted in durene (106) where $D_{zz} = -3 \times 10^9$ cps; $D_{++} = D_{--} = -0.21 \times 10^9$ cps; g = 2.0133, and γ_c is taken to be 10^{-11} sec. T_2^{-1} would be greater than two hundred gauss. It would thus not be a simple matter to see the naphthalene spectrum in solution. Weissman (107) has discussed this problem in some detail.

This seems to rule out the assignment of the EPR absorption in sedimm-ethylenedismine solutions to a triplet state M_2^{\dagger} : species. Since the line width at 22° C is only of the order of 0,5 gauss, both the fine structure interaction and the correlation time would have to be extremely small to account for the observed spectra. For example, if a correlation time of 10^{-11} sec is chosen, the fine structure tensor would have to be only 10 G.

A second possibility of an EPR absorption arising from the molecule-ion would be the interaction of the paramagnetic electron of the \mathbb{M}_2^+ core with the two equivalent metal nuclei.

Kivelson (108) has shown that such interaction will result in a contribution to the line width given by

$$T_2^{-1}(im,m) = I(0)[\langle a^2 \rangle - \langle a \rangle^2] n_1^2/2$$

where $\langle a \rangle$ is the hyperfine splitting constant, I(0) is the amplitude of the resonance. The secular line widths for Na_2^+ are given in Table IXIII as a function of m_1^- . The predicted dependence of T_2^{-1} upon m_1^- is most interesting. Unfortunately since no hyperfine interaction

TABLE IXIII. Celemisted Secrice Linewidths of He.

Æ	8	8	2	#	*	*	0	0	0	0
ζ_{Im}	3/2	3/2	2/2	3/2	2/17	1/2	-3/5	3/5	7/2	2/15
$z_{(n_1)_2}$	3/2	1/2	3/5	-1/2	3/2	3/2	3/2	-3/2	-1/2	1/2
ZT2(1mm)	1.13	0.50	0.5	973	0.13	613	0	•	0	6
272(1se.m)b	09°0	0.19	0.19	0.05	\$0.0	\$0.0	0	•	•	•

Por this case, the two moties cerry out a correlated out-of-chase motion in which the For this calculation the molet are considered to filt shruptly between 0° and 90°. Instantaneous hyperfine splitting constants a_1 and a_2 wary between 0 and a as the model relate through 90° .

attributable to H_2^+ is observed the above equation is of little use to us directly. We observe, however, that since the absorption in sedium-ethylemedismine solutions displays no hyperfine structure and dince in the above relationship T_2^{-1} is proportional to the square of the hyperfine splitting, we must assume that since $T_2(\text{obs}) = 6 \times 10^{-7}$ see that $\langle a \rangle$ is very small. The argument that this resonance is exchange narrowed is unlikely since the dissociation of H_2^+ would be expected to be slow and all other exchange and chamical processes would lead to breadening rather than narrowing.

On the basis of these two arguments, the author feels that the EPR absorption present in sedium-ethylenedismine solutions cannot be attributed to a triplet M_2^+ . \bullet^- or M_2^+ . It is possible that the valence electron of M_2^+ . \bullet^- experiences very little or no triplet state interaction or nuclear hyperfine interaction and is sufficiently notionally narrowed to account for the observed linewidth.

It may also be noted that H2*** could exist as a singlet in which case it would be expected to be disanguetic.

There are four characteristics of the visible band which appear to the author to be very difficult to describe on the basis of surrently-existing models. These characteristics are (1) the narrowness and high energy at which the band occurs, (2) the independence of the band position on the metal used, (3) the dependence of the absence or presence of the band upon metal, (4) the slew rate of interconversion of the band. No assignment at the present time, including the assignment to M^{*}, satisfactorily explains all of these characteristics.

B. The Assignment of the EPR Absorptions

1. The hyperfine species. As has already been stated, the mature of the spectrum indicates unambiguously that the species giving rise to hyperfine splitting must involve a single paramagnetic electrem interacting with a single alkali metal nucleus.

The magnitude and temperature dependence of the hyperfine splitting procludes assignment of the monomeric species colely to solvated atems. In order to explain the temperature and solvent dependence of the hyperfine interaction, workers in this field have been forced to resert to either complex stationary state models or multi-state models involving equilibrium between several species.

In this dissertation we shall attempt to discuss g-shifts and the temperature dependence of these shifts in the light of surrent models.

Let us first review the phenomenological theory for g-shifts.
We shall start with the following Hamiltonian for an unpaired electron
in an external magnetic field

$$\mathcal{H} = 2.0023 \,\beta \,\tilde{\mathbf{S}} \cdot \tilde{\mathbf{B}} + \left(\frac{e\hbar}{2\pi} Z_0^2\right) \,\tilde{\mathbf{S}} \cdot \left[\tilde{\mathbf{E}} \times \left(\tilde{\mathbf{p}} + \frac{e}{4}\tilde{\mathbf{A}}\right)\right] + \frac{e}{2\pi e} \left(\tilde{\mathbf{p}} \cdot \tilde{\mathbf{A}} + \tilde{\mathbf{A}} \cdot \tilde{\mathbf{p}}\right) \quad (32)$$

where the second term gives the spin-orbit interaction in which \overline{A} is the vector potential that gives a static magnetic field externally applied, and \overline{p} is the linear momentum operator, \overline{E} is an electric field in which an electron moves. The third term describes the orbital Zeeman interaction. The g shift caused by the combined effect of the spin-orbit and the orbital Zeeman coupling is given by

$$\Delta g_{g} = \frac{e}{n^{2}e^{2}} \cdot \frac{1}{B_{e}} \times \Sigma^{\dagger} \frac{\langle e/(\vec{E} \times \vec{p})_{g}/n \rangle \langle n/(\vec{p} \cdot \vec{A} + \vec{A} \cdot \vec{p})_{g}/e \rangle}{E_{e} - E_{g}}$$
(33)

where B denotes the magnitude of the external magnetic field.

Regardless of whether we employ a stationary state model or an equilibrium model we must at some point consider a species exhibiting appreciable spin-orbit coupling. Traditionally spin-orbit coupling has been viewed as arising from interaction between the ground and excited exbitals of one paramagnetic electron localized on a central metal atom or ion. In such a situation the ground and excited state energy levels are said to be coupled through spin-orbit coupling. Such coupling gives rise to a negative g-shift, that is, a g-value less than the free electron.

As can be seen from consulting Table II this is in the right direction for g-values observed in this work. However if one considers Fig. 15 and Table I one sees that the g-values are strengly temperature dependent for rubidium and cosium solutions. This behavior is unexpected in terms of the classical picture.

In further considering g-shifts and the temperature dependence of these shifts it is most convenient to proceed in the context of the several models developed for metal-smine solutions. We shall follow the treatment of Dalton et al. (42) and divide the models into two classes. It must be kept in mind that any model proposed to explain g-shifts must also explain the observed hyperfine interactions.

Stationary single-state models

a) The expanding orbital model. As has been previously discussed, this model views the monomeric species as being an alkali metal ion surrounded by several solvation spheres of solvent molecules with the

paramagnetic or valence electron density spread over these layers but with the density maximum localized upon the outer solvation sphere. The solvation binding energy of the secondary solvation spheres is viewed as being on the order of kT so that as the temperature is raised the outer solvation spheres drop off. This is viewed as resulting in the electron density moving closer to the metal mucleus thus increasing the hyperfine interaction. Quantum mechanically this is viewed as an expanding spherically symmetric wavefunction

$$\psi(s) = K \psi_{c}(s/c)$$

From normalization it is easily shown that $K = e^{-3/2}$. If s is a dimensionless radial variable, e is simply a scaling factor which determines a new variable $s^{\dagger} = s/e$ expressed in units e times as large as those in which s is measured.

Since for such a model $\beta=0$, the Ag would be predicted to be sere. This result is rigorously true and is completely independent of the nature of the excited state to which the ground state would be expected to be coupled.

Thus we must completely reject the simple (spherically symmetrical) expanding orbital model.

b) The admixture model. The simple admixture model views the wavefunction of the paramagnetic electron of the monomeric species as
being an admixture of ground state s and excited state orbitals.

For example, the wavefunction for the potassium monomer would be

$$\Psi = \alpha \Psi(4s) + \beta \Psi(3d) + \Psi \Psi(4p) + E\Psi(5s) \tag{34}$$

Since the 4p and 3d orbitals have nodes at the medicus and the 5s orbital is epposite in sign to the 4s orbital at the medicus, any such admixture would reduce the centast density without requiring

so drastic a change in the mean radius of the electron distribution as required by the simple expanding orbital model. The coefficients of the various orbitals are viewed as being temperature dependent. To explain the observed increase in hyperfine splitting with temperature the ratio of ground state orbital contribution to excited or higher state contribution is viewed as increasing with increasing temperature.

Let us now examine such a model in the light of g-shifts. Although such an admixture does predict the correct sign of the g-shift the magnitude of the g-shift would be expected to decrease with increasing temperature if the admixture of states of non-zero critical angular momentum is to be viewed as important in determining the observed hyperfine splitting. As has already been noted the magnitude of the negative g-shift is experimentally observed to increase with increasing temperature.

If we are to retain the simple admixture model we must view the decrease in hyperfine splitting with decreasing temperature as entirely due to the mixing of higher s criticals into the wavefunction. In fact such excited s-state admixture must effect the reverse trend for states of non-sere orbital angular momentum.

e) The expanding admixture model. This model is equivalent to viewing the change in hyperfine splitting as arising from the expansion or contraction of the electron cloud as described for the expanding orbital model and the g-shift as arising from the admixture of states of mon-zero p. This is equivalent to the case discussed above of the admixture of ground and excited s-state orbitals accounting for changes in the hyperfine interaction and the admixture of $p \neq 0$ states accounting

for changes in the g-shift with the exception that the expanding admixture model would require greater changes in the mean radius of the electron distribution.

d) The covalent bonding or charge-transfer model. As can be seen from the phenomenological equation for g-shifts, the magnitude and sign of the g-shift will depend upon four properties of the material under investigation. These are (1) the orbital angular momentum of the electron, (2) the nature of the ground state wavefunction, (3) the nature of the excited state wavefunction, and (4) the energy separation of the ground and excited state. It is to be noted that these parameters are not independent.

Traditionally the ground and excited state wavefunctions have been those of the metal stom or central metal ion and the energy separation has been that between the ground and excited electronic energy levels of the metal.

We now wish to consider the case where ligand-metal bonding (particularly covalent) or ligand-electron interaction are sufficiently strong that we can no longer represent the ground and excited wavefunctions to a good approximation in terms of metal critials.

The ground state wavefunction which we must consider is new a melecular orbital wavefunction of the type

$$Y_{\bullet} = \mathbb{I}\left\{\widehat{\Phi}_{\bullet} - \rho(\mathbf{n})^{-\frac{1}{2}} \sum_{\mathbf{i}=1}^{n} \sigma_{\bullet}(\mathbf{s}^{\mathbf{i}})\right\}$$
 (35)

where Φ_0 denotes the s erbital of the alkali metal monomer (or atom) and $\sigma_0(s^4)$ is the σ molecular orbital of the 1th solvent molecule directed toward the alkali metal atom or ion. The σ orbital is

assumed to be constructed from the sp³ hybridised orbitals of carbon and nitrogen and from the atomic s orbitals of the hydrogens. In the above expression, we denote the antibending orbital by positive ρ .

It is to be noted that this expression will give rise to a g-shift even though a spherically symmetrical s-state of the alkali metal atom is used. In such a case the g-shift is seen to arise from the nem-zero orbital angular mements of the solvent molecule orbitals.

The metal wavefunction Φ of Eq. 35 can also be an admixture of ground state s and higher or excited as in Eq. 34.

A similar expression can be written for the wavefunction of the valence electron interacting directly with the selvent,

$$\underline{\underline{Y}}_{\bullet}^{\bullet} = \mathbb{P}\left\{\phi_{\bullet} - \rho(\mathbf{n})^{-\frac{1}{2}} \sum_{i=1}^{n} \sigma_{\bullet}(\mathbf{s}^{1})\right\}$$
(36)

where $\phi_{f e}$ is the wavefunction of an electron in a spherical square well.

As with the previous expression the spin-orbit coupling arises from the $\vec{p} \neq 0$ character of the selvent σ^*s .

If we substitute Eq. 35 into Eq. 33 the fellowing expression for g is obtained

$$\Delta \mathbf{g} = \xi(\mathbf{x}) \left[\frac{\mathbf{g}_1}{\Delta \mathbf{g}^b} - \frac{\mathbf{g}_2}{\Delta \mathbf{g}^a} \right] \tag{37}$$

where ξ is the one-electron spin-orbit interaction parameter for the 2p orbital of nitrogen (The nature of the interaction of the suine nelecule with the notal ion is such that ξ (carbon) \approx 0).

If the admixture of the ground state s orbital of the notal with higher non-zero orbital angular memoratum orbitals of the notal is permitted one obtains the following equation

$$\Delta g = \xi \text{ (mitrogen P)} \left[\frac{K_1}{\Lambda E^b} - \frac{K_2}{\Lambda E^a} \right] + \xi \text{ (metal P)} \left[\frac{K_1}{\Lambda E^b} - \frac{K_2}{\Lambda E^a} \right] + \xi \text{ (metal P)} \left[\frac{K_1}{\Lambda E^b} - \frac{K_2}{\Lambda E^a} \right]$$

As can be seen from Eqs. 37 and 38, charge transfer interaction $(\Delta E^b = \text{the separation between the ground state and the charge transfer state) results in a positive g-shift.$

 K_1 and K_2 in Eqs. 37 and 38 relate to the bonding coefficients between the notal atom or ion and the solvent molecules. ΔE^a is the separation between ground and excited molecular orbital energy levels.

An evaluation of the experimental data given in Tables IX and X in terms of equations 37 and 38 is given in Appendix I.

The temperature dependence of the g-shift in the case of Eq. 37 would be viewed as arising from either an increase in metal-solvent bonding or a decrease in charge-transfer interaction with increasing temperature.

Although the "solvent spin-orbit interaction" model, as we shall eall the model of Eq. 37, explains the g-shifts and temperature dependence of a given metal-same system, a look at Table IX causes us to question its applicability. As can be seen from Table IX the g-value is relatively independent of solvent for a given metal but is strongly dependent on metal for a given solvent. This forces us to the conclusion that $\bar{p} \neq 0$ states or orbitals of the metal are important in determining Δg and the temperature dependence of Δg . This does not exclude the possibility of some contribution to Δg from nitrogen 2P orbitals.

Since the observed Δg is large and negative we conclude that probably $K_1 \ll K_2$.

In conclusion we feel that the most appropriate expression for $\triangle g$ involving a single state model is

$$\Delta_{g} = \left\{ (\beta \xi (MP) + \gamma \xi (MD) + \delta \xi (MP) + K \xi (M2P) \right\} \left[\frac{K_{1}}{\Delta E^{b}} - \frac{K_{2}}{\Delta E^{a}} \right]$$
where $K_{1} \ll K_{2}$ and $K_{1} \approx 0$.

Multi-State Equilibrium Model

As has been stated in the Historical, Dalton et al. (42) have described the temperature and solvent dependence of the hyperfine splitting and spin concentration in terms of an equilibrium among monomeric species. Because of the large values of the his observed at high temperatures they took the selvated atom as the high temperature limit.

The g-shifts of gaseous metal atoms are observed to be very nearly zero as can be seen in Table IX. From Fig. 15 it is obvious that the observed g-shift will be quite large at high temperatures (The curve apparently levels off at zero to a constant value, i.e., Δg (Cs in EtNH₂) = 0.0075).

Thus if we take the selvated atom as the high temperature limit we must view the g value of this species as being greatly affected by the solvation process. It must be noted that on the basis of previous arguments this shift must arise largely from the admixture of $p \neq 0$ erbitals of the metal.

In analogy with the treatment of Delten ot al. we assume the low temperature species to be a solvated monomer. The temperature dependence of the g-shift forces us to the conclusion that the g-value is greater in the solvated monomer than in the solvated atom. This

would have to result from an increase in the importance of higher s states relative to $\bar{p} \neq 0$ states in the wavefunction for the monomer. The experimental observed Δg is related to the Δg of the stom and monomer by

$$\Delta g(obs.) = p_A \Delta g_A + p_B \Delta g_B$$

where p_A and p_B are the concentrations of atoms and monomers respectively. The lack of agreement between the values of p_A/p_B obtained by the two methods forces us to conclude that the equilibrium responsible for the g-shift cannot be the atom-monomer equilibria.

We must now assign the process resulting in the temperature dependence of the g-shift to an equilibrium between solvated monomers and a third species which we shall assume to be an ion pair. Since the square of the wavefunction of the paramagnetic electron in a solvated ion-pair would be expected to have only a very small contact density at the metal nucleus we take a value of g = 2.0019 (the value of the solvated electron) for the g-value of the ion pair. The g-shift is now given by

$$\Delta g(obs.) = p_0 \Delta g_0 + p_0 \Delta g_0$$

where the subscripts B and C refer to the monomer and ion pair respectively. The values of $p_B/p_B + p_C$) obtained from analysis of the g-shifts using the monomer-ion pair equilibrium and the values of $p_B/(p_B + p_C)$ obtained from analysis of the hyperfine splitting in terms of an atom, monomer, ion-pair equilibria are compared in Table IXIV and the plot of p_B vs. temperature is shown in Fig. 20. The improvement in agreement provides strong support for the existence of the monomer-ion pair equilibrium.

TABLE IXIV. The ratio $p_{\rm p}/(p_{\rm C}+p_{\rm B})$ obtained from g-shift analysis and independently from analysis of hyperfine splitting for a solution of costum in othylamine.

Temperature	$p_{\rm p}/(p_{\rm B}+p_{\rm C})$	$p_{\mathrm{B}}/(p_{\mathrm{B}}+p_{\mathrm{C}})$
•c	from his data	from g-shift data
-20	0.90	0.86
-30	0.84	0.80
- ₽0	0.78	0.75
• r0	0.72	0.70
-60	0.65	0.65
-70	0.60	0.59
-80	0.55	0.55

This being the case we are now foced with the problem of comsidering the effect of the atom-memorr equilibrium upon the temperature dependence of the g-shifts. Two possible alternatives confront us as we consider the high temperature behavior of the g-shifts. These are summarised schematically in Fig. 21.

- 1) Case 1. If we view the observed g-shift as being constant at the higher temperatures then we must see the atem and monemer as having equivalent amounts of $\bar{p} \neq 0$ orbitals of the notal mixed into their wavefunctions. The difference in the magnitude of the hyperfine interestion in the two species would be viewed in this case as arising from the greater extent of admixture of excited a states in the menemer.
- 11) Case 2. Since there is considerable scatter in the data at higher temperature it may be that the g-value increases with increasing temperature. If such a case $\beta \psi(MP) + \gamma \psi(MD) + \delta \psi(MP)$ would be viewed as making only a slight contribution to the total wavefunction.

On the basis of existing experimental evidence Case 1 appears to be the more realistic of the two.

In summary we conclude that the observed hyperfine splitting and g-shifts can be explained on the basis of equilibria between atoms, memomers, and ion pairs. The nature of the g-shifts permits the detailed specification of the wavefunction of these species.

The wavefunction of the ion-pair is viewed as

$$\Psi$$
(ion pair) = $\mathbb{I}\left\{\bar{\Phi}_{\bullet} - \rho(\mathbf{n})^{-\frac{1}{2}} \sum_{i=1}^{n} \sigma_{\bullet}(\mathbf{s}^{1})\right\}$

where $\Phi_{\mathbf{e}}$ is the wavefunction of an electron in a cavity interesting only weakly with an adjacent noted medicus. This gives as an expression for the g-shift

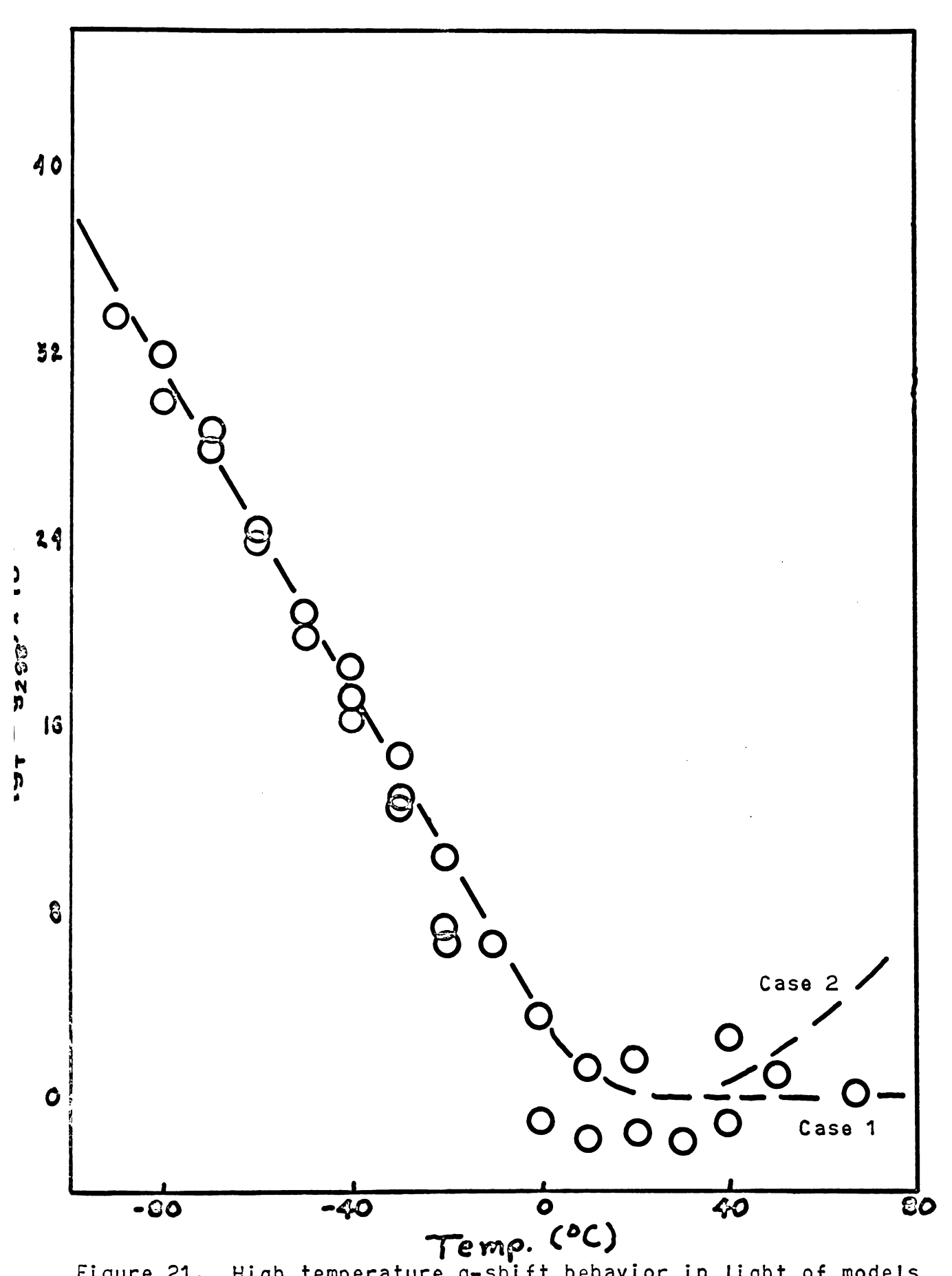


Figure 21. High temperature g-shift behavior in light of models for the solvated atom.

$$\Delta g(\text{ion pair}) = \left(\xi(\text{M2P})\right) \left[\frac{K_1}{\Delta E^b} - \frac{K_2}{\Delta E^a}\right]$$

or, neglecting charge transfer interaction

$$\Delta g(\text{ion pair}) = -\frac{E_2 \xi(\text{H2P})}{\Delta E^2}$$

Calculations involving the evaluation of this equation in the light of experimental evidence is given in Appendix I.

The wavefunction of the monomer is seen to be

$$\Psi$$
 (monomor) = π { α Ψ (MS) + β Ψ (MP) + δ Ψ (MD) + δ Ψ (MF) + ϵ Ψ (MES)

This gives rise to an expression for the g-shift given by

$$\Delta g(\text{monomer}) = \left\{ a \, \xi(\text{MP}) + b \, \xi(\text{MD}) + a \, \xi(\text{MF}) + d \, \xi(\text{M2P}) \right\} \left[\frac{K_1}{AE^b} - \frac{K_2}{AE^a} \right]$$
We shall assume that $\frac{K_1}{AE^b} = 0$.

Thes

$$\Delta g(monomer) = -\left\{a \xi(MP) + b \xi(MD) + e \xi(MP) + d \xi(M2P)\right\} \frac{K_2}{\Delta E^a}$$

A consideration of the dependence of spin-orbit coupling on notal in going from sodium to costum permits us to evaluate the contribution of each of the $\bar{p} \neq 0$ metal and ligand(solvent) orbitals to the total spin-orbit coupling. The details of this treatment are given in Appendix I.

Continuing we view the wavefunction for the atom as

$$\Psi(\text{atom}) = \Psi(\text{(MS)} + \beta^{\text{(MP)}} + \gamma^{\text{(MD)}} + \delta^{\text{(MP)}} \\
-\rho(n)^{-\frac{1}{2}} \frac{n}{2\pi i} \sigma_{0}(s^{1})$$

The difference between the hyperfine splitting in the atom and in the moment requires that $\alpha' >> \infty$.

Neglecting charge transfer we derive for the atom

$$\Delta g(aton) = -\left\{a'\xi(MP) + b'\xi(MD) + c'\xi(MF) + d'\xi(M2P)\right\} \frac{K_2}{\Delta E^a}$$

In Case 1, $b'K_2 = c'K_2 = d'K_2 = 0$ while in Case 2 it is likely that $aK_2 \approx a'K_2$, $bK_2 \approx b'K_2$, $aK_2 \approx c'K_2$, and $dK_2 \approx d'K_2$.

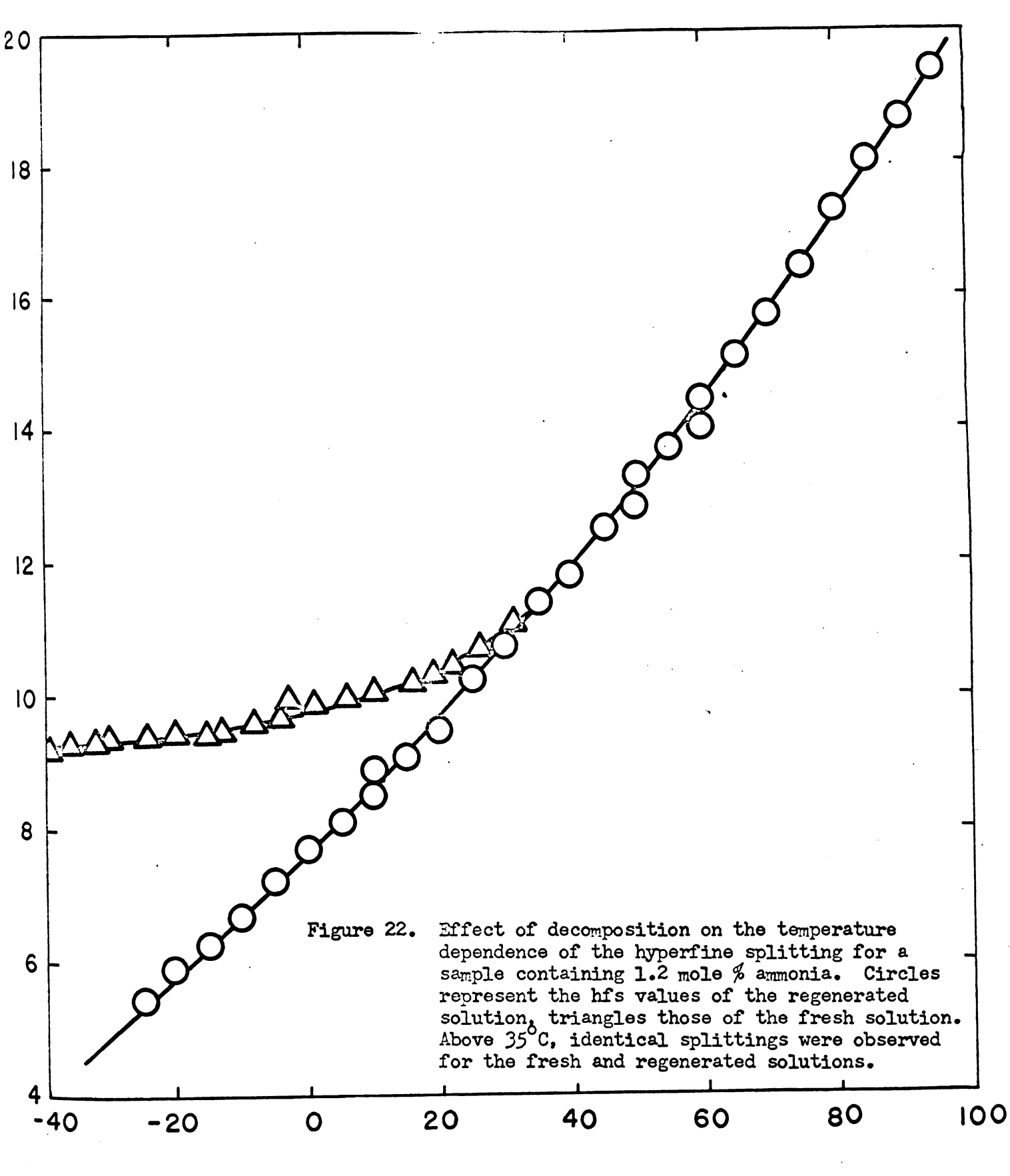
Whether we use a stationary state or equilibrium model, any explanation of the temperature dependence of the g-shifts must also explain the temperature dependence of the hyperfine splitting since both of these physical variables are intimately related to the nature of the wavefunction of the paramagnetic electron. For example

$$\frac{A}{g} = \frac{2 \beta \beta_{n} n}{I} \left\langle r^{-3} \right\rangle \frac{\langle J | \pi | J \rangle}{\langle J | \wedge | J \rangle}$$

As can be seen from Appendix I the K_2 's calculated from g-shifts explain the correct progression of hyperfine splitting values from metal to metal and from solvent to solvent.

The reader may wonder why only two species (atoms and monomers) were required to explain the temperature dependence of the hyperfine interaction in potassium-ethylamine solutions while three species were required to explain the hyperfine interaction and g-shifts in cosium-amine solutions.

The most reasonable explanation for this is that the concentration of the ion-pair is nearly sero in petassium-ethylamine solutions. In fact this assumption explains the observed temperature independence of the g-shifts. It also serves to explain the unusual change in temperature dependence of a petassium-ethylamine solution after decomposition and regeneration (see Fig. 22 and Ref. 42). The build-up of decomposition



TEMPERATURE (°C)

products is viewed as favoring the ism-pair. (It has been pointed out to the author that this can occur only as a result of a change in the activity coefficient.) This concept can also be used to explain the fact that the ism-pair concentration is higher in freshly prepared cosimm-amine solutions than in potassium-amine solutions. Cosium solutions are more subject to decomposition than potassium solutions. The favoring of the ism-pair in occium solutions may also result from the presence of small amounts of amonia in the amines used. Cosium-amine solutions were invariably the last to be prepared from a given solvent purification. Upon standing over notal the purified amine may have decomposed somewhat, resulting in the build-up of amonia. The ism-pair appears to be favored by increasing amonia concentration.

The three-state equilibrium model also serves to explain the temperature dependence of the g-shift and hyperfine interestion observed in rubidium-othylamine solutions. As has been proviously mentioned (42) potassium and rubidium do not appear to be soluble in high purity othylamine. When samples containing rubidium and othylamine were allowed to stand at elevated temperatures for extended periods of time blue solutions were formed. The temperature dependence of the hfs and g-shifts suggest that the ion-pair is favored at the expense of the momenter. Indeed if one considers an equilibrium between only ion-pairs and atoms (case 1), one can obtain a reasonable quantitative fit of the data. Such an atom-ion pair equilibrium appears to have been successfully applied by Catterall and Symons (109) to certain potassium-amine solutions.

In fact at this writing there appear to be no results which cannot be at least qualitatively described using the equilibrium medel.

Multi-State Matribution Model

The observed temperature dependence of the g-shift can also be explained in terms of a temperature dependent distribution of g-values. The g-value distribution would be viewed as arising from a distribution of the admixture coefficients. The quantitative treatment of such a model involves a knowledge of the distribution of g-shifts as a function of temperature. At this time it is not clear how this distribution should be determined.

- 2. The selvated electron. We assign the EPR singlet observed at $g=2.0019\pm0.0002$ to the selvated electron. The reasons for this assignment are as follows:
- a) The ebserved g-value is close to that of the free electron ($g_{\rm e}$ = 2.0023). The molecular orbital expendation given in Appendix I supports the contention that the observed g-shift ($\Delta g({\rm obs.}) = 0.0004$) can be viewed as arising from interaction of the paramagnetic electron with the solvent. Moreover, the g-value and honce the g-shift is independent of the metal and solvent used, the metal concentration, and temperature. If the paramagnetic electron were experiencing significant interaction with metal model this independence of experimental

conditions would not be expected. Since the spin-orbit coupling induced by solvent interaction arises from the nitrogens (at least in the simple N.O. approximation) of the solvation structure, the g-shift of the solvated electron would not be expected to change as a result of changing the alkyl group of the same or dissine.

b) Catterell, Symons, and Tipping (51,52) have shown that the ratio $[singlet]^2/[hyperfine species]$ is independent of concentration for dilute solutions of potassium dissolved in the higher alkylamines. In contrast, the ratio of the intensities [singlet]/[hyperfine species] is independent of concentration in the presence of an excess of cations (e.g. H⁺). These observations are quantitatively in accord with expected concentration ratios for the equilibrium

$$H^{\dagger}(solv.) + o^{\ast}(solv.) \rightleftharpoons H(solv.)$$

Although these relationships are not observed in rubidium and comium solutions this may be due to the interference of additional equilibria.

e) The observed linewidth behavior of these solutions is in accord with processes expected for the solvated electron.

C. Ruelear Spin-Dependent Relexation

The rationale which we wish to employ in considering medear spin-dependent relaxation in notal-smine solutions is to smalyse these processes in the light of models developed by analyses of hyperfine interestions and g-shifts. It is to be emphasized that an analysis of relaxation data alone cannot distinguish between the various models. Hevertheless any model capable of explaining hyperfine interestions and g-shifts must also be capable of explaining the nature of paramagnetic relaxation in these solutions. We shall now examine the

•

. .

various models espable of giving rise to an n₁-dependent paramagnetic relaxation.

The McCouncil Mechanian

In an attempt to obtain a more realistic evaluation of the experimental coefficients of Eq. 16 in terms of a McConnell mechanism we have measured the viscosity of ethylamine as a function of temperature. The values of the coefficients plotted versus η/T are shown in Fig. 23.

As can be seen from Fig. 23 and from Fig. 4, the equificients of the terms in m, tend to go to sere as the freezing point of the selution is approached. One might reason that this would indicate that a McConnell--type mechanism commot be operative in these solutions since for this medal the coefficients would be expected to increase with decreasing temperature (see References 57 and 59) and the separation into non--symmetrical components (e.g. $A_{\parallel e}$ $A_{\perp e}$ $g_{\parallel e}$ g_{\perp} if the system is axially symmetrical) would be expected upon freezing. While this argument is true to a cortain extent and the temperature dependence of the coefficients of the equation in m, does comes us to doubt the applicability of the McConnell mechanism to those solutions, the experimental behavior does not rule out this possibility. The reason for this is that an increase in the coefficients of the my-dependent relaxation equation implies a decrease in the correlation time of the motion everaging the existropic hyperfine and g-tensor interactions. In cases where the McCouncil mechanism is operative the usual averaging process is the tambling of the peremagnetic microcrystal (central ion, immediate es-erdinated ligands, and more distant but nevertheless eriented seemsdary solvation layers). In these cases the coefficients will be preportional to the viscosity of the solution and for normal solvents

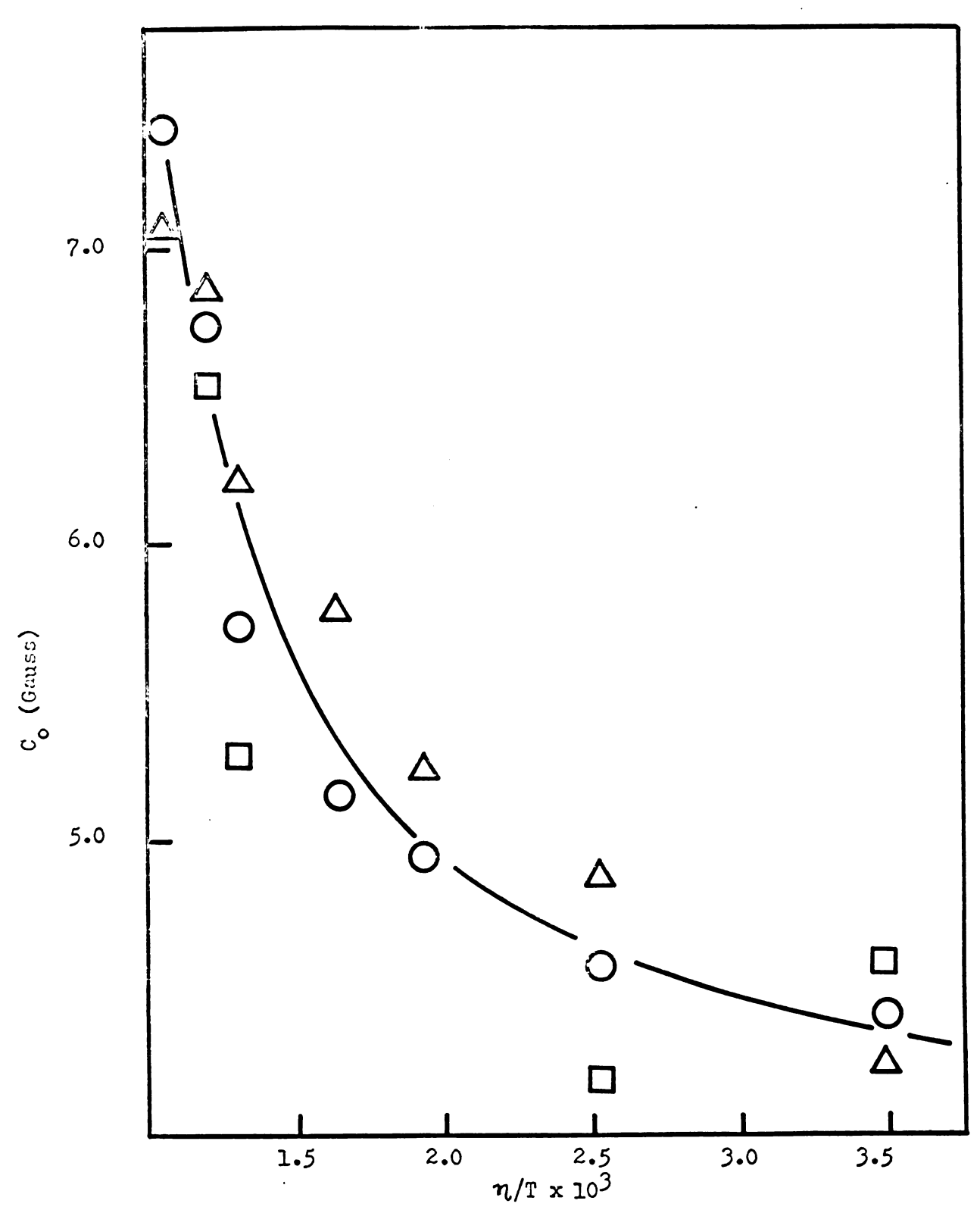


Figure 23a. Variation of the residual linewidth (C_0) with n/T: Cs in EtNH₂. Results are shown for three different sample preparations.

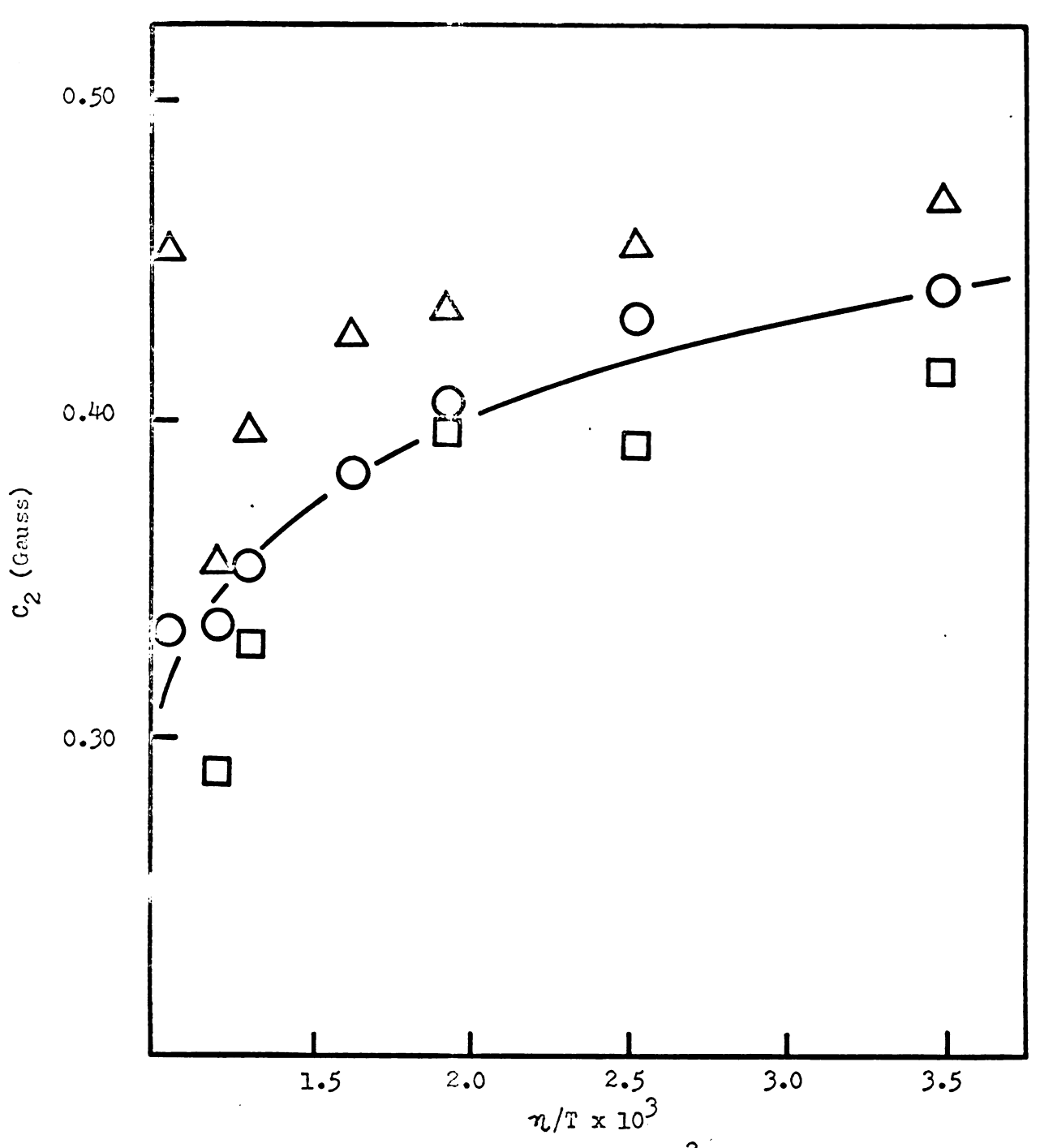


Figure 23c. Variation of the coefficient of $m_{\rm I}^2$ (C₂) with n/T: Cs in EtNH₂. Results are shown for three different sample preparations.

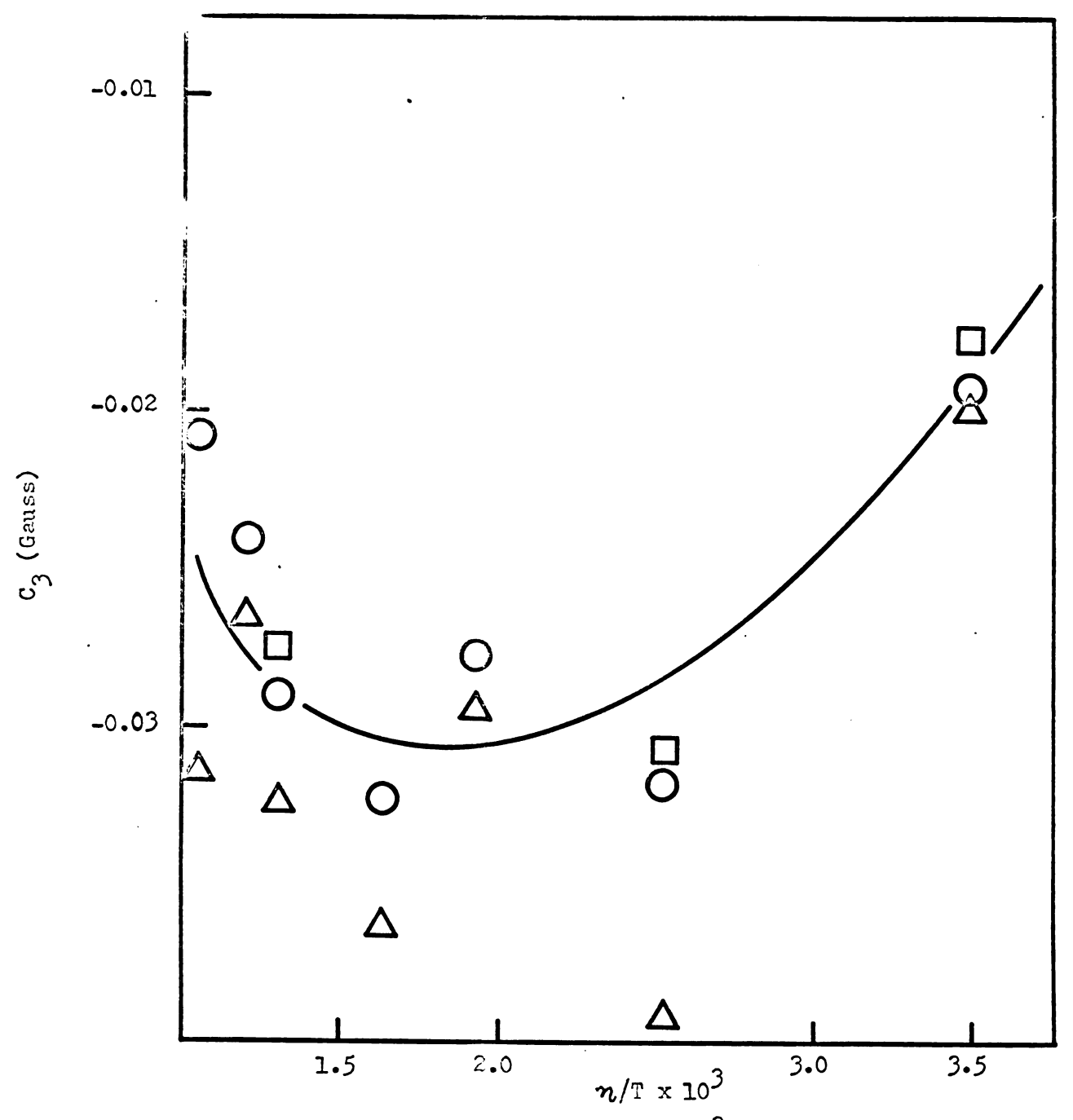


Figure 23d. Variation of the coefficient of $m_{\rm I}^{-3}$ (C₃) with η/T : Cs in EtNH₂. Results are shown for three different sample preparations.

would be expected to increase with decreasing temperature. Actually, however, the asymmetric microcrystalline unit can also experience modulation of the A and g tensor asymmetries through lattice vibrations, magnetic interactions (e.g., exchange) with other paramagnetic substances, and through a rotation of the central motal atom or ion with respect to the remainder of the microcrystal.

Thus, although the temperature dependence of the coefficients example arise from the tumbling of an asymmetric monomeric species, it is possible that a McConnell mechanism involving some other form of symmetry modulation could result in the observed dependence upon $\mathbf{n}_{\mathbf{r}}$.

It is highly unlikely, however, that the weak interestions entieipsted between an alkali metal measurer and the same solvent sould result in the large asymmetries required by this model.

It may also be observed that the strong temperature dependence of the hyperfine and spin-orbit coupling would not be expected for a single asymmetric species.

In concluding our discussion of the McConnell mechanism it should be noted that for natorials in which this mechanism is operative, one example use the equation of Bloombergen, Purcell, and Pound (92,109) to relate T_2 to T_1 quantitatively. This is because, although the spin-lattice relaxation affect (T_1) alone would be expected to give the usual Lorentzian curve, the transverse relaxation due to the anisotropies of the hyperfine and Zouman tensor, T_2 , is expected to give quite unsymmetrical broadening since, in the limiting case of a perfectly rigid glass the reconsise would be extranely unsymmetrical. Thus we must relate T_2 and T_3 by the following relationship

$$\frac{1}{x_2} = \frac{1}{x_2} + \frac{1}{x_3}$$

As this relation indicates the shorter the correlation time of the process modulating the anisotropies the more the observed line shape will appreach a Lorentzian curve.

In metal-anime solutions showing n_1 -dependent relaxation the resonances were more closely approximated by a Gaussian shape function. The Equilibrium Model

For conserveness, let us first consider a particularly simple example of the time-dependent variation in hyperfine splitting: suppose that the redical can exist in only two forms, A and B, and that these are in rapid equilibrium with each other. A model such as this is a reasonable representation, for example, of the nitrobensone emion radical when it is prepared by reduction of nitrobensone with potassium (76). The ion-pair complex between the radical anion and the alkali-motal cation can be represented by Form A and the uncomplexed radical anion by Form B. If Form A could be isolated and were not undergoing transitions to Form B, a mucleus of spin I with hyperfine splitting $A_{\hat{A}}$ would give rise to an EFR spectrum of 2I + 1 equal-intensity lines with a constant inter-line spacing $A_{\hat{A}}$. Similarly, Form B would give a spectrum of 2I + 1 lines with specing $A_{\hat{B}}$. Each line in the two spectra corresponds to a particular value of the quantum number $n_{\hat{A}}$ specifying the field-direction component of the maclear spin angular momentum.

When the two forms are interchanging rapidly, an average of the two spectra is obtained which consists of 2I + 1 lines with a mean splitting

$$X = p_A A_A + p_B A_B$$

where $\mathbf{p}_{\mathbf{A}}$ and $\mathbf{p}_{\mathbf{B}}$ are the probabilities of finding Forms A and B, respectively.

This result for the mean hyperfine splitting follows from the general relaxation-matrix theory (110) and also from the Bloch equations (93) as modified to include the effects of exchange (111). In the Bloch-equation formulation, lines which appear at (angular) frequencies $\omega_{\underline{A}}(n_{\underline{I}})$ and $\omega_{\underline{B}}(n_{\underline{I}})$ in the spectra of the two isolated forms coalesce, in the limit of fast exchange, to an average frequency

$$\omega(\mathbf{m}_{\mathrm{T}}) = \mathbf{p}_{\mathrm{A}} \omega_{\mathrm{A}}(\mathbf{m}_{\mathrm{T}}) + \mathbf{p}_{\mathrm{B}} \omega_{\mathrm{B}}(\mathbf{m}_{\mathrm{T}}) \tag{40}$$

It is important to note that we consider a particular paramagnetic species in Fern A with medicar-spin quantum number n. in equilibrium with a Fern B of the same nuclear spin quantum number n. Effects which cause nuclear-spin transitions can thus not be treated by use of the Bloch formulian.

It can be shown that for repid interchanges the contribution to the transverse relaxation time, T₂, from the modulation of the isotropic hyperfine interaction is inversely proportional to the mean-square fluctuation in splitting (80,110),

$$\langle (\delta A)^{2} \rangle = \langle [\bar{A}(t) - \bar{A}]^{2} \rangle$$

$$= p_{\bar{A}}(A_{\bar{A}} - \bar{A})^{2} + p_{\bar{B}}(A_{\bar{B}} - \bar{A})^{2}$$

$$= p_{\bar{A}}p_{\bar{B}}(A_{\bar{A}} - A_{\bar{B}})^{2}$$

$$(41)$$

The rates of the reactions also affect the widths, and if $\tau_{\rm A}$ and $\tau_{\rm B}$ are the lifetimes of Ferms A and B, respectively, the widths are

$$T_{2}^{-1}(\mathbf{n}_{I}) = \mathbf{p}_{A}T_{2A}^{-1} + \mathbf{p}_{B}T_{2B}^{-1} + \mathbf{Y}_{o}^{2}\tau \langle (\delta A)^{2} \rangle \mathbf{n}_{I}^{2}$$

$$= \mathbf{p}_{A}T_{2A}^{-1} + \mathbf{p}_{B}T_{2B}^{-1} + \mathbf{Y}_{o}^{2}\tau \mathbf{p}_{A}\mathbf{p}_{B}(A_{A} - A_{B})^{2}\mathbf{n}_{I}^{2}$$
(42)

where Y_o = the electron gyromegnetic ratio and

$$\tau = \tau_A \tau_B / (\tau_A + \tau_B)$$
 and

 T_{2A}^{-1} and T_{2B}^{-1} , the contribution to the widths from other line-

-breadening mechanisms, is assumed to be independent of $\mathbf{n}_{\mathbf{I}}$. The quantity $T_2(\mathbf{n}_{\mathbf{I}})$ is the transverse relaxation time for the line corresponding to the modesr-spin quantum number $\mathbf{n}_{\mathbf{I}}$. The shape of each line is Lorentzian and given by (on an angular frequency basis)

$$I_{n_{1}}(\omega) = [I_{2}(n_{1})/\pi] \{1 + I_{2}^{2}(n_{1}) [\omega - \bar{\omega}(n_{1})]^{2}\}^{-1}$$
 (43)

In magnetic field units, the width is

$$[\omega(\mathbf{n}_{1}) - \omega_{0}(\mathbf{n}_{1})]_{\frac{1}{2}} = [|\gamma_{0}| \gamma_{2}(\mathbf{n}_{1})]^{-1}.$$

This is the half-width at half-maximum intensity, and is related to the separation of the extrema in the first derivative spectrum by

$$s_p = (2/\sqrt{3})[\omega(\mathbf{n}_1) - \omega(\mathbf{n}_1)]_1$$

The above equations result from the Block-equation formalism, according to which the widths are

$$T_2^{-1}(n_T) = T_2^{-1}(0) + \gamma \langle [\delta \omega(n_T)]^2 \rangle$$
 (44)

where for two species undergoing exchange

$$T_2^{-1}(0) = p_A T_{2A}^{-1} + p_B T_{2B}^{-1}$$

and

$$\langle [\delta \omega (\mathbf{n}_{\mathbf{I}})]^2 \rangle = \mathbf{p}_{\mathbf{A}} \mathbf{p}_{\mathbf{B}} [\omega_{\mathbf{A}}(\mathbf{n}_{\mathbf{I}}) - \omega_{\mathbf{B}}(\mathbf{n}_{\mathbf{I}})]^2$$

Precised (80) has shown that the relaxation-matrix gives the same results for this simple two-jump model. Since this is also applicable to much more complicated situations (such as an equilibrium involving many states or a distribution) we shall briefly review this treatment. To understand the method of calculation, several new quantities have to be introduced. The fluctuations in hyperfine splittings enter through a correlation function

$$g(t^{\dagger}) = \gamma_0^2 \langle [A(t) - \overline{A}] [A(t+t^{\dagger}) - \overline{A}] \rangle$$
 (45)

which is a time average of the product of deviations in hyperfine splittings at time t, $[A(t) - \overline{A}]$, and at time t + t', $[A(t + t') - \overline{A}]$. The linewidths are related to this correlation function through its Fourier cosine transform,

$$J(\omega) = \int_{0}^{\infty} g(t^{*}) \cos \omega t^{*} dt^{*}, \qquad (46)$$

in which, when only secular terms are significant, $\omega=0$. Finally, the linewidths are given by (110)

$$T_2^{-1}(\mathbf{m}_1) = j(0)\mathbf{m}_1^2 + T_2^{-1}(0)$$
 (47)

As an illustration of the precedure for evaluating the correlation function, we again treat the simple two-jump model considered above. The reaction between Forms A and B is

$$A \xrightarrow{k_{A}} B$$

and the differential equation for the mole fraction of A, I_A , is

$$dX_A/dt = -k_AX_A + k_BX_B$$

The solution of this equation is

$$I_A(t) = p_A + [I_A(0) - p_A] \exp(-t/\gamma)$$

where

$$\gamma = \gamma_A \gamma_B / (\gamma_A + \gamma_B) \quad \text{with } \gamma_A = k_A^{-1}, \ \gamma_B = k_B^{-1}, \text{ and}$$

$$p_A = I_A(\infty) = k_B / (k_A + k_B) = \gamma_A / (\gamma_A + \gamma_B).$$

Thus, the probability that Species A at time t=0 will still be in Ferm A at time $t\geq 0$ is given by

$$P(A/A,t) = p_A + p_B \exp(-t/\tau)$$

while the probability that it will be in Form B at time t is

$$P(A/B,t) = p_{R} [1 - \exp(-t/\gamma)],$$

with similar expressions if the paramagnetic species is initially in Form B.

The correlation function becomes

$$Y_{\bullet}^{-2}g(t^{*}) = \sum_{H} p_{H}[A(H) - \bar{A}] \sum_{Y} P(\mu/Y_{\bullet}t^{*})[A(Y) - \bar{A}]_{\bullet}$$

$$= p_{A}[p_{A} + p_{B} \exp(-t^{*}/\gamma)] (A_{A} - \bar{A})^{2}$$

$$+ p_{B}[p_{B} + p_{A} \exp(-t^{*}/\gamma)] (A_{B} - \bar{A})^{2}$$

$$+ 2p_{A}p_{B}[1 - \exp(-t^{*}/\gamma)] (A_{A} - \bar{A})(A_{B} - \bar{A})$$

$$= p_{A}p_{B}(A_{A} - A_{B})^{2} \exp(-t^{*}/\gamma)$$

The Fourier transform of g(t') is thus

$$J(\omega) = Y_{A}^{2} \tau (1 + \omega^{2} \tau^{2})^{-1} p_{A} p_{B} (A_{A} - A_{B})^{2}$$
 (49)

Substituting this expression into Eq. 47 gives Eq. 42.

The relaxation-matrix procedure is readily extended to quite general types of motion modulation as, for example, complicated jump mechanisms and models in which the hyperfine splitting is a continuously varying function of the time (77.78.79.110). It is also a rigorous theory which is limited only by the requirement that the metion has to be sufficiently rapid when compared to the magnitude of the fluctuations in splittings $\left[\frac{2}{2}Y_0^2 < (\delta A)^2\right] < 1$, and shows that a result of the form of Eq. 47 is valid without recourse to specific medels for the calculation of the spectral density j(0).

The Block equations can also be employed for simple jump models of the type considered above when the characteristic times are long. In the limit of very long times, the results can be simply expressed, but in the intermediate region, detailed numerical computations of

the spectra are required (111,112,113). For example, at long times the two-jump model reduces to two superimposed spectra each of 2I+1 lines. The spectrum with hyperfine splitting A_A has relative intensity p_A , while the one with splitting A_B has relative intensity p_B . The widths in the spectrum from Ferm A are

$$T_{2A}^{-1}(\mathbf{n}_{\underline{I}}) = T_{2A(\infty)}^{-1}(\mathbf{n}_{\underline{I}}) + \gamma_{\underline{A}}^{-1}$$

with a similar expression for the spectrum from B, where $T_{2A(\infty)}^{-1}(m_{\tilde{I}})$ is the width in the absence of reaction between the two forms. As the rates increase, the lines begin to coalesce as well as to breaden.

The nuclear spin-dependent relaxation observed in notal-animo solutions appears to be characterised by two equilibria involving three species. Above subject temperatures the linewidth variation appears to be determined by an atom-monomer equilibrium, while at lower temperatures a monomer-ion pair equilibrium is effective in accounting for the nuclear spin-dependent relaxation.

A difficulty in treating the stem-momener equilibrium srices from the fact that the splittings of potassium stems, and of rebidium and cosium atoms and monomers are sufficiently large that the high field approximation breaks down. Hence frequencies of the hyperfine lines as obtained from the Breit-Rebi formulism (83) or from the expansion of Fessenden and Schuler (84) should be used with Eq. 44.

At low temperatures the coefficient of the $n_{\rm I}^2$ is the predominant higher order term in accord with the predictions of Eq. 44 and the monomer-ion pair equilibrium.

D. Huclear Spin-Independent Relexation

The effects of metal concentration, salt addition (e.g., IBr or K(EtHH)), and decomposition indicate that spin exchange processes involving H⁺ and the species giving rise to the optical absorption at 650 to 725 mp are particularly important in determining the residual or muclear spin-independent linewidths. Under certain conditions spin exchange processes involving the solvated electron and solvent exchange can result in a slight contribution to linewidths.

APPENDIX I

In order to perform the molecular orbital calculation of metal—solvent bonding coefficients we need to know the energy separation, E^8 , between the ground and excited state molecular cristal energy levels and the spin-orbit coupling constants of the cristals of the ground-state wavefunction which we have constructed. In the simple H_*O_* , treatment the ΔE^8 's must be obtained from experiment. We have obtained approximate values of ΔE^8 by comparison of vapus phase and solution spectra of the stomic and dimeric transitions of the alkali metals. This treatment is summarised in Table XXV. The spin-orbit coupling constants of the orbitals used in forming the ground state wavefunction of the solveted species were obtained from Reference 12O*. These together with the necessary E^8 are given in Table XXVII. The K^* s calculated at $23^{\circ}C$ are given in Table XXVII.

TABLE XXV. Optical Absorptions of M. M. 2. and e in the Vaper Phase and in Solution (in cm 1)

P S Transition for H in gas phase

	x	Rb	Ce	
,	13,017.5	12,700.2	11.451.7	
'Σ'- Έ	Transition for H2 in gas phase			
	K ₂	Rb ₂	Cs ₂	
	11,670.9	11,190	10,100	
Try - Ig	Trensition for M ₂ in gas phase			
, 0	r ₂	Rb ₂	Cs ₂	
	15,369.2	12,700.2	11.451.7	
Trite-12g	Transition for M2 in solution			
	r ₂	Rb ₂	Ca ₂	
١	11,834	11,236	9709	
\Z, - \Za	Trensition for M2 in solution			
,	r ₂	m ₂	Cs ₂	
	8,340*	7.768*	6.769*	
(Pesado) P	(Pseudo) S Trensiti	on for N in solution		
	K	Rb	Ce	
	9,686•	9.2780	8,120*	
*Predicted	9,686° from enalogy with shift of	of The Zyapon	solvation of diser.	

TABLE MAVI. Parameters used in Molecular Orbital Calculation.

Solveted Flootron Ion-Pair **∆ g = -0.000**4 \$ (beauces) → -0.0004 A E - 7,813 a -1 △E*(assumed) = 7,813 cm 1 ξ(E) golvent = 4.57 cm-1 (E) solvent = 4.57 cm-1 Lithium A = -0.0004 A = 11.169 cm-1 E(11) solvent = 4.97 cm-1 号(2P)14 - 0.509 cm-1 Softon **∆** g = -0.0008 AE - 9.696 -1 E (N) solvent = 4.57 cm⁻¹ E (𝔻)_{Na} = 25.78 cm⁻¹ Potassina 8000.0008 Δ E = 9.686 cm-1 ξ(H) solvent = 4.57 cm-1 E (47) = 86.54 cm ξ(3d)_x = 1.95 **~**⁻¹ **Jubicius** △ E = -0.0025 △ 5° - 9.278 ξ (3) solvent = 4.57 cm⁻¹ ξ (5P)_{3b} = 221 cm⁻¹ \$(4d)_{2b} = 1 cm⁻¹ Contin ∆E = 8,120 m-1 ξ(E) solvent = 4.57 cm⁻¹

€(6P)c= 677 m-1

141

TABLE IXVII. Calculated Values for E at 23°6 for Species Present in Motal-Amine Colutions.

Species	X
Solvated electron	0.11
Ion-pair	•.11
14	1 6
Xe.	0.15
K	0.07
Rb	0.09
Cs	0.07
K Rb	0.07

REFERENCES

- 1. W. Weyl. Arm. Physik. 121, 601 (1864).
- 2. C. A. Kraus, J. M. Chos. Soc., 30, 1323 (1908).
- 3. S. Freed and N. J. Sugarman, J. Chem. Phys., 11, 354 (1943).
- 4. E. Huster, Ann. Physik, 33, 477 (1938).
- 5. E. Huster, Ann. Physik, 4, 183 (1948).
- 6. C. A. Rutchison, Jr. and R. C. Paster, J. Chem. Phys., 21, 1959 (1953).
- 7. D. E. O'Reilly, Ph. D. Dissertation, University of Chicago, Chicago (1955).
- 8. C. A. Frans. J. An. Chan. Spe., 36, 864 (1914).
- 9. E. C. Evers, A. E. Young II, and A. T. Penson, J. Am. Chem. Sog., 72, 5113 (1957).
- 10. J. L. Dye, R. F. Sankuer, and G. E. Saith, J. An. Chem. Spc., 82, 8797 (1960).
- 11. H. M. McConnell and C. H. Holm, J. Chem. Phys., 25. 1517 (1957).
- 12. J. V. Acrivos and K. S. Pitser, J. Phys. Chem., 66, 1693 (1962).
- 13. T. R. Hughes, Jr., J. Chem. Phys., 35, 202 (1963).
- 14. D. E. O'Reilly. J. Chem. Phys. 51, 3729 (1964).
- 15. C. A. Kraus, E. S. Carney, and W. C. Johnson, J. Am. Cham. Soc., 19, 2206 (1927).
- 16. W. C. Johnson and A. W. Heyers, J. An. Chen. 500., 50, 3621 (1932).
- 17. R. C. Douthit and J. L. Dye, J. Im. Chem. Soc., 62, 4472 (1960).
- 18. N. Gold and W. L. Jolly. Inorg. Chem., 1, 818 (1962); M. Gold. Ph. D. Pissertation, University of California, Berkeley. (1962); U.S.A.E.C., 1962, U.C.R.J.,-10062.
- 19. J. Corset and G. Lepoutre, "Metal-Assemble Solutions: Physiochemical Properties," eds. G. Lepoutre and M. J. Sienko, W. A. Benjamin, Inc., New York, 1964, p. 186.

- 20. D. F. Burow and J. J. Lagowski. Advances in Checistry Series, 50.
 "Solvated Flootron," edited by R. F. Gould, American Chemical Seciety,
 Washington, D. C., 1965, 125.
- 21. J. Replan and C. Kittel. J. Chem. Press. 22, 1439 (1953).
- 22. R. Pocker, R. H. Lindquist, and R. J. Alder, J. Chem. Phys. 25. 971 (1956).
- 23. E. Armold and A. Patterson, Jr., J. Chem. Phys., bl. 3009 (1964).
- 24. S. Goldon, C. Cuttman, and T. R. Tuttle, Jr., J. Am. Chan. Foc., £7, 135 (1965); J. Chan. Phys., bt. 3791 (1966).
- 25. R. Cattorall and M.C.R. Symons, J. Chom. Foc., (1966) 13.
- 26. H. Flades and J. W. Rodgins, Con. J. Chan. 33. 411 (1955).
- 27. N. C. R. Symons, J. Chem. Phys. 20, 1628 (1999); Quarterly Reviews, 13, 99 (1959).
- 28. H. Clark and M. C. R. Symons, J. Cham. Sec., (1957).
- 27. F. A. Cafasco and B. R. Sundheim, J. Chon. Phys., 31, 809 (1959).
- 30. G. W. A. Fordes, W. R. Follogor, and M. C. R. Symons, J. Chom. 200... (1957) 3339.
- 31. S. B. Finder and R. R. Sundheim, J. Phys. Chem. 66, 1254 (1962).
- 32. F. S. Dainton, D. N. Wiles, and A. S. Wright, J. Cham. Coc. (1960) 4283.
- 33. J. L. Tye and R. R. Dewald, J. Phys. Chem., (8, 135 (1964).
- 24. G. Herrberg, Opentra of Distoric Molecules, D. Van Mostrond Co., New York, 1950.
- 35. R. R. Foweld and J. L. Dye, J. Phys. Chem., 63, 121 (1964).
- 36. H. J. Eding. D. D. Diecis. Stanford University, Stanford. 1952.
- 37. K. D. Vos and J. L. Dye, J. Chop. Phys. 23, 2033 (1963).
- 30. K. Ber-Ull and T. R. Tuttle, Jr., Phil. Mr. Phys. Soc. 8, 352 (1963).
- 37. H. Ottolenghi. E. Par-Fli. H. Linschits, and T. R. Tuttle. Jr., J. Chem. Phys., 40, 3729 (1964).
- 40. W. Ottolenghi. E. Bar-Eli. and E. Linschits, J. Chem. Phys., \$3, 205 (1965).
- 41. J. L. Dye, L. R. Dalton, and E. H. Hanson, Abstracts, 1/1/11 Retional Recting of the American Charical Society (April, 1965), p. 455.

- 42. L. R. Dalton, J. D. Rynbrandt, E. K. Hansen, and J. L. Dyo, J. Chan-Phys., 44, 3969 (1966).
- 43. E. Bar-Ell and T. R. Tuttle, Jr. J. Chos. Phys. 40, 2508 (1964).
- 44. H. Anbar and E. J. Hart. J. Phys. Chem. 60, 1244 (1965).
- 45. D. N. J. Compton, J. F. Bryant, R. A. Cesena, and B. L. Gehman, Polog Padiolyzia, editors N. Ebert, J. P. Keene, A. J. Swallow, and T. H. Bamoniale, Academic Press, London and New York, 1965, p. 43.
- 46. L. R. Delton, J. L. Dye, E. M. Fielden, and E. J. Hart, J. Phys. Chem., in press.
- 47. J. D. Rymbrandt, private communication.
- 43. D. E. O'Reilly, J. Chem. Phys., 51, 2736 (1964).
- 49. D. E. O'Roilly and T. Tsang. J. Chon. Phrs., 52, 3333 (1965).
- 50. The value a = 6.4 at 0°C and 0°Redlly's (26) graph of spin density vs. the "strongth" of the repulsive potential. Y a2, were used. This requires that the quadrupole-moment term Q has a value of 4.7. While the experimental quadrupole moment tensor for ethylamine is not known, the corresponding value for amonia is 0.8.
- 51. R. Catterall, M. C. R. Symons, and J. W. Tipping, International Conference on Chemical Aspects of Electron Spin Resonance, Cardiff, July, 1966.
- 52. R. Catterall, M. C. R. Symons, and J. W. Tipping, J. Chom. Som. to be published.
- 53. J. L. Lye and L. R. Dalton. Symposium on Flactron Spin Resonance Spectroscopy. East Lansing. August. 1966; J. Five. Chem. to be published.
- 50. R. H. McCommell. J. Chap. Phys., 25, 709 (1956).
- 55. R. H. Rogers and G. E. Peke. J. Char. Phys., 23, 2107 (1960).
- 56. D. Kivelson, L. Chem. Phys., 33, 1090 (1960).
- 57. R. Wilson and D. Kivolson, J. Chan. Phys., 54, 15 (1966).
- 58. A. J. Marriage, Must. J. Chon., 18, 463 (1965).
- 57. Le Re Dalton. J. D. Rymbrandt. J. L. Dye, and C. H. Brubsker, Jr., to be published.
- 60. D. Kivelson, J. Chem. Phys., 27, 1007 (1957).
- 61. A. W. Cverbauser, Phys. Rev., 27. 607 (1950).
- 62. R. J. Fillott. Phys. Rev., 95, 266, 280 (1954).

- 63. Y. Infot, Pres. Rev., 65, 473 (1952).
- 64. H. Brooks, Phys. Rev. . 25, 1/11 (A) (1951).
- 65. G. Feher and A. F. Kip, Phys. Ext., 20, 337 (1955); G. Feher, Ph. P. Thoris, University of California, Perkeley, 1974.
- 66. R. A. Leny, Phys. Box. 98, 264 (1955).
- 67. R. A. LOTY, Phys. Rev., 102, 31 (1956).
- 68. R. D. Vos. M. D. Theris. Michigan State University, East Lancing. 1762.
- 69. L. B. Feldman, R. B. Denmid, and J. L. Dye, Advances in Charletry Surious 50. "Solvated Ploctron," edited by R. F. Could, American Charles Society, Markington, D. C., 1965, p. 163.
- 70. L. H. Feldman, M. D. Thoris, Michigan State University, East Landing, 1966.
- 71. R. R. Domid, D. D. Doris, Hichigan State University, East Lansing, 1963.
- 72. I. L. Szo end H. L. Borke, And. Cher. 35, 240 (1963).
- 73. H. A. Kuska and M. T. Rogers, J. Ches. Phys., 50, 910 (1964).
- 7%. T. Colo, J. Eushida, and H. C. Heller, J. Com. Phys., 23, 2015 (1963).
- 75. Calculated constants were obtained using the values of fundamental physical constants as recommended by the Estional Academy of Sciences Estional Research Council and reported in the Cotober issue of the Estional Dureau of Standards Technical News Pulletine
- 76. G. H. Fraenkal. Symposium on Electron Spin Resonance Spectroscopy. East Lansing. August. 1766; i. Five. Chem. to be published.
- 77. J. H. Freed and G. K. Freenkel. J. Chem. Phys., 41, 699 (1964).
- 73. J. H. Freed and G. K. Freenkel. J. La. Chom. 120. 56. 3777 (1964).
- 79. J. K. Freed and G. K. Fracakel, J. Chem. Phys., 51, 3623 (1964).
- 80. G. K. Fraenkol. J. Chap. Days., 52, 4275 (1965).
- El. B. F. Ramsey, Holocular Reces, Caford University Press, London, 1956.
- 82. S. Millman. I. I. Rahi. and J. R. Lacharias, Phys. Pers. 53, 324 (1938).
- 83. G. Breit and I. I. Rabi. Phys. Rov. 25, 2022 (1931).
- Ch. R. W. Fessenden and R. H. Schuler, J. Ches. Phys. 53, 2700 (1965).

- 85. M. A. Gareten, Phys. Rov., 93, 1228 (1994).
- 86. G. E. Pake and E. H. Purcell, Phys. Rev., 74, 1184 (1948).
- 87. S. A. Altehuler, Zhur. Eksptl. 1 Tooret. Fis., 20, 1047 (1950).
- 88. If one performs an accurate double integration of the derivative curve for a Lorents-shaped absorption neglecting the wings beyond a 48, an error of 27% results.
- 89. L. S. Singer, W. J. Spry, Jr., and W. H. Smith, <u>Proceedings of the Third Conference on Carton</u>, Pergason Press, New York, 1959, p. 123.
- 90. R. T. Weidner and C. A. Whitmer, Phys. Rev., 91, 1279 (1953).
- 91. N. Bloombergen, J. Appl. Phys., 23, 1379 (1952).
- 92. S. Bloombergen, E. M. Purcell, and R. V. Pound, Phys. Rev. 23, 679 (1948).
- 93. F. Block, Phys. Rev., 70, 460 (1946).
- 94. P. F. Chester, P. E. Wagner, and J. G. Castle, Jr., Quantum Klectronics, Columbia University Press, New York, 1960, p. 359.
- 95. D. J. E. Ingrem. Free Radicals as Studied by Ricotron Spin Resonance. Butterworths, London, 1958, p. 128.
- 96. A. H. Portis, Phys. Rev., 91, 1071 (1953).
- 97. H. Weger, Bell System Tech. J., 29, 1013 (1960).
- 98. E. R. Andrew, Phys. Rev., 91, 425 (1953).
- 99. (a) E. L. Hahn, Phys. Rev., 80, 580 (1950):
 - (b) L. L. Pollack, J. Chem. Phys., 30, 864 (1961); (c) R. T. Blume, Phys. Rev., 109, 1867 (1958);
 - (d) D. Cutler and J. G. Poules, Proc. Phys. Sec., 80, 130 (1962);
 - (e) D. Cutler and J. G. Posies, Colleges de Eindhoven, 93 (1962).
 - (f) D. E. Kaplen, N. E. Browne, and J. A. Cowen, Rev. Sci Inst., 32, 1182 (1961):
 - (g) R. C. Pastor and R. H. Hoskins, J. Chem. Phys., 32, 269 (1969).
- 100. J. Smidt. Appl. Sci. Research 68. 353 (1957).
- 101. The "integrated intensities" were assumed to be $h(s_p)^2$, where h and s_p are the derivative peak to peak height and width.
- 102. R. C. Douthit and J. L. Dye, J. Am. Chem. Sec., 82, 14072 (1960).
- 103. J. L. Dye and L. H. Feldman, Rev. Sci. Instr.
- 104. R. R. Dowald and J. L. Dye. J. Phys. Chem., 68, 128 (1964).

